

EVALUATION OF THE USE OF RECLAIMED ASPHALT PAVEMENT
IN STONE MATRIX ASPHALT MIXTURES

Except where referenced is made to the work of others, the work described in this thesis is my own or was done in collaboration with my advisory committee. This thesis does not include proprietary or classified information.

Adriana Vargas-Nordbeck

Certificate of Approval:

David Timm
Assistant Professor
Civil Engineering

Elton Ray Brown, Chair
Director
National Center for
Asphalt Technology

Randy West
Assistant Director
National Center for
Asphalt Technology

George T. Flowers
Interim Dean
Graduate School

EVALUATION OF THE USE OF RECLAIMED ASPHALT PAVEMENT
IN STONE MATRIX ASPHALT MIXTURES

Adriana Vargas-Nordbeck

A Thesis

Submitted to

the Graduate Faculty of

Auburn University

in Partial Fulfillment of the

Requirements for the

Degree of

Master of Science

Auburn University
December 17, 2007

EVALUATION OF THE USE OF RECLAIMED ASPHALT PAVEMENT
IN STONE MATRIX ASPHALT MIXTURES

Adriana Vargas-Nordbeck

Permission is granted to Auburn University to make copies of this thesis at its discretion,
upon request of individuals or institutions and at their expense. The author reserves all
publication rights.

Signature of Author

Date of Graduation

VITA

Adriana Vargas-Nordcbeck, daughter of Mario Vargas and Shirley Nordcbeck, was born November 26, 1977 in San Jose, Costa Rica. She graduated from the University of Costa Rica with a Bachelor of Science degree in Civil Engineering in August, 2003. She also attended the State University at Distance in San Jose, Costa Rica, and graduated with a Masters Degree in Business Administration in July, 2005. She began her studies as a graduate student at Auburn University in September, 2005. She married Fabricio Leiva-Villacorta on May 19, 2007.

THESIS ABSTRACT

EVALUATION OF THE USE OF RECLAIMED ASPHALT PAVEMENT IN STONE MATRIX ASPHALT MIXTURES

Adriana Vargas-Nordbeck

Master of Science, December 17, 2007
(MBA, UNED-Costa Rica, 2005)
(B.S., University of Costa Rica, 2003)

171 Typed Pages

Directed by E. Ray Brown

Mixtures that contain reclaimed asphalt pavement (RAP) can typically perform as well or better than conventional HMA mixes. However, use of RAP has generally not been extended to stone matrix asphalt (SMA) production. This study evaluated the effect of RAP on combined aggregate properties, asphalt binder properties, and overall performance of SMA mixtures. The effect of type and size of RAP, as well as aggregate source on overall mix performance was also evaluated. Four types of RAP were combined at four levels (0%, 10%, 20% and 30%) with four aggregate sources. One source of virgin asphalt cement (PG76-22) was used in this study.

Testing was performed to evaluate LA abrasion and flat and elongated particle content of the virgin and recycled aggregate blends. The effect of RAP addition on the rheological properties and performance grades of the combined binder blends was also evaluated. Finally, testing was performed to determine potential binder effect on resistance to moisture susceptibility, resistance to rutting, thermal cracking potential and fatigue life of the recycled mixtures.

Results showed that only fatigue life of the mixes decreased significantly with the addition of RAP, but damage can be minimized by limiting the use of recycled SMA mixes to the top layers of the pavement and ensuring a good bond with the underlying layer. Overall, up to 20% RAP could be used without significantly affecting the performance of the mixes.

ACKNOWLEDGMENTS

The author would like to thank Dr. E. Ray Brown and Donald Watson for all their guidance and support in this endeavor. The author also acknowledges the advisory committee including Dr. David Timm and Dr. Randy West for all of their time and assistance during this project. Thanks are also due to the staff at the National Center for Asphalt Technology for all their assistance. Special thanks are due to her parents Mario and Shirley and to her sister Marcela, for all of their love and support throughout all academic endeavors. Finally to her husband Fabricio, for all of his encouragement and support in every step of the way.

Style manual used: Proceedings, Association of Asphalt Paving Technologists

Computer software used: Microsoft Word, Microsoft Excel, Minitab

TABLE OF CONTENTS

LIST OF TABLES.....	xi
LIST OF FIGURES.....	xv
CHAPTER 1. INTRODUCTION.....	1
1.1 BACKGROUND AND PROBLEM STATEMENT.....	1
1.2 OBJECTIVES.....	2
1.3 SCOPE OF STUDY.....	2
CHAPTER 2. LITERATURE REVIEW.....	4
2.1 INTRODUCTION.....	4
2.2 REVIEWS.....	5
2.3 SUMMARY.....	36
CHAPTER 3. RESEARCH TEST PLAN.....	38
3.1. PART 1 – EVALUATION OF MATERIALS.....	39
3.1.1 Evaluation of Aggregate Properties.....	39
3.1.2 Evaluation of Asphalt Binder Properties.....	47
3.2 PART 2 – MIX DESIGNS.....	53
3.3 PART 3 – PERFORMANCE TESTS.....	59
3.3.1 Moisture Susceptibility.....	59
3.3.2 Rutting Susceptibility.....	60

3.3.3	Creep Compliance.....	61
3.3.4	Flexural Beam Fatigue.....	65
CHAPTER 4. TEST RESULTS AND ANALYSIS.....		67
4.1	MATERIAL PROPERTIES	67
4.1.1	Aggregates	67
4.1.2	Asphalt Binder	69
4.2	MIX DESIGNS	83
4.3	PERFORMANCE TESTS	87
4.3.1	Moisture Susceptibility.....	87
4.3.2	Rutting Susceptibility.....	96
4.3.3	Indirect Tensile Creep Compliance	100
4.3.4	Flexural Beam Fatigue.....	107
4.3.5	Summary.....	119
CHAPTER 5. CONCLUSIONS AND RECOMMENDATIONS		125
CHAPTER 6. REFERENCES		128
APPENDIX A.....		133
APPENDIX B		148

LIST OF TABLES

Table 2.1. Rutting of Fine SMA vs. Standard Hot Mix: I-85 Test Section (2).....	5
Table 2.2. Friction Values for Fine SMA Mix: I-85 Test Section (2).	6
Table 2.3. Procedures for the Design of Mixtures Containing RAP (9).....	20
Table 2.4. Mix Design Parameters (14).....	25
Table 2.5. Strength, Stiffness and Critical Pavement Temperature of the Mixes (16)....	27
Table 2.6. Change of IDT Properties for Long-Term Aged Mixture (17).....	29
Table 2.7. Summary Results of Fatigue Constants and Allowable Number of Loads (18).	34
Table 2.8. Analysis of Moisture Damage Potential (18).	34
Table 3.1. Test Matrix for Mix Variables.	39
Table 3.2. Properties of Virgin Aggregates.	40
Table 3.3. Gradations for Mt. View Aggregates.....	40
Table 3.4. Gradations for Lithia Springs Aggregates.	41
Table 3.5. Gradations for Camak Aggregates.....	41
Table 3.6. Gradations for Ruby Aggregates.	41
Table 3.7. RAP Gradations.	45
Table 3.8. Asphalt Contents in RAP.....	46
Table 3.9. Gradations for Control Mixes.....	54
Table 3.10. Gradations of Recycled SMA Mix Using DG1 RAP.	54

Table 3.11. Gradations of Recycled SMA Mix Using DG2 RAP.	55
Table 3.12. Gradations of Recycled SMA Mix Using -4 RAP.....	55
Table 3.13. Gradations of Recycled SMA Mix Using +4 RAP.....	55
Table 4.1. Aggregate Properties for Combined Blends.	68
Table 4.2. Analysis of Variance for Aggregate Properties.	68
Table 4.3. Aggregate Properties for RAP Material.....	68
Table 4.4. Average Results for Aggregate Sources.	69
Table 4.5. Average Results for RAP Contents.	69
Table 4.6. Critical Temperatures and Performance Grades of Virgin and Recovered RAP Binders.	70
Table 4.7. Measured Binder Properties of +4 RAP Blends.	71
Table 4.8. Measured Binder Properties of -4 RAP Blends.	71
Table 4.9. Measured Binder Properties of DG1 RAP Blends.....	72
Table 4.10. Measured Binder Properties of DG2 RAP Blends.....	72
Table 4.11. Performance Grades of RAP Blends.	76
Table 4.12. Rate of Increase in $G^*/\sin\delta$ for Unaged Blends.	78
Table 4.13. Rate of Increase in $G^*/\sin\delta$ for RTFO-Aged Blends.....	79
Table 4.14. Rate of Increase in $G^*\sin\delta$ for RTFO and PAV-Aged Blends.	80
Table 4.15. Rate of Increase in Creep Stiffness.....	82
Table 4.16. Rate of Decrease in Creep Rate.	83
Table 4.17. Volumetric Properties of RAP Mixtures.	84
Table 4.18. Virgin and RAP Binder Contents for SMA Mixes.....	85
Table 4.19. Savings in Virgin Binder (%) for RAP Mixtures.	87

Table 4.20. Tensile Strengths for SMA Mixtures.....	88
Table 4.21. Analysis of Variance for Tensile Strengths.	89
Table 4.22. Tensile Strength Comparisons for SMA Mixes with Various RAP Contents.	90
Table 4.23. Tensile Strength Comparisons for SMA Mixes with Various RAP Types. ..	91
Table 4.24. Unconditioned Tensile Strengths Comparisons for Aggregate Source – RAP Type Interaction.....	92
Table 4.25. Conditioned Tensile Strengths Comparisons for Aggregate Source – RAP Type Interaction.....	92
Table 4.26. Moisture Susceptibility Results for Control Mixes.	93
Table 4.27. Moisture Susceptibility Results for SMA Mixes Using +4 RAP.	93
Table 4.28. Moisture Susceptibility Results for SMA Mixes Using -4 RAP.....	94
Table 4.29. Moisture Susceptibility Results for SMA Mixes Using DG1 RAP.....	94
Table 4.30. Moisture Susceptibility Results for SMA Mixes Using DG2 RAP.....	94
Table 4.31. Analysis of Variance for TSR.....	95
Table 4.32. Average TSR Values for Various RAP Contents.	95
Table 4.33. Tensile Strength Ratios Comparisons for RAP Contents.	95
Table 4.34. Rutting Susceptibility Results for RAP Mixtures.....	96
Table 4.35. Analysis of Variance for Rut Depths.....	97
Table 4.36. Average Rut Depths for Various RAP Contents.	97
Table 4.37. Differences in Rut Depth for Aggregate Sources.	97
Table 4.38. Rut Depth Comparisons for RAP Types.....	98
Table 4.39. Rut Depths for RAP Content – RAP Type Interaction.....	100

Table 4.40. m-values for SMA Mixes.	104
Table 4.41. Analysis of Variance for m-value.	105
Table 4.42. m-value Comparisons for Aggregate Sources.	106
Table 4.43. m-value Comparisons for RAP Types.	107
Table 4.44. Test Results for High Strain Beams (800 $\mu\epsilon$).	108
Table 4.45. N_f Comparisons for RAP Contents (800 $\mu\epsilon$).	109
Table 4.46. Effect of RAP Binder on Fatigue Life (800 $\mu\epsilon$).	109
Table 4.47. N_f Comparisons for Aggregate Sources (800 $\mu\epsilon$).	110
Table 4.48. N_f Comparisons for RAP Content – Aggregate Source Interaction	111
Table 4.49. Initial Stiffness Comparisons for Recycled SMA with Various RAP Contents (800 $\mu\epsilon$).	112
Table 4.50. Initial Dissipated Energy Comparisons for RAP Contents (800 $\mu\epsilon$).	113
Table 4.51. Average Test Results for Low Strain Beams.	114
Table 4.52. N_f and Percent Drop Comparisons for RAP Contents (400 $\mu\epsilon$).	115
Table 4.53. Initial Stiffness Comparisons for Aggregate Sources (400 $\mu\epsilon$).	117
Table 4.54. Initial Stiffness Comparisons for RAP Content – Aggregate Source Interaction (400 $\mu\epsilon$).	118
Table 4.55. Fatigue Life Comparisons for Strain Levels.	119

LIST OF FIGURES

Figure 2.1. Distribution of Rut Measurements on SMA Pavements (3).....	7
Figure 2.2. Los Angeles abrasion loss versus change in percent passing 4.75 mm sieve (5).....	10
Figure 2.3. F/E particle content versus change in percent passing 4.75 mm sieve (5).	11
Figure 2.4. Percent passing 4.75 mm sieve versus VMA (5).	12
Figure 2.5. Percent passing 4.75 mm sieve versus VCA (5).	13
Figure 2.6. Example of Superpave high temperature sweep blending charts (8).	17
Figure 2.7. Load Vs. Number of Cycles to Failure in SCB Fatigue Test for PG64-22 Mixtures (17).	30
Figure 2.8. Number of Cycles to Failure in Strain Controlled Beam Fatigue Test (17)..	31
Figure 2.9. Effect of Test Temperature on Indirect Tensile Strength (18).	33
Figure 3.1. Gradations for Mt. View Aggregates.	42
Figure 3.2. Gradations for Lithia Springs Aggregates.....	42
Figure 3.3. Gradations for Camak Aggregates.	43
Figure 3.4. Gradations for Ruby Aggregates.....	43
Figure 3.5. RAP Gradations.....	46
Figure 3.6. Rolling Thin Film Oven (20).....	48
Figure 3.7. Pressure Aging Vessel (20).	49
Figure 3.8. Basics of Dynamic Shear Rheometer (20).	50

Figure 3.9. Schematic of Bending Beam Rheometer (20).....	52
Figure 3.10. Superpave Binder Specification Example (20).	53
Figure 3.11. Gradations for Control Mixes.....	56
Figure 3.12. Gradations of Recycled SMA Mix Using DG1 RAP.....	56
Figure 3.13. Gradations of Recycled SMA Mix Using DG2 RAP.....	57
Figure 3.14. Gradations of Recycled SMA Mix Using -4 RAP.	57
Figure 3.15. Gradations of Recycled SMA Mix Using +4 RAP.	58
Figure 3.16. Indirect Tension Test Creep Compliance Curves (23).	63
Figure 3.17. Prony Series Fit to Master Creep Compliance Curve (23).....	64
Figure 3.18. Determination of m, the Slope of the Log Creep Compliance Curve (23)...	65
Figure 4.1. Critical High Temperatures for Binder Blends.	74
Figure 4.2. Critical Intermediate Temperatures for Binder Blends.	74
Figure 4.3. Critical Low Temperatures for Binder Blends.	75
Figure 4.4. $G^*/\sin\delta$ Trends for Unaged RAP Blends.	77
Figure 4.5. $G^*/\sin\delta$ Trends for RTFO-Aged RAP Blends.....	79
Figure 4.6. $G^*\sin\delta$ Trends for RTFO+PAV-Aged RAP Blends.	80
Figure 4.7. Creep Stiffness Trends for RAP Blends.....	81
Figure 4.8. Creep Rate Trends for RAP Blends.....	83
Figure 4.9. Old to New Asphalt Ratio vs RAP Content.	85
Figure 4.10. Asphalt Contents for SMA Mixtures.....	87
Figure 4.11. Strength Values from Moisture Susceptibility Test.	89
Figure 4.12. Effect of RAP Percentage on Tensile Strength.	90
Figure 4.13. Strength Values for RAP Types.	91

Figure 4.14. Effect of Aggregate Source on Rut Depth.....	98
Figure 4.15. Average Rut Depths for Various RAP Types.....	99
Figure 4.16. Effect of RAP Content on Creep Compliance for Recycled Mixes Using +4 RAP.....	101
Figure 4.17. Effect of RAP Content on Creep Compliance for Recycled Mixes Using -4 RAP	101
Figure 4.18. Effect of RAP Content on Creep Compliance for Recycled Mixes Using DG1 RAP.....	102
Figure 4.19. Effect of RAP Content on Creep Compliance for Recycled Mixes Using DG2 RAP.....	102
Figure 4.20. Creep Compliance Master Curves for RAP Mixtures.....	103
Figure 4.21. Average m-values for RAP Mixtures.....	105
Figure 4.22. Effect of Aggregate Source on m-value.....	106
Figure 4.23. Average m-values for RAP Types.....	107
Figure 4.24. Number of Cycles to Failure for RAP Mixtures (800 $\mu\epsilon$).....	109
Figure 4.25. Effect of Aggregate Source on N_f (800 $\mu\epsilon$).....	110
Figure 4.26. Relationship between Initial Stiffness and Number of Cycles to Failure (800 $\mu\epsilon$).....	112
Figure 4.27. Relationship between Drop in Initial Stiffness at 1,000,000 Cycles and Estimated N_f (400 $\mu\epsilon$).....	115
Figure 4.28. Relationship between Initial Stiffness and N_f (400 $\mu\epsilon$).....	116
Figure 4.29. Effect of Aggregate Source on Initial Stiffness (400 $\mu\epsilon$).....	117
Figure 4.30. Number of Cycles to Failure for High and Low Strain Levels.....	119

CHAPTER 1. INTRODUCTION

1.1 BACKGROUND AND PROBLEM STATEMENT

Economic and environmental considerations have prompted the use of reclaimed asphalt pavement (RAP) in new asphalt mixes. Asphalt pavement is the most recycled product in the United States, both in terms of tonnage (73 million tons, more than any other material) and in terms of percentage (80 percent of reclaimed asphalt pavement is recycled, a higher percentage than any other substance) (1). RAP is used HMA pavement that has been milled up or crushed. It can be used as a constituent in new mixtures, with characteristics similar to those of virgin HMA mixtures. Benefits of using recycled HMA include lower costs, reduced waste and conservation of natural resources.

Although RAP has been successfully incorporated in HMA applications, its use by many agencies has not been extended to the production of open-graded friction courses and stone matrix asphalt (SMA) mixtures. When SMA technology was first implemented in the United States in 1991, there was no experience with the use of RAP in this specialty mixture. Its effect on special requirements for SMA mixes, such as more cubical aggregate and use of polymer-modified asphalt and fiber stabilizers was uncertain, and therefore, its use in SMA mixtures has generally not been allowed.

Based on the success obtained with the incorporation of RAP in conventional mixtures, the use of RAP in SMA mixtures needed to be evaluated. This research

evaluated the effect of RAP on aggregate, asphalt binder and combined mixture properties.

1.2 OBJECTIVES

The objectives of this study were to:

- 1) Evaluate the effect of various RAP contents and sources on combined aggregate properties such as toughness/abrasion, and flat and elongated particles.
- 2) Evaluate the effect of RAP on asphalt binder properties such as dynamic shear and fatigue.
- 3) Determine the feasibility of using SMA mixtures as future RAP sources.
- 4) Evaluate the performance of SMA mixtures containing fractionated RAP and the potential economical benefits of using this type of material.
- 5) Evaluate the effect of various RAP sources of different gradation, asphalt content and aggregate properties on the overall performance of SMA mixtures.

1.3 SCOPE OF STUDY

To accomplish the aforementioned objectives, this study started with a literature search and review of the information pertaining to the design of SMA mixtures and mixtures containing RAP and their performance. Based on the results of the literature study, a research plan was developed involving extensive laboratory testing, which included performing mix designs for different aggregate sources, RAP types and RAP proportions. For each blend, aggregate properties were determined, as well as optimum asphalt

content and volumetric properties. Performance tests were conducted to evaluate the mixtures at different RAP levels. A blend with no RAP was used as a baseline for the study for comparisons of mix performance.

CHAPTER 2. LITERATURE REVIEW

2.1 INTRODUCTION

Several projects have studied the use of SMA mixes in the United States. Results have shown that the same benefits found in European mixes can be obtained with local materials and procedures. However, many specifications for material properties, gradation and volumetrics needed to be modified, and in some cases new requirements were developed.

Use of RAP in HMA applications has also been widely investigated. Inclusion of RAP in HMA mixes has been shown to have not only economic and environmental benefits, but also in some cases it has improved performance. Combining RAP with virgin materials may affect mixture properties, and therefore it has been necessary to develop guidelines for the design of mixtures containing RAP. Performance tests conducted on recycled mixtures indicate that for the most part, they have been found to perform as well as virgin mixtures if properly accounted for in the mix design.

2.2 REVIEWS

1. Summary of Georgia's Experience with Stone Matrix Asphalt Mixes by GDOT (2)

This report summarizes the results of various research projects conducted by GDOT to assess the viability of using SMA mixes on the Georgia road system. Research Project No. 9102 evaluated the performance of SMA asphalt under stresses of heavy truck loadings and compared it to the performance of conventional GDOT mixes. Research Project No. 9202 evaluated the use of SMA as an overlay for Portland cement concrete (PCC) pavements. Both projects used the 50-blow Marshall Mix Design procedure, which is used in the design of European SMA.

In Project No. 9102, coarse and fine SMA mixes were designed for use as intermediate layers and wearing courses, respectively. The mixes were placed in a 2.5-mile, high traffic volume test section on Interstate 85 northeast of Atlanta. Following the construction of the I-85 test section in 1991, rutting measurements were conducted between 1993 and 1995 to monitor rutting in the fine SMA and conventional mixes. The results indicated that SMA mixes exhibited significantly less rutting than conventional mixes (Table 2.1).

Table 2.1. Rutting of Fine SMA vs. Standard Hot Mix: I-85 Test Section (2).

Year	SMA (mm)	Standard (mm)
1993	0	3.0
1994	2.3	5.3
1995	2.5	6.8

The test section on I-85 was also used to monitor the friction provided by SMA mixes. Results indicated that the thick asphalt film in SMA mixes did not affect frictional properties, since the thicker film wears quickly at the surface (Table 2.2).

Table 2.2. Friction Values for Fine SMA Mix: I-85 Test Section (2).

Friction Number	
Date	Number
11/91	42
2/92	50
1/96	50

A mix optimization research study was conducted in a joint study with Georgia Tech to learn more about methods of enhancing SMA performance. Findings from this study showed that GDOT fine SMA mixes undergo at least 30% to 40% less rutting than a typical GDOT dense-graded surface mix, and these fine SMA mixes typically have a fatigue life of 3 to 5 times that of a conventional surface mix.

The study also indicated that by relaxing the aggregate quality requirements for SMA mixes important production cost savings could be realized without significantly reducing the performance of the mixes. In Europe, aggregate quality requirements for SMA mixes are typically very rigorous. Based on this research, GDOT implemented use of aggregates which have no more than 45% abrasion loss and which have no more than 20% flat and elongated particles when measured at the 3:1 ratio.

Based on the combination of GDOT and European experience, SMA has proven to have the following intrinsic benefits:

- 30-40% less rutting than standard mixes
- 3 to 5 times greater fatigue life in laboratory experiments

- 30-40% longer service life
- Lower annualized cost

2. Performance of Stone Matrix Asphalt (SMA) Mixtures in the United States by Brown et al. (3)

This report provides a summary of mix design and performance data obtained between 1994 and 1996 from 86 SMA projects involving a total of 140 test sections in 19 different states. All mixtures were designed using the 50-blow Marshall procedure and used a stabilizer (or special asphalt binder) to prevent draindown of the asphalt cement. In most cases, a fiber (cellulose or mineral) or a polymer was used as the stabilizer.

The various SMA mixtures were inspected to determine performance. The study indicated that over 90% of the projects had rutting measurements less than 4 mm. Approximately 25% of the projects had no measurable rutting (Figure 2.1).

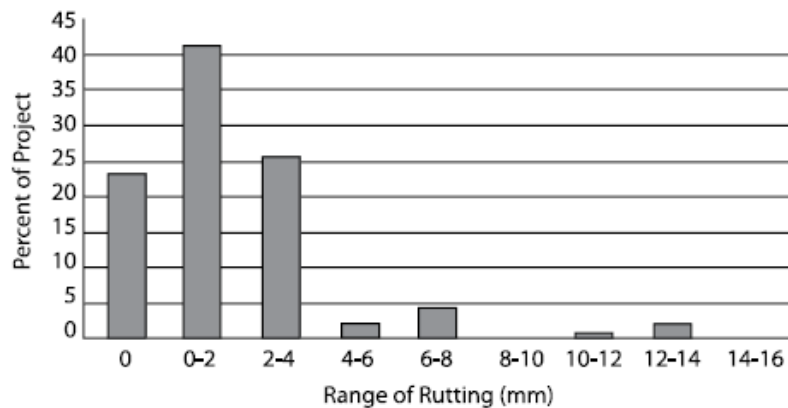


Figure 2.1. Distribution of Rut Measurements on SMA Pavements (3).

Cracking (thermal and reflective) did not represent a significant problem. SMA mixtures appeared to be more resistant to cracking than dense mixtures, most likely due

to the relatively high asphalt content and its resulting high film thickness. There was no evidence of raveling, and the biggest performance problem was the occurrence of fat spots, which is caused by segregation, draindown, high asphalt content or improper type or amount of stabilizer.

The study concluded that SMA mixtures provided good performance in high traffic volume areas and that the increased benefits should compensate for the extra cost of construction.

3. Updated Review of Stone Matrix Asphalt and Superpave Projects by Watson (4).

A second study (4) was conducted in September 2001 to evaluate long-term performance on some of the same SMA projects studied by Brown et al. The survey found that SMA mixtures had given exceptional rut-resistant performance, even when placed on high-traffic volume routes. Only one out of the 11 projects visited exhibited rutting in excess of 6 mm.

Only one project had significant block-type cracking, believed to be caused by the stiff binder. The biggest long-term performance problem was transverse, reflective cracking. However, this problem appeared to be related to the use of SMA as a thin-lift overlay of PCC pavements. Comparisons between SMA mixes and conventional sections indicated that SMA mixtures may significantly reduce the rate of crack propagation when used as an overlay for concrete pavements.

The fat spots, noted as the major performance problem in the original study (2) had been worn off by traffic over time and were not noticeable during the 2001 review. In

general, several projects were still in excellent condition after 9 years of service and based on an overall project condition rating, SMA mixes can be expected to last up to 25% longer than conventional mixes.

4. Development of a Mixture Design Procedure for Stone Matrix Asphalt (SMA) by Brown et al. (5).

This study developed a mixture design procedure for SMA and evaluated material and mixture criteria for these mixes. Data were collected from a laboratory study conducted with various types of aggregates, fillers, asphalt binders and stabilizing additives. Parameters evaluated included aggregate toughness, flat and elongated particles, aggregate gradation, volumetric mix properties, asphalt binder content, compactive effort and asphalt binder draindown. Results indicated that there was a good correlation between aggregate breakdown and aggregate toughness as measured by the Los Angeles abrasion test for both Marshall ($R^2 = 0.62$) and SGC ($R^2 = 0.84$) compaction, as seen in Figure 2.2.

To evaluate the effect of flat and elongated particles, mixtures were prepared with 0%, 25%, 50%, 75% and 100% flat and elongated aggregate. Samples were compacted with 50 blows of the Marshall hammer and aggregate breakdown was measured. Figure 2.3 shows that increased F/E particle content increases aggregate breakdown ($R^2 = 0.89$).

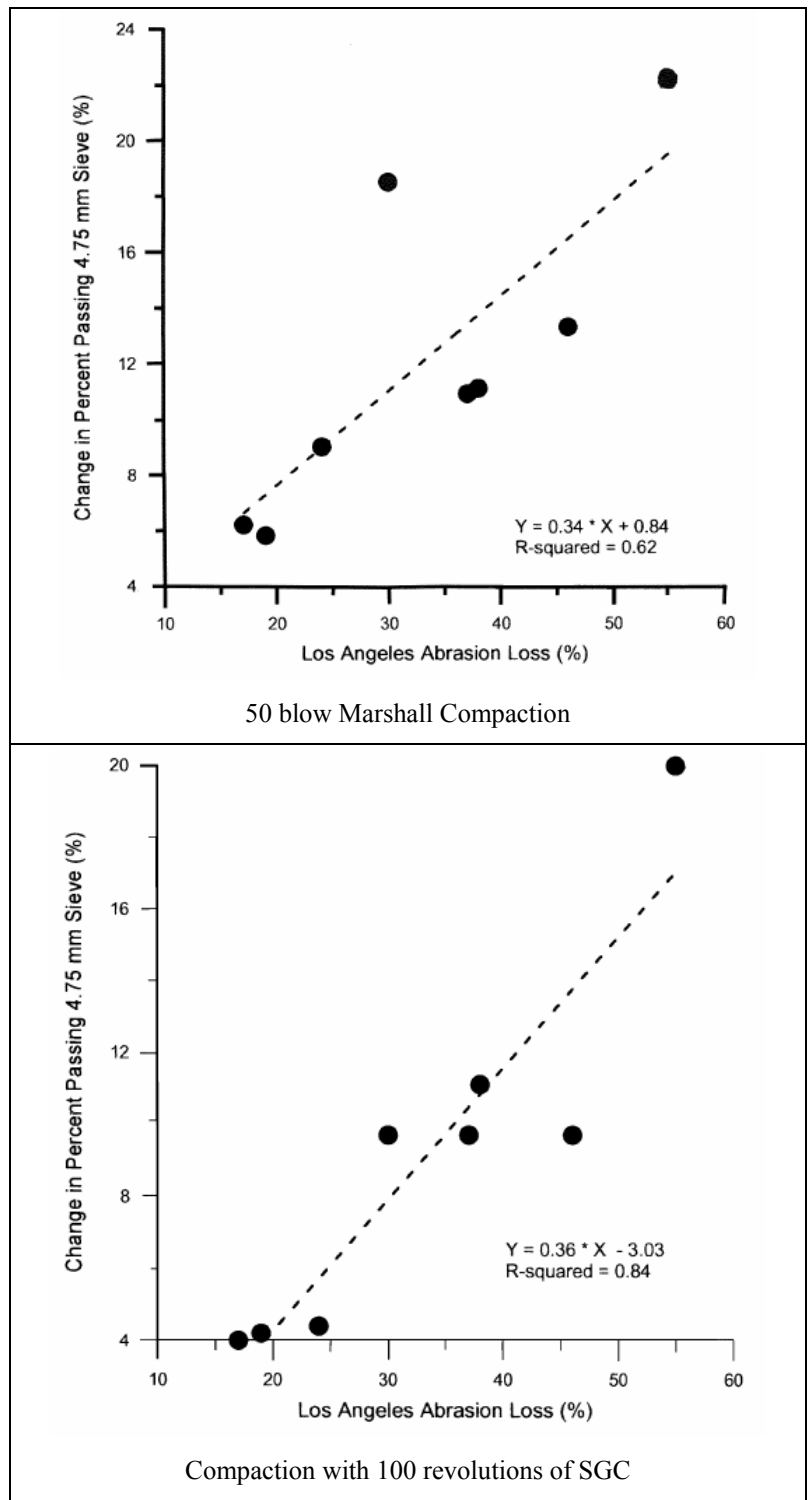


Figure 2.2. Los Angeles abrasion loss versus change in percent passing 4.75 mm sieve (5).

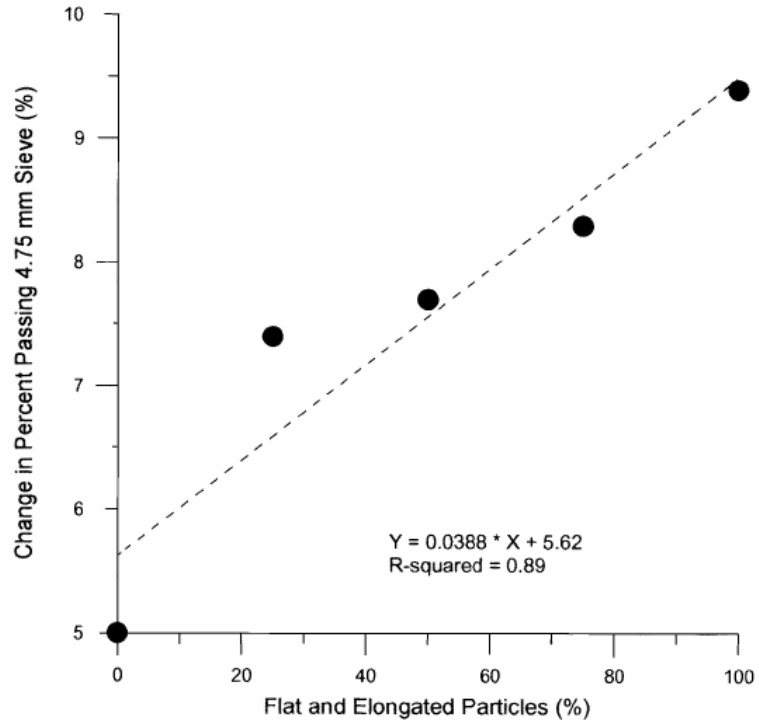


Figure 2.3. F/E particle content versus change in percent passing 4.75 mm sieve (5).

Increased aggregate breakdown resulted in lower VMA. High Los Angeles abrasion values (40% or higher) make meeting the VMA requirements and ensuring a reasonable high asphalt content more difficult. Figure 2.4 shows the change in VMA with change in percent passing the 4.75 mm sieve. As the percent passing the 4.75 mm sieve decreases, the VMA remains nearly constant, and then begins to increase once the percent passing the 4.75 mm sieve reaches 30-40 percent. The point at which the VMA begins to increase defines the condition at which stone-on-stone contact begins to develop. To ensure the formation of stone-on-stone contact, the percent passing the 4.75 mm sieve should be kept below 30 percent.

The presence of an adequate aggregate skeleton can also be verified by measuring the voids in the coarse aggregate (VCA) of the mix. Figure 2.5 shows that as the percent passing the 4.75 mm sieve decreases, the VCA of the mix also decreases. At

approximately 30 percent passing the 4.75 mm sieve, the slope of the curve begins to decrease slightly, setting the point at which stone-on-stone contact begins to develop.

The design air void range should be kept between 3 and 4 percent. To minimize fat spots and rutting, the air voids in warmer climates should be designed closer to 4 percent. Also, use of polymer modified asphalt produced better rut resistant mixes, while fiber stabilizers were superior in preventing draindown. A combination of stabilizers may provide the best properties in SMA mixes.

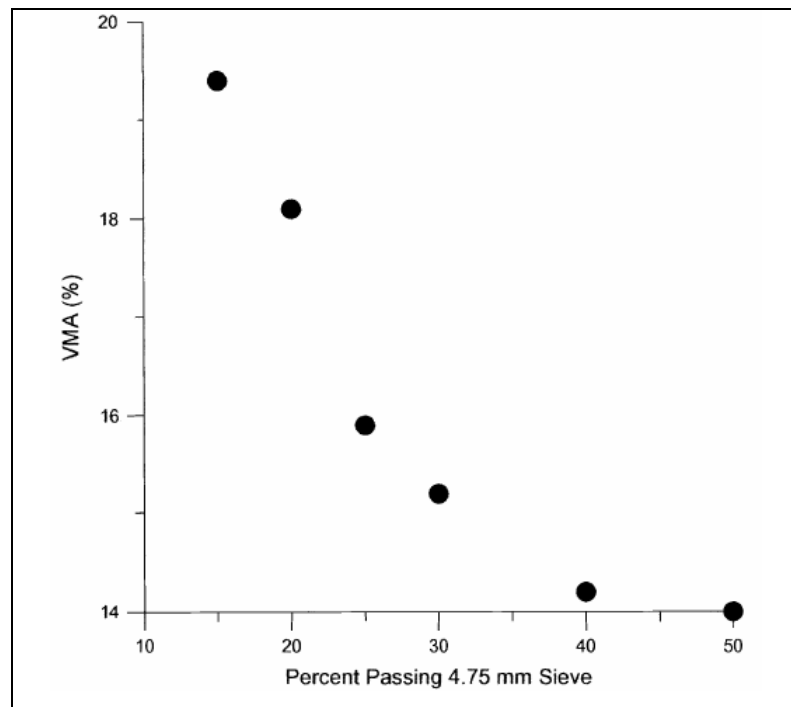


Figure 2.4. Percent passing 4.75 mm sieve versus VMA (5).

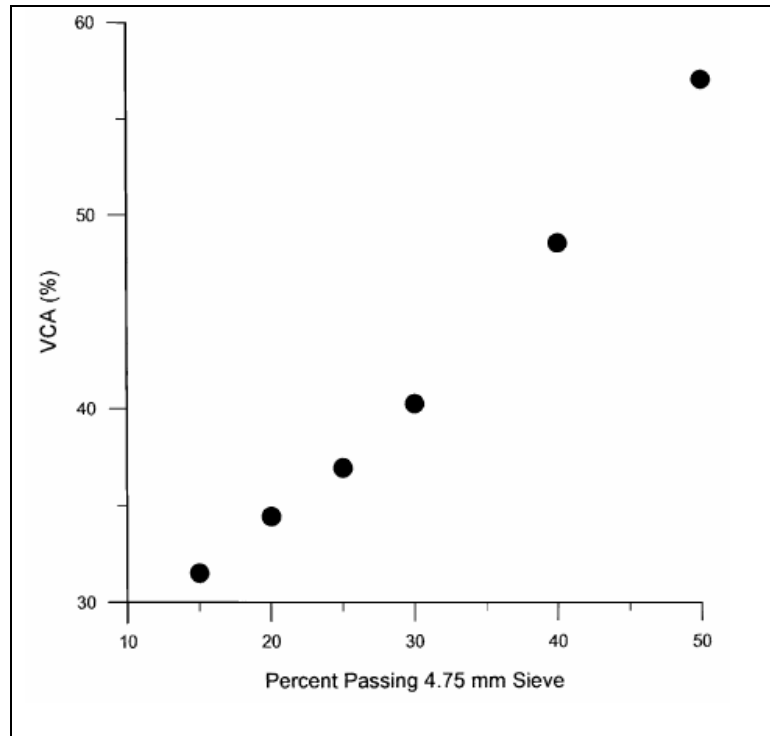


Figure 2.5. Percent passing 4.75 mm sieve versus VCA (5).

5. NCHRP Project 9-12 (6).

Research for Project 9-12, *Incorporation of Reclaimed Asphalt Pavement in the Superpave System*, was conducted in three separate, but related, studies:

Black Rock Study

The objective of this study was to determine whether RAP acts like a black rock or whether some blending occurs between the old and new binders. Three cases simulating possible interactions between the old and new binders were studied to investigate the behavior of RAP blends. Black Rock (BR) samples were made using virgin and recovered RAP aggregate with virgin binder (no RAP binder). Actual Practice (AP) samples were made using virgin binder and aggregate, mixed with RAP with its binder film intact. Total Blending (TB) samples were made using virgin and recovered RAP

aggregate. RAP binder was recovered, then blended with virgin binder in the specified percentages before mixing. All the samples were prepared on the basis of an equal volume of total binder.

Three different RAPs, two different virgin binders, and two RAP contents (10 and 40 percent) were investigated in this primary phase of the project. The different cases of blending were evaluated through the use of various Superpave shear tests at high temperatures and of the indirect tensile creep and strength tests at low temperatures. Results indicate that even though there is no significant difference at low RAP contents, RAP does not act like a black rock, and blending of the old and new binders occurs to a significant extent. This means that at high RAP contents the hardened RAP binder must be accounted for in the virgin binder selection.

Binder Effects Study

This study investigated the effects of RAP content and stiffness on the blended binder properties. The same three RAPs and two virgin binders were evaluated in this phase of the project at RAP binder contents of 0, 10, 20, 40, and 100 percent. The blended binders were tested according to the AASHTO MP1 binder tests. The response variables for the experiment were the individual test results and critical temperatures determined at high and intermediate temperatures from the Dynamic Shear Rheometer (DSR) tests and at low temperatures from the BBR tests. The specific parameters studied were complex shear modulus (G^*) and phase angle (δ) from the DSR and stiffness and m-value from the BBR.

It was found that at low RAP contents, the effects of the RAP binder are negligible. At intermediate RAP contents, these effects can be compensated for by using

a virgin binder that is one grade softer on both the high- and low- temperature grades. Higher RAP contents require the use of blending charts to determine the appropriate virgin binder grade.

Mixture Effects Study

This study investigated the effects of RAP on total mixture properties. Shear tests and indirect tensile tests were conducted to assess the effects of RAP on mixture stiffness at high, intermediate, and low temperatures. Beam fatigue testing was also conducted at intermediate temperatures. RAP contents of 0, 10, 20, and 40 percent were evaluated.

The tests indicated that high RAP contents increase the mixture stiffness, and therefore, a softer virgin binder must be used to improve the fatigue and low-temperature cracking resistance of the mixture.

6. Laboratory Investigation of Mixing Hot-Mix Asphalt with Reclaimed Asphalt Pavement by Huang et al. (7).

This study analyzed the blending process of RAP with virgin mixture. One type of screened RAP consisting only of –No. 4 particles was blended with virgin coarse aggregate at different percentages, and binder rheological tests were performed to characterize properties of binders at different layers of aggregate particle coating.

An extreme case was evaluated by mixing RAP and virgin aggregates without any new asphalt binder. The objective was to find out to what extent the aged asphalt will “get away” from the RAP particles under pure mechanical mixing. Results indicated that only a small proportion of the aged binder would be available to blend with the virgin binder.

A blended mixture containing 20% RAP and PG 64-22 binder was used to simulate actual plant mixing. The mixture was subjected to staged extraction and recovery by soaking it in trichloroethylene solution for 3 minutes and then decanting the solution, repeating the process several times. This process allowed the formation of different layers of asphalt around the RAP particles. Results showed that the influence of RAP on the virgin binder was very limited. Only a small portion of RAP asphalt participated in the remixing process; other portions formed a stiff coating around RAP aggregates, and RAP acted as a “black rock”.

7. Designing Recycled Hot-Mix Asphalt Mixtures Using Superpave Technology by Kandhal and Foo (8).

This project developed a procedure for selecting the performance grade (PG) of virgin asphalt binder in a recycled HMA mixture based on the Superpave PG grading system. Blending charts were constructed and evaluated based on test parameters obtained from the dynamic shear rheometer (DSR) and therefore, only high and intermediate test temperatures were considered. Two blending charts were used to determine the high temperature value of recycled asphalt binder. The first high temperature sweep blending chart determined the temperature at which $G^*/\sin\delta$ of the unconditioned recycled asphalt binder is 1.0 kPa. The second high temperature sweep blending chart determined the temperature at which $G^*/\sin\delta$ of RTFO residue of the recycled asphalt binder is 2.2 kPa. The high temperature value of the recycled asphalt binder is defined as the lower temperature value given by these two high temperature sweep blending charts. The

intermediate temperature sweep blending chart determined the temperature at which $G^*/\sin\delta$ of RTFO+PAV residue of the recycled asphalt binder is 5 MPa.

These charts indicated a linear relationship between the logarithm of binder shear stiffness (expressed as $G^*/\sin\delta$) and percent of virgin asphalt in a virgin and RAP binder blend, as shown in Figure 2.6.

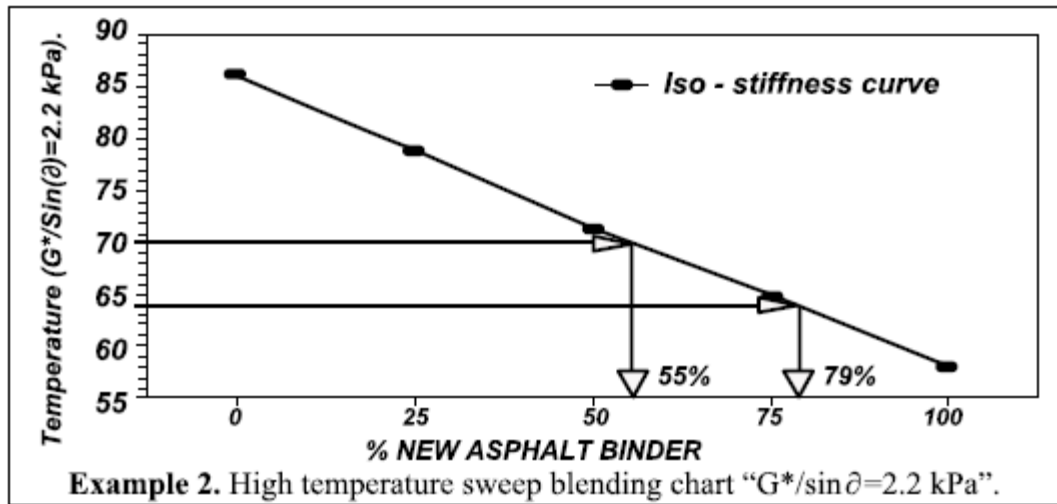
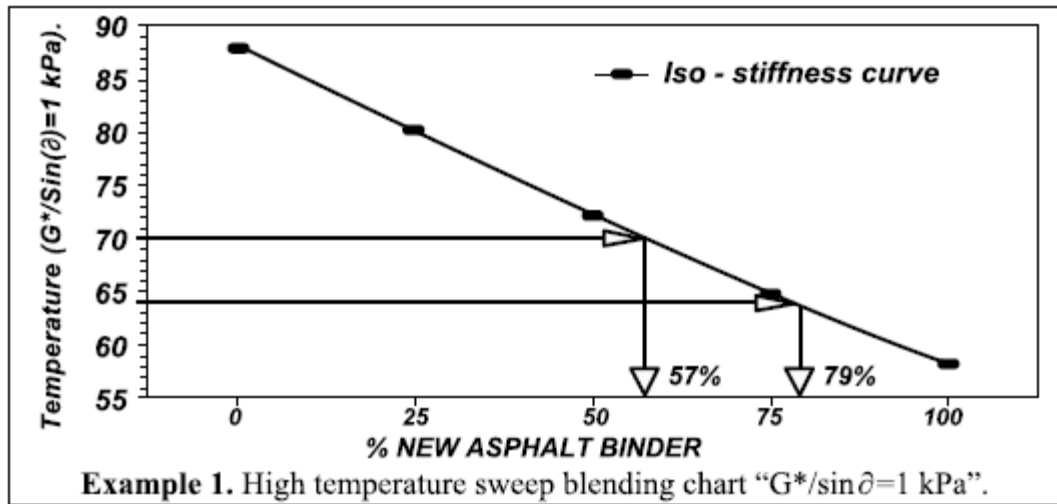


Figure 2.6. Example of Superpave high temperature sweep blending charts (8).

The following recommendations were made for proper selection of PG asphalt binder:

- High temperature value of the recycled asphalt binder performance grade can be determined by using only one high temperature sweep blending chart. High temperature sweep blending chart “ $G^*/\sin \delta = 1.0 \text{ kPa}$ ” is recommended over high temperature sweep blending chart “ $G^*/\sin \delta = 2.2 \text{ kPa}$ ” because it does not require running the RTFO test.
- Although the intermediate temperature sweep blending chart “ $G^*\sin\delta = 5 \text{ MPa}$ ” was expected to determine the maximum amount of RAP, it allowed unusually high percentages of RAP, which are inconsistent with the field experience with recycled HMA. Use of the intermediate temperature sweep blending chart is not recommended at the present time.
- A three-tier system of selecting the PG grade of the virgin asphalt binder was recommended for recycled mixes:

Tier 1: If the amount of RAP in the HMA mix is equal to or less than 15%, the selected PG grade of the virgin asphalt binder should be the same as the Superpave specified PG grade.

Tier 2: If the amount of RAP in the HMA mix is more than 15% but equal to or less than 25%, the selected PG grade of the virgin asphalt binder should be one grade below (both high and low temperature grade) the Superpave specified PG grade. The use of a specific grade blending chart to select the high temperature grade of the virgin asphalt binder is optional.

Tier 3: If the amount of RAP in the HMA mix is more than 25%, use the specific grade blending chart to select the high temperature grade of the virgin asphalt binder. The low temperature grade should be at least one grade lower than the binder grade specified by Superpave.

8. Guidelines for the Design of Superpave Mixtures Containing Reclaimed Asphalt Pavement (RAP) by Bukowski (9).

This guideline was developed by the FHWA Superpave Mixtures Expert Task Group and outlines the proper means for incorporating RAP in Superpave mixtures. It suggests that aggregate and asphalt binder in the RAP should be considered as part of the aggregate and asphalt binder contents of the total mix, respectively. Also, all aggregate requirements for the aggregate blend must be satisfied.

Asphalt binder grade must be adjusted depending upon the amount of RAP included in the mixture, according to the following three categories:

Tier 1: Up to 15% RAP by weight of total mixture

Tier 2: 16% to 25% RAP by weight of total mixture

Tier 3: Above 25% RAP by weight of total mixture

Tier 1 does not require any modification of the mix design process, and the selection of the grade of virgin asphalt binder is based on typical requirements for climatic conditions and predicted traffic. Determination of asphalt binder content in RAP is left to the discretion of the agency. Tier 2 requires determination of the asphalt binder content in the RAP. For Tier 3, the grade of virgin asphalt binder is either set to one grade lower than that usually selected for given climatic conditions, or selected from a blending

chart. Table 2.3 summarizes the tests required on the RAP and selection of asphalt binder grade.

Table 2.3. Procedures for the Design of Mixtures Containing RAP (9).

Tier	Determine RAP AC Content	Measure RAP Gradation	Measure RAP AC Stiffness	Measure Agg Blend Properties	PG Grade Change
1	(a)	x	no	x	none
2	x	x	no ^(b)	x	one grade lower ^(c)
3	x	x	yes	x	use blending chart

^(a) At the discretion of the agency

^(b) Unless blending chart is used

^(c) Or use blending chart

9. Effect of Reclaimed Asphalt Pavement on Binder Properties Using the Superpave System by Kennedy et al. (10).

In this study, rheological properties were measured for different combinations and percentages of aged asphalts and virgin asphalts. It includes test results from Superpave binder tests conducted on unaged binders at the high-temperature range, as well as test results on blends aged using the rolling thin film oven test (RTFOT) and pressure aging vessel (PAV) conducted at high-, low-, and intermediate-temperature ranges.

Six asphalts were chosen from the Material Reference Library (MRL) for this experiment. Two of the binders were chosen arbitrarily to be aged to simulate RAP binder and then combined with the four virgin binders at different percentages (0, 15, 25, 55 and 100%). Engineering characteristics of the virgin-RAP blends were determined with the aid of a dynamic shear rheometer (DSR) and a bending beam rheometer (BBR).

The result of this study is a methodology for determining the effect of RAP on rheological properties of PG binders in the Superpave system. Specific conclusions drawn from this study include:

- The stiffness of the binder is higher at higher percentages of RAP binder.
- The rate of change of stiffness ($G^*/\sin \delta$, $G^*\sin \delta$, or creep stiffness) is either constant from 0–100% RAP binder or increases with lower temperatures.
- The rate of change of stiffness is either constant from 0–100% RAP or increases at higher percentages of RAP in the blend.

10. Determination of Recycled Asphalt Pavement (RAP) Content in Asphalt Mixes Based on Expected Mixture Durability by Abdulshafi et al. (11).

This study developed a method to evaluate the effects of RAP content on long-term durability of a bituminous concrete mixture, which may be used to select an optimum RAP content. The procedure includes preparation of test specimens at different levels of RAP addition. Each set of specimens is divided into two subsets to be tested for indirect tensile strength; one is tested in dry condition and the other is subjected to vacuum saturation, followed by a freeze cycle and warm water soaking prior to testing. During the testing, load and deformation data are continuously collected, and the resultant energy needed to fail a specimen is calculated. Numerical indices of absorbed energy are computed from the test data obtained for the dry and conditioned subsets of specimens. The mix that has the greatest index of absorbed energy is selected as having the optimum RAP content.

11. Recycled Asphalt Pavement (RAP) Effects on Binder and Mixture Quality by Li et al. (12).

This study investigated the effect of various types and percentages of RAP on asphalt binder and asphalt mixture properties. Ten mixtures were prepared using two asphalt binders (PG58-28 and PG58-34) and two RAP sources, identified as follows:

- Millings – RAP from a single source, milled up from I-494 in Maple Grove
- RAP – RAP combined from a number of sources and crushed at the HMA plant.

In addition to the control mixtures, asphalt mixtures were prepared with 20% and 40% of each of the RAP sources. The dynamic modulus proposed by the recent AASHTO design guide was used to determine the effect of various percentages of RAP on mixture properties. Stiffness and moisture susceptibility results were also used to determine the effect of RAP on the asphalt mixture properties.

From the complex modulus test results, it was observed that addition of RAP to a mixture generally increased the complex modulus and mixture stiffness. However, this does not always occur at low temperatures. Asphalt binder grade and RAP source had a significant effect on mixture stiffness. The complex modulus for the mixtures made with PG 58-28 asphalt binder was always higher than that from the mixtures made with a softer PG 58-34 asphalt binder. Also, addition of the millings led to a larger increase in stiffness than the similar addition of RAP. Mixtures containing RAP showed significant variability and the variability increased with the increase in RAP content.

The IDT creep test was performed at temperatures of -18°C and -24°C. Results indicated that generally stiffness increases as the percentage of RAP or millings increases. The mixtures with PG 58-34 binder were softer than the mixtures with PG 58-

28 binder. For the mixtures with PG 58-28 binder, as the percentage of RAP or millings increased, the IDT strength increased, while the mixtures with PG 58-34 binder did not show the same trend. Moisture susceptibility test data indicated that as the percentage of RAP increased the strength also increased, while the tensile strength ratio decreased.

Binder tests showed that the addition of RAP improved the binder grade in terms of high temperature performance, while the low temperature performance did not change significantly except for the case when 40% RAP was added, meaning that the resulting binder blends would be more resistant to rutting and equally resistant to thermal cracking compared to virgin binders. The tests on the binders indicated that using 20% RAP in asphalt mixtures does not significantly affect the performance. RAP amounts of 40% have a significant effect on the performance of the mixtures.

12. Use of Reclaimed Asphalt Pavement in Superpave Hot-Mix Asphalt Applications by Stroup-Gardiner and Wagner (13).

This research evaluated the effectiveness of screening RAP stockpiles into coarse and fine fractions. This practice was found to maximize the use of RAP and produce a range of HMA mixtures that meet Superpave requirements.

The coarser fraction was used in a typical 12.5 mm below-the-restricted-zone Superpave gradation, while the finer fraction was used in a 12.5 mm above-the-restricted-zone gradation. Screening the RAP increased uniformity in coarser aggregate fractions and allowed up to 40 percent of this material to be used and still meet below-the-restricted-zone Superpave gradation requirements by reducing the amount of finer

aggregate fractions, especially the minus 0.075 mm material. The use of RAP in these mixtures reduced neat asphalt requirements by 18 to 33 percent.

The use of the finer RAP fraction in above-the-restricted-zone Superpave gradations resulted in a reduction in neat asphalt of about 25 percent. Addition of this material decreased rutting potential and temperature susceptibility. However, the amount of material to be used was limited to a maximum of 15 percent in order to meet above-the-restricted-zone gradation requirements.

13. Mechanistic and Volumetric Properties of Asphalt Mixtures with Recycled Asphalt Pavement by Daniel and Lachance (14).

This research examined how the addition of RAP changes the volumetric and mechanistic properties of asphalt mixtures. Two RAP sources, a processed RAP and an unprocessed RAP (grindings), were used to study the change in volumetric properties and one RAP source was used for dynamic modulus and creep testing. A control mixture containing only virgin materials (0% RAP) was tested along with mixtures containing 15, 25 and 40% RAP.

The volumetric properties of the different mixes are shown in Table 2.4. For the processed RAP mixtures, the VMA and VFA values for the 25% and 40% RAP contents were higher than those for the control and 15% mixtures. For the grindings RAP mixtures, the VMA values increase with RAP content and the VFA values for all mixtures are higher than for the control mix. It is hypothesized that this difference is due to the extent of blending of the RAP material with the virgin materials.

Table 2.4. Mix Design Parameters (14).

	Control	Processed			Grindings		
		15% RAP	25% RAP	40% RAP	15% RAP	25% RAP	40% RAP
% AC	4.8	5.1	5.4	4.9	4.9	5.2	5.2
Gmm	2.451	2.483	2.445	2.466	2.452	2.460	2.475
VMA	13.1	13.3	16.3	15.2	13.8	14.3	14.7
VFA	69.4	69.9	75.4	73.6	71.8	71.0	73.0
DP	1.14	1.10	0.88	1.02	0.91	0.75	0.75

% AC = asphalt content; Gmm = maximum theoretical specific gravity; DP = dust proportion.

The study also indicated that there is an optimal preheating time for RAP to allow the particles to soften, break down, and blend with the virgin materials. At 15% RAP, the stiffness of the mixture increased and the compliance decreased, which indicates that the mixture will be more resistant to permanent deformation and less resistant to fatigue and thermal cracking, due to the addition of aged binder contained in the RAP. However, mixtures containing 25 and 40% RAP did not follow the expected trends and behaved similar to the control mixture. A combination of gradation, asphalt content and volumetric properties is likely the cause of these trends.

14. Five Year Experience of Low-Temperature Performance of Recycled Hot Mix by Tam et al. (15).

This project investigated the relative resistance of recycled hot mixes to thermal cracking, as compared to conventional mixes. Two criteria were used: limiting stiffness and fracture temperature (FT). Materials were selected from five recycling contracts covering different regions, virgin asphalt cements, and recycling ratios.

Direct tension tests were performed at different temperatures to determine the tensile strengths, strains, and stiffnesses of the different mixtures. Results indicated that when using the limiting stiffness approach, the recycled mixes had higher stiffness values

than the conventional mix, which would translate into higher thermal cracking susceptibility. Thermal contraction was used to estimate the induced strain due to thermal shrinkage under a restrained condition. In this case, only one mixture had a fracture temperature below the FT of the virgin mix, confirming the findings from the direct tension tests.

Results from field data and laboratory tests revealed that mixes with low RAP content or high penetration virgin asphalt cement had better performance than those with high RAP content or using low penetration virgin asphalt cement. It was also found that fracture temperature, stiffness and viscosity increased with aging of the pavement, reducing its resistance to low temperature cracking.

15. Investigation of Properties of Plant-Produced RAP Mixtures by McDaniel et al. (16).

This experiment examined the influence of RAP content in the mixture and recovered binder properties of plant-produced hot mix asphalt. For low temperature properties the plant-produced mixtures were tested for creep compliance and tensile strength. For high temperature properties the mixtures were tested for dynamic modulus ($|E^*|$). The virgin and recovered RAP binders were also tested for complex shear modulus (G^*). Three percentages of RAP were added (15%, 25% and 40%) using two binder grades (PG64-22 and PG58-28).

Indirect tensile strength results showed that, in general, mixtures with higher strength also showed higher stiffness values. Mixtures with lower stiffness values have a better ability to relax the thermal stresses that develop as the pavement cools. In addition,

high strength is also required to resist cracking by traffic loads. Table 2.5 shows that the mixture with the highest RAP content (Mixture D) had the highest strength and stiffness; hence, the warmest critical temperature (T_c). Mixture E with the lowest strength also had the lowest stiffness and a low T_c value. Mixtures with the softer binder (PG58-28) showed lower strengths at a given RAP content than the corresponding mixtures with PG64-22, as expected.

Table 2.5. Strength, Stiffness and Critical Pavement Temperature of the Mixes (16).

Mixture	RAP %	Binder	Strength (kPa)				Stiffness (GPa)	T_c (°C)
			Rep1	Rep2	Rep3	Avg.		
A	0	PG64-22	3284	3393	2785	3154	14.7	-28.9
B	15	PG64-22	3359	3525	2831	3238	17.3	-23.3
C	25	PG64-22	3498	3245	3150	3298	17.7	-25.6
D	40	PG64-22	4056	4165	3390	3870	19.2	-22.8
E	25	PG58-28	3153	3143	2413	2903	13.1	-27.2
F	40	PG58-28	3272	3370	2988	3210	16.1	-23.9

16. Laboratory Study of Fatigue Characteristics of HMA Mixtures Containing RAP by Huang et al. (17).

This project evaluated the laboratory fatigue characteristics of asphalt mixtures containing RAP. A typical surface mixture commonly used in the state of Tennessee was evaluated at 0, 10, 20 and 30 percent of No. 4 sieve screened RAP materials. One type of aggregate (limestone) and two types of asphalt binders (PG64-22 and PG76-22) were considered in this study. Fatigue characteristics of mixtures were evaluated through indirect tensile strength (IDT), beam fatigue, and semi-circular fatigue tests (SCB). These three tests represented three different test modes: indirect tensile at monotonic loading, SCB at cyclic constant stress, and third-point beam at cyclic constant strain. Half of the specimens were subjected to laboratory long-term aging prior to performance tests.

The indirect tensile stress (ITS) and strain test was used to determine the tensile strength and strain of the mixtures. This test was conducted at 25°C and a 2 inch/min deformation rate. The toughness index (TI), a parameter describing the toughening characteristics in the post-peak region, was also calculated from the indirect tensile test results. The TI compares the performance of a specimen with that of an elastic perfectly plastic reference material, for which the TI remains a constant of 1. For an ideal brittle material with no post-peak load carrying capacity, the value of TI equals zero. In this study, the values of indirect tensile toughness index were calculated up to tensile strain of one percent.

Results from the IDT test revealed that increasing the percentage of screened RAP materials generally increased the tensile strengths, and decreased toughness indices for both un-aged and aged mixes. Increasing RAP percentages had significantly different effects in IDT properties for mixtures with PG64-22 than those with PG76-22, especially for the mixtures subjected to laboratory long-term aging. As shown in Table 2.6, the increase of RAP had more tensile strength gains (about 5 to 10% greater for PG64-22 mixtures), no (or less) tensile strain loss at failure (1% smaller for the PG64-22 mixture at 30% RAP content), and less decrease in post-failure toughness index (9.8 to 24.3% less for PG64-22 mixtures), suggesting that the recycled mixes would have an increased fatigue life.

Table 2.6. Change of IDT Properties for Long-Term Aged Mixture (17).

IDT Properties	Tensile Strength Change, %		Strain at Failure Change, %		Toughness Index Change, %	
	PG76-22	PG64-22	PG76-22	PG64-22	PG76-22	PG64-22
AC						
%RAP						
10	4.94	10.9	2.14	9.41	-13.6	-3.82
20	12.2	17.1	-9.57	4.38	-34.5	-11.9
30	18.82	28.9	-12.3	-11.3	-45.0	-20.7

Note: The values in the table indicated the increase or decrease of properties relative to the control mix (with 0% RAP).

In the SCB fatigue test, the inclusion of RAP generally increased the fatigue life of the mixtures in this study, as well as the total dissipated energy. Long-term aging also increased fatigue life. For mixes subjected to long-term aging, the slope of fatigue curves in load versus $\log(N_f)$ increased significantly when the RAP increased to 30 percent, which indicated potential lower fatigue life for these mixes at lower stress levels (Figure 2.7).

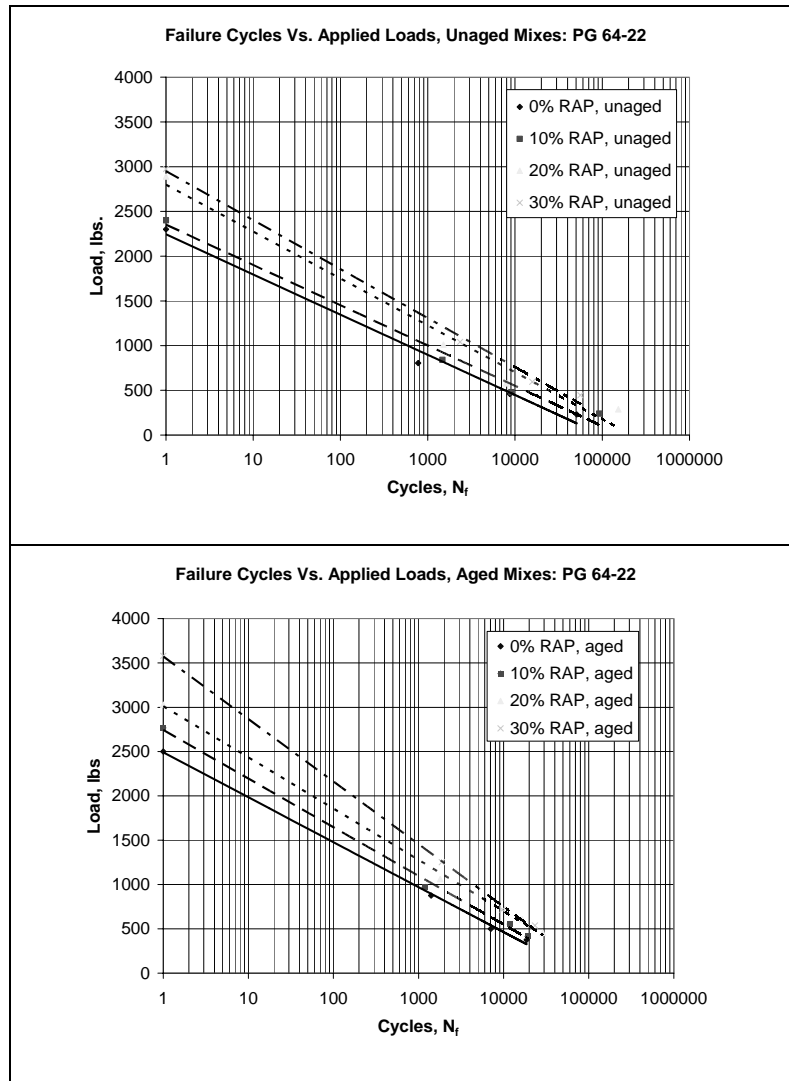


Figure 2.7. Load Vs. Number of Cycles to Failure in SCB Fatigue Test for PG64-22 Mixtures (17).

Results from beam fatigue tests indicated that the inclusion of RAP generally increased the flexural stiffness of the mixtures. Fatigue life as defined by AASHTO TP8-94 generally increased with the increase of RAP percentages. The percentage of increase in fatigue life is more significant for long-term aged mixtures with PG64-22 asphalt (up to 1.8 higher than the virgin mix) than those with PG76-22 (up to 0.6 times higher than

the virgin mix). For mixtures with PG76-22 asphalt, without long-term aging, the fatigue life decreased with the inclusion of RAP (Figure 2.8).

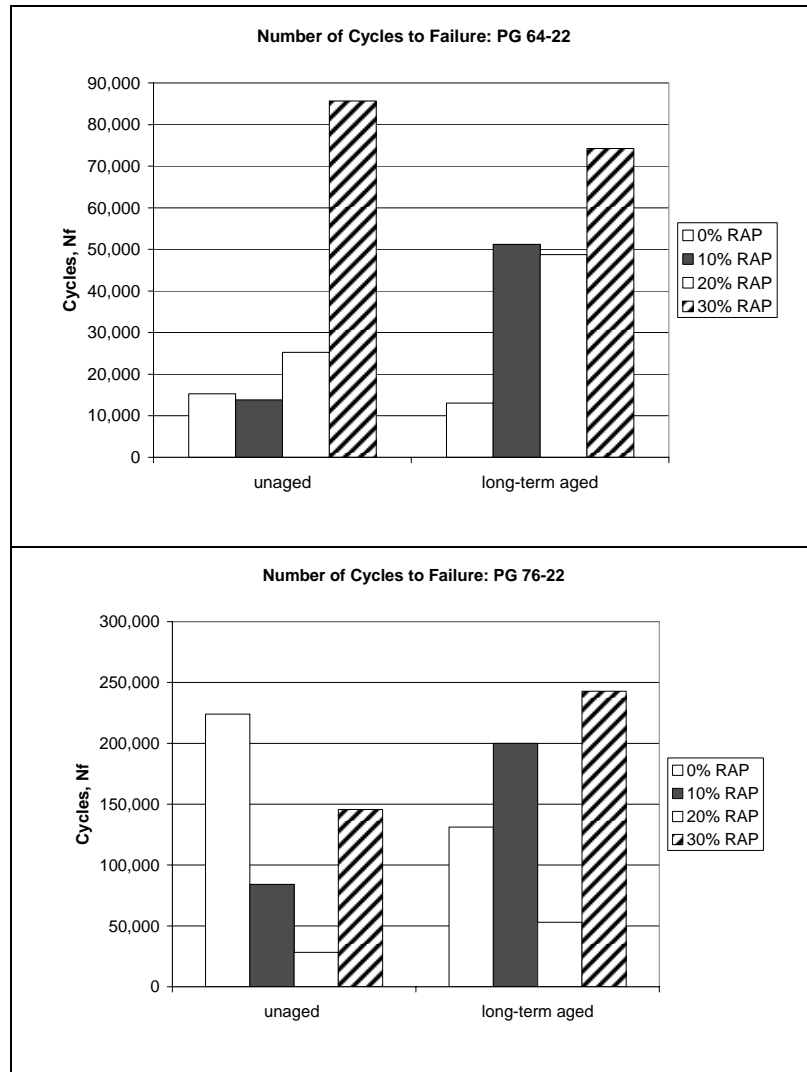


Figure 2.8. Number of Cycles to Failure in Strain Controlled Beam Fatigue Test (17).

In summary, the results from this study indicated that the inclusion of RAP generally increased the stiffness, indirect tensile strength and laboratory fatigue resistance

for the mixtures studied. Mixture properties changed significantly at 30% RAP content as compared to those with 10 and 20 percent.

17. A Comparison of the Predicted Performance of Virgin and Recycled Mixes by Puttagunta et al. (18).

This study compared the fatigue and moisture damage potential of virgin and recycled mixes through the use of indirect tensile strength and resilient modulus tests, as stipulated by the Asphalt Aggregate Mixture Analysis System (AAMAS) guidelines, which recommend the use of indirect tensile strength and resilient modulus to assess both fatigue and moisture damage potential. One source of RAP was used to prepare mixes with recycling ratios of 25% and 50%.

Results for the indirect tensile strength test indicated that the virgin mix had a tensile strength about 1,000 kPa higher at low temperatures as compared to the recycled mixes (Figure 2.9). The tensile strength of all mixes decreased as temperature increased, but the rate of decrease was higher for the virgin mix (about 5 kPa/°C higher). The difference in the tensile strengths of the 25% and 50% recycled materials was small at all temperatures (less than 100 kPa).

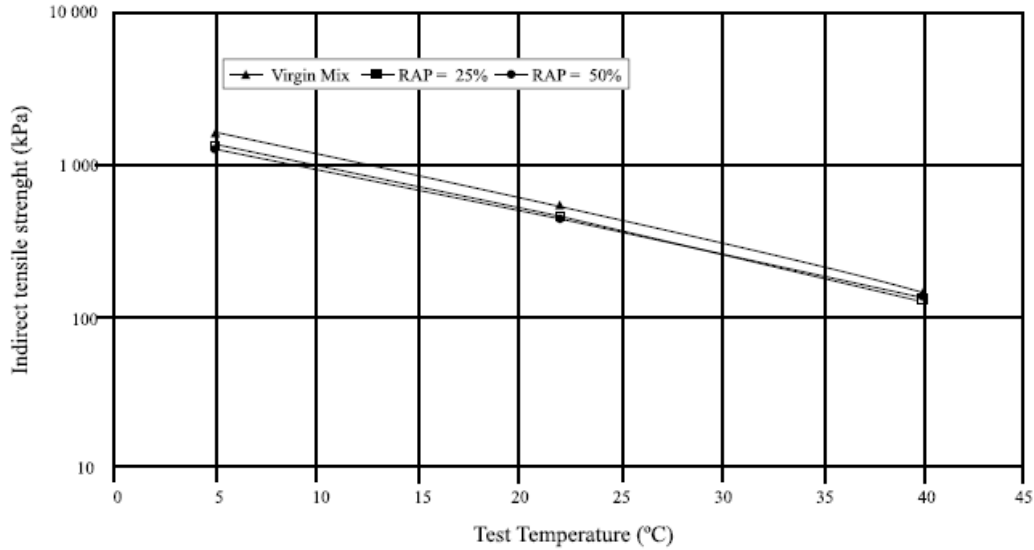


Figure 2.9. Effect of Test Temperature on Indirect Tensile Strength (18).

From the results of the resilient modulus test it was concluded that the virgin mix had a higher resilient modulus than the recycled mixes at all temperatures (from 238 MPa at 40°C to 1,667MPa at 5°C for mixtures with 25% RAP and from 255 MPa at 40°C to 1,548MPa at 5°C for mixtures with 50% RAP). The rate of decrease of resilient modulus with test temperature for the virgin mix was 68 to 73 MPa/°C higher than for the recycled mixes between 5 and 22°C but was almost equal between 22 and 40°C (only 8 to 10 MPa/°C higher). Again, at all temperatures the difference between the results of the 25% and 50% recycled mixes was small (not more than 120 MPa).

The fatigue analysis showed that in general, the virgin mix had higher resistance to fatigue cracking than the recycled mixes (up to 7.86×10^8 repetitions higher at 5°C). The AAMAS procedure utilizes the resilient moduli and failure strain from the indirect tensile strength test to calculate the fatigue coefficients K_1 and K_2 . The fatigue performances of the 25% and 50% recycled mixes were relatively similar at all temperatures, with a maximum difference of 2.8×10^7 repetitions at 5°C (Table 2.7).

Table 2.7. Summary Results of Fatigue Constants and Allowable Number of Loads (18).

	Temperature (°C)	Mixture		
		Virgin Mix	25% RAP	50% RAP
Resilient modulus (MPa)	5	6,928	5,261	5,380
	22	2,020	1,594	1,621
	40	1,259	1,021	1,004
Fatigue constant, K_1	5	4.83×10^{-8}	1.45×10^{-7}	1.33×10^{-7}
	22	6.68×10^{-6}	1.72×10^{-5}	1.61×10^{-5}
	40	4.43×10^{-7}	1.0×10^{-4}	1.0×10^{-4}
Fatigue constant, K_2	5	3.59	3.47	3.48
	22	3.05	2.95	2.96
	40	2.85	2.76	2.75
Allowable number of loads, N_f	5	8.34×10^8	4.83×10^7	7.61×10^7
	22	7.64×10^6	2.35×10^6	2.61×10^6
	40	1.99×10^5	1.42×10^5	1.52×10^5

Moisture damage analysis based on retained stability as defined by the Marshall design method indicated that the virgin and recycled mixes offered good resistance to moisture damage (over 90% retained stability). However, the AAMAS procedure, which involves the use of the indirect tensile strength and resilient modulus, predicted a resistance to moisture damage that falls below the minimum criteria. The AAMAS procedure also predicted resistance to moisture damage that increased with increasing recycling ratios (up to 0.32 higher, as shown in Table 2.8). This may be attributed to the fact that recycled aggregates allow a better coating with new asphalt as compared to virgin aggregates.

Table 2.8. Analysis of Moisture Damage Potential (18).

	Virgin mix	Reclaimed Asphalt Pavement		AAMAS criterion
		25%	50%	
Tensile strength ratio	0.59	0.81	0.91	>0.80
Modulus of resilient ratio	0.68	0.85	0.90	>0.80

18. Behavior of Recycled Asphalt Pavements at Low Temperatures by Sargious and Mushule (19).

This study was conducted to evaluate the behavior of recycled asphalt pavements with respect to low-temperature cracking. A recycled mix consisting of 45% RAP and 55% virgin materials as well as a virgin control mix were used. Using mix properties that were determined experimentally in the laboratory, thermal stresses resulted from drop in temperature and the expected cracking temperatures were determined for both mixes. An experimental analysis based on laboratory tests that consider the pavement properties only, as well as a more complete theoretical analysis based on a finite element computer program were included.

The mix properties that were determined experimentally included density, resilient modulus, tensile strength, coefficient of thermal contraction, thermal conductivity, and specific heat. The data required by the program are the ambient air temperature, the cross-section geometry, the thermal and elastic properties of pavement and subgrade, and the surface thermal characteristics.

The results for both experimental and laboratory-based experimental analyses indicated that the performance of recycled asphalt pavements with respect to low-temperature cracking is superior to that of virgin asphalt pavements of comparable initial properties. Recycled mixtures had lower crack temperatures (-27°C for the virgin and -31.5°C for the recycled materials), which may be due to factors such as the use of a soft asphalt in the recycled mix as a modifier. Recycled mixtures also had higher coefficient of thermal conductivity (0.37 to 0.50 W/(m $^{\circ}\text{C}$) higher), higher tensile strength (360 to 1260 kPa higher) and lower coefficient of thermal contraction ($0.12 \times 10^{-5}/^{\circ}\text{C}$ to

0.19x10⁵/°C lower) than those of virgin mixtures. The theoretical work showed that pavement thickness and subgrade type play an important role in low-temperature cracking for both virgin and recycled asphalt pavements.

2.3 SUMMARY

The literature review revealed that studies conducted on SMA mixture design and performance (2, 3, 4, 5) concluded that SMA mixes had benefits such as reduced rutting, greater fatigue life and longer service life. Certain modifications in the requirements have been made to adapt the mixtures to the material characteristics and conditions found in the United States.

Research on the use of recycled asphalt pavement has found that RAP does not act like a black rock and partial blending occurs (6, 7, 8, 9). Guidelines have been developed to incorporate RAP in conventional HMA mixtures, establishing that at low RAP contents (up to 15%) the binder effects are negligible and no modification is required in the design process. At intermediate RAP contents (16% to 25%), these effects can be compensated for by using a virgin binder that is one grade softer on both the high- and low- temperature grades. Higher RAP contents (over 25%) require the use of blending charts to determine the appropriate virgin binder grade.

It has also been found that addition of RAP increases the binder stiffness (6, 10), and hence, the mixture stiffness. This may affect low temperature performance (14, 15) and fatigue life (17, 18). On the other hand, increase in mix stiffness resulted in higher indirect tensile strength (17, 18), which improved rutting and moisture resistance (12, 14, 18).

Fractionated RAP has been successfully used in Superpave mixtures (13). RAP material passing the 1.18 mm sieve represents the fine aggregates bound in small conglomerates by the RAP asphalt, which cannot be separated during milling or sieving operations. RAP sources studied had similar gradations at and above the 1.18 mm size, but showed significant differences in the amount of material passing the 1.18 mm sieve. By removing this material, the uniformity between the RAP sources in the coarser fractions could be increased.

The fine RAP fractions generally have a higher asphalt content than the coarse fractions due to the higher surface area per unit weight associated with fine aggregate gradations. This higher binder content may reduce the required virgin binder content noticeably while using a lower percentage of RAP material. It has also been observed that using the fine RAP fraction increases the mixture stiffness which reduces rutting potential.

The information collected suggests that use of RAP in SMA mixtures could produce important benefits in terms of performance. The effect of increased stiffness must be carefully studied, since SMA mixes could be especially vulnerable to distresses associated with this property, such as thermal and fatigue cracking.

CHAPTER 3. RESEARCH TEST PLAN

The research approach was divided into three parts as they relate to the objectives of the study: evaluation of materials, mix designs and performance tests. The experiment was planned as a 4x4x4 factorial design, with three factors (aggregate source, RAP content and RAP type) at four levels each. This allowed studying the contributions that each of the factors make individually to the response, as well as the effect of the interaction of treatment factors.

The full factorial design would require 64 treatment combinations, but due to time constraints and a need to keep research costs in a reasonable range, a one-fourth fraction was selected so that the number of mix designs to be evaluated could be limited without sacrificing the integrity of the experiment. Table 3.1 shows the test matrix for the fractional factorial design.

Table 3.1. Test Matrix for Mix Variables.

Aggregate source	RAP source	RAP content, %			
		0	10	20	30
Mountain View	Regular	X			
	SMA			X	
	Fine-graded		X		
	Coarse-graded				X
Lithia Springs	Regular		X		
	SMA				X
	Fine-graded	X			
	Coarse-graded			X	
Camak	Regular				X
	SMA		X		
	Fine-graded			X	
	Coarse-graded	X			
Ruby	Regular			X	
	SMA	X			
	Fine-graded				X
	Coarse-graded		X		

3.1. PART 1 – EVALUATION OF MATERIALS

This study involved evaluating material properties of aggregates, asphalt binder and the combined blend of virgin materials and RAP.

3.1.1 Evaluation of Aggregate Properties

Four aggregate sources were used in this study: Florida Rock at Mt. View, Martin-Marietta at Ruby, Martin-Marietta at Camak, and Vulcan at Lithia Springs. These sources were chosen because they have been widely used in SMA production in Georgia with positive results. Their properties are shown in Table 3.2. Tables 3.3 through 3.6 and Figures 3.1 through 3.4 show the aggregate gradations for each source. The “M”

denomination on some of the aggregates means that they are manufactured screenings, while the “W” denominations correspond to washed screenings, which have a lower dust content.

Table 3.2. Properties of Virgin Aggregates.

Aggregate Source	General Character of Material	Specific Gravities			Absorption, %
		Bulk	SSD	App.	
Mt. View	Granite Gneiss/ Amphibolite	2.640	2.659	2.691	0.72
Lithia Springs	Granite Gneiss	2.591	2.608	2.635	0.62
Camak	Granite Gneiss	2.638	2.655	2.682	0.62
Ruby	Gneiss/ Amphibolite	2.734	2.746	2.767	0.43

Table 3.3. Gradations for Mt. View Aggregates.

Sieve Size	Percent Passing		
	007	089	W10
1"	100.0	100.0	100.0
3/4"	100.0	100.0	100.0
1/2"	97.0	100.0	100.0
3/8"	48.0	100.0	100.0
#4	3.0	22.0	99.0
#8	3.0	4.0	83.0
#16	2.0	2.0	66.0
#30	2.0	2.0	53.0
#50	2.0	1.0	37.0
#100	1.0	1.0	18.0
#200	1.0	1.0	6.0

Table 3.4. Gradations for Lithia Springs Aggregates.

Sieve Size	Percent Passing		
	007	089	810
1"	100.0	100.0	100.0
3/4"	100.0	100.0	100.0
1/2"	85.0	100.0	100.0
3/8"	50.0	100.0	100.0
#4	6.0	30.0	84.0
#8	2.0	2.0	62.0
#16	1.0	2.0	50.0
#30	1.0	1.0	41.0
#50	1.0	1.0	28.0
#100	1.0	1.0	21.0
#200	1.0	1.0	10.0

Table 3.5. Gradations for Camak Aggregates.

Sieve Size	Percent Passing	
	007	M10
1"	100.0	100.0
3/4"	100.0	100.0
1/2"	94.0	100.0
3/8"	56.0	100.0
#4	10.0	98.0
#8	3.0	82.0
#16	3.0	62.0
#30	2.0	50.0
#50	1.0	36.0
#100	1.0	25.0
#200	1.0	12.0

Table 3.6. Gradations for Ruby Aggregates.

Sieve Size	Percent Passing	
	007	M10
1"	100.0	100.0
3/4"	100.0	100.0
1/2"	96.0	100.0
3/8"	55.0	100.0
#4	2.0	99.0
#8	1.0	82.0
#16	1.0	62.0
#30	1.0	49.0
#50	1.0	37.0
#100	1.0	27.0
#200	1.0	18.0

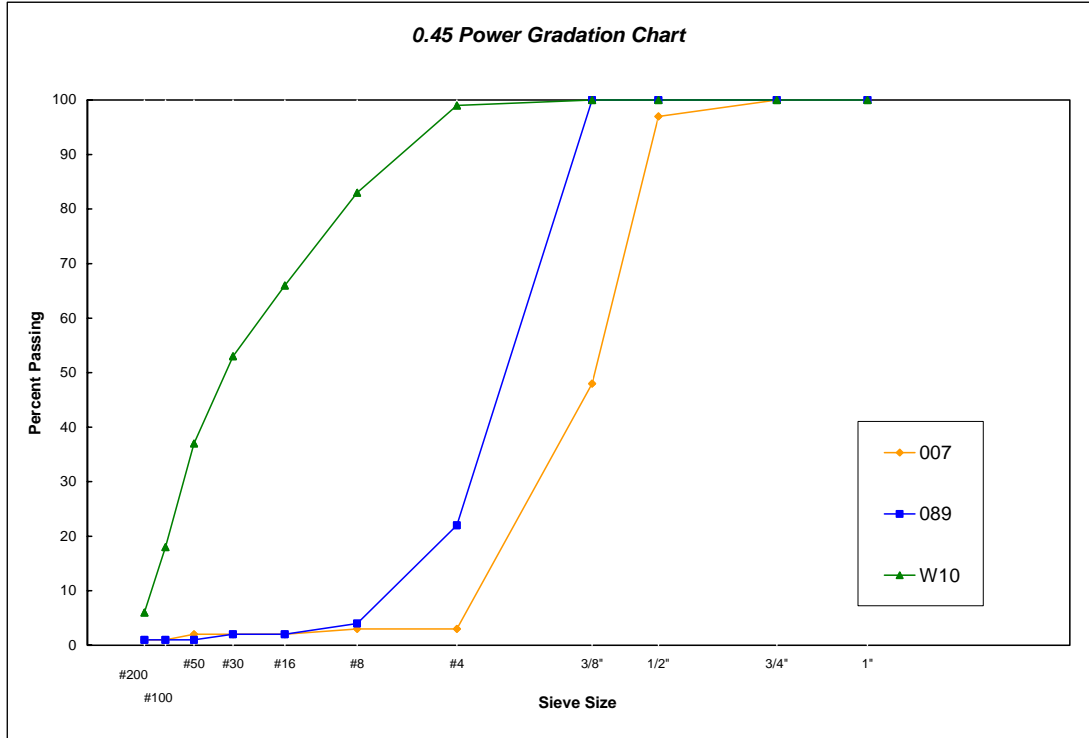


Figure 3.1. Gradations for Mt. View Aggregates.

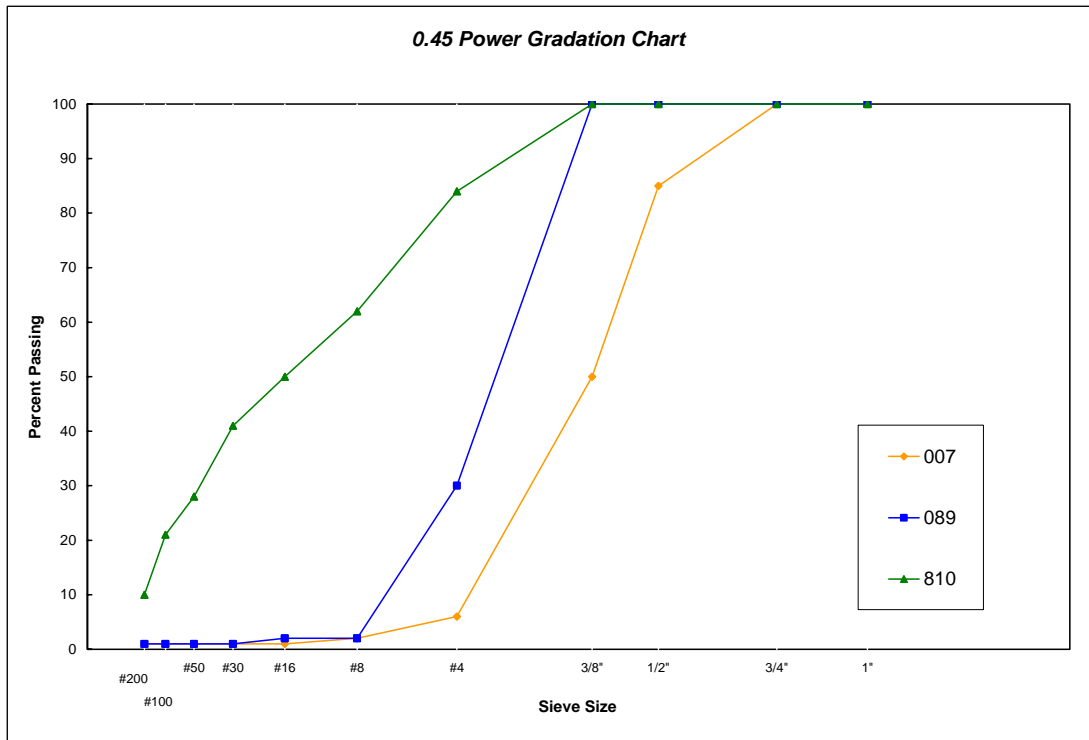


Figure 3.2. Gradations for Lithia Springs Aggregates.

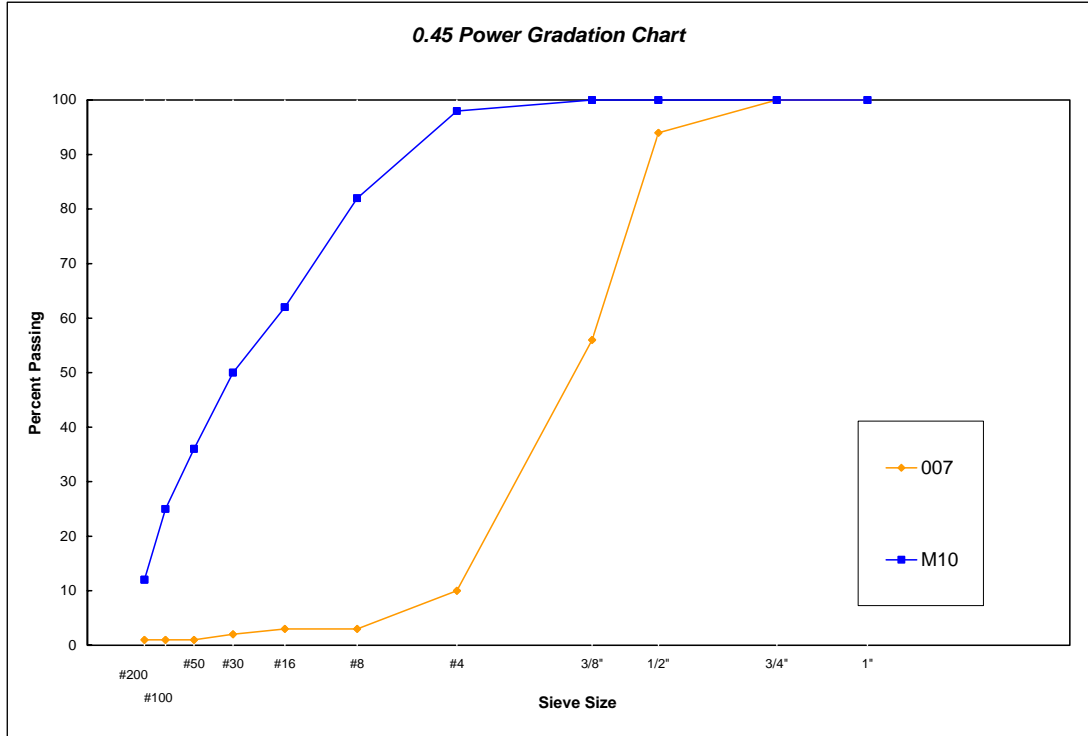


Figure 3.3. Gradations for Camak Aggregates.

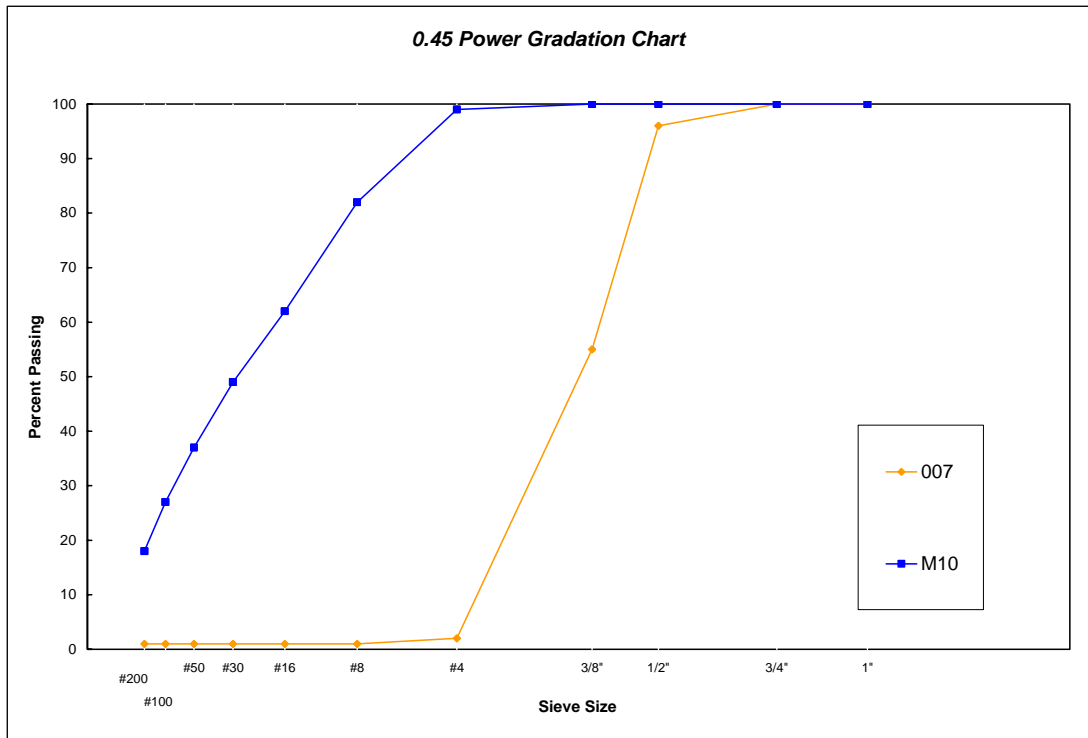


Figure 3.4. Gradations for Ruby Aggregates.

Four RAP sources were used in this study: conventional RAP, RAP from reclaimed SMA, fine-graded RAP (-4 RAP), and coarse-graded RAP (+4 RAP). Table 3.7 and Figure 3.5 show the RAP gradations used in this study and Table 3.8 shows the asphalt cement content of each RAP source.

SMA RAP was included in this study to evaluate the possibility of recycling SMA material back into an SMA mixture. As the first SMA projects reach the end of their service life, it is important to determine if the stiff mastic in an SMA mix might prevent it from being recycled or if the proportion of RAP may have to be reduced. However, when the SMA RAP received from GDOT was tested it was found that its gradation and asphalt content did not match those of an SMA mix. SMA mixes generally have about 25 percent of the material passing the No. 4 sieve, and in this case, that amount was 77 percent. It is known that this RAP material was crushed to achieve the 12.5 mm NMAS and this may have affected its gradation.

The asphalt content of the SMA RAP was unusually low with an average of only 4.4 percent based on weight of total mix (the usual asphalt content being about 6 percent). Based on this result, it is likely that the RAP from the SMA project also included a portion of the underlying 19 mm Superpave mixture as a result of the milling process. Overall, there was no significant difference between the gradations of conventional and SMA RAP, and from this point on they will be treated and referred to as dense-graded RAP 1 (DG1 RAP) and dense-graded RAP 2 (DG2 RAP), respectively.

The use of fractionated RAP material into coarse and fine-graded stockpiles was also considered in this study. +4 RAP was used as a substitute of a portion of the No. 7 stone, typically used in high quantities in SMA production. This option would be

beneficial in the event that quarries were faced with a supply shortage of No. 7 stone due to its high demand in other HMA and concrete mix applications. -4 RAP was used as a substitute for a portion of the asphalt content, since its higher surface area makes it richer in asphalt cement. This would represent an advantage because asphalt cement is typically the most expensive component of a mixture.

Table 3.7. RAP Gradations.

Sieve Size	Percent Passing			
	DG1 RAP	DG2 RAP	-4 RAP	+4 RAP
1"	100.0	100.0	100.0	100.0
3/4"	100.0	100.0	100.0	99.0
1/2"	99.0	100.0	100.0	96.0
3/8"	93.0	95.0	100.0	84.0
#4	73.0	77.0	100.0	37.0
#8	58.0	61.0	81.0	25.0
#16	47.0	50.0	65.0	21.0
#30	38.0	42.0	53.0	18.0
#50	29.0	32.0	40.0	15.0
#100	19.0	20.0	25.0	10.0
#200	11.2	12.0	15.0	6.2

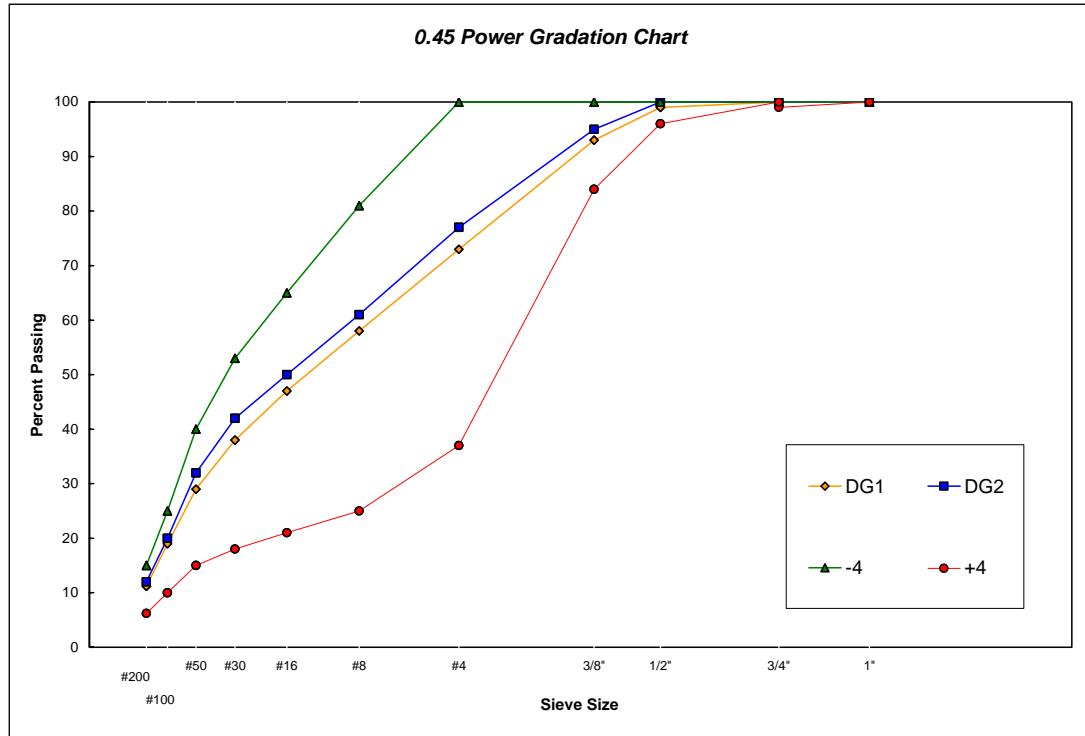


Figure 3.5. RAP Gradations.

Table 3.8. Asphalt Contents in RAP

RAP Source	Asphalt Content, %
+4	4.5
-4	6.2
DG1	5.6
DG2	4.4

Aggregate toughness was determined by the Los Angeles abrasion test (ASTM C131), which measures the resistance of coarse aggregates to degradation by abrasion and impact. The aggregate is placed in a metal drum along with a charge of steel balls, and the drum is rotated 500 times at a speed of 30 - 33 revolutions per minute (RPM). The inside of the drum is equipped with an angle iron which runs longitudinally. This causes the charge of aggregate and balls to fall with a heavy impact once during each revolution, breaking the aggregate particles into smaller particles. At the completion of

the test, the aggregate is shaken over a No. 12 sieve and the amount which passes through the sieve, expressed as a percentage of the total charge, is the Los Angeles abrasion value designated "percent loss".

Aggregates must be tough in order to prevent crushing and abrasive wear during manufacturing, placing and compaction of HMA. This aggregate property is especially critical in gap-graded mixtures such as SMA because excessive aggregate breakdown will fill void spaces within the mixture and thereby reduce the amount of asphalt cement that would otherwise be needed. As the asphalt content is reduced, the durability of the mixture suffers and results in premature aging and deterioration.

The flat and elongated property was determined by GDT-129. This characteristic is defined as the percentage by weight of coarse aggregates that have a length in excess of three times its average thickness, in accordance with the test procedure. This test was performed to ensure that the aggregate contained cubical particles capable of distributing traffic loads through the stone-on-stone coarse aggregate skeleton of an SMA mix. This also contributes to the improved rutting resistance of SMA mixes as compared to conventional mixtures.

3.1.2 Evaluation of Asphalt Binder Properties

The binder from RAP materials was recovered through Abson recovery tests (ASTM D1856) and its properties were evaluated by means of the Dynamic Shear Rheometer (DSR) and Bending Beam Rheometer (BBR). Asphalt cement from samples of the

proposed blends was also extracted and analyzed for rheological properties and performance grade.

Short-term aging of the blended binders was achieved using the Rolling Thin Film Oven (RTFO) procedure according to AASHTO T240, which simulates aging during construction. In this test, a moving film of asphalt binder is heated in an oven for 85 minutes at 163° C. The moving film is created by placing the asphalt binder sample in a small jar then placing the jar in a circular metal carriage that rotates within the oven (Figure 3.6). This rotation is used to continually expose fresh films of the binder to hot air.

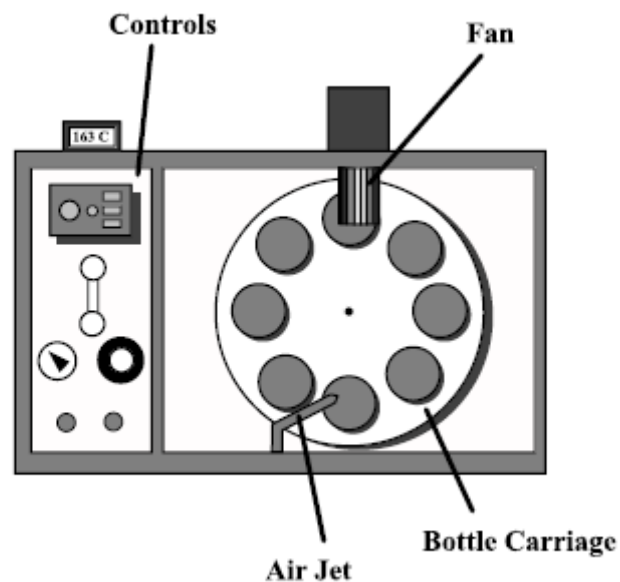


Figure 3.6. Rolling Thin Film Oven (20).

Long-term aging, which simulates several years of exposure to the environment, was achieved using the Pressure Aging Vessel (PAV) in accordance to AASHTO PP1. The PAV is an oven-pressure vessel combination that takes RTFO aged samples and

exposes them to high air pressure (2070 kPa) and temperature (90°C, 100°C or 110°C, depending upon expected climatic conditions) for 20 hours.

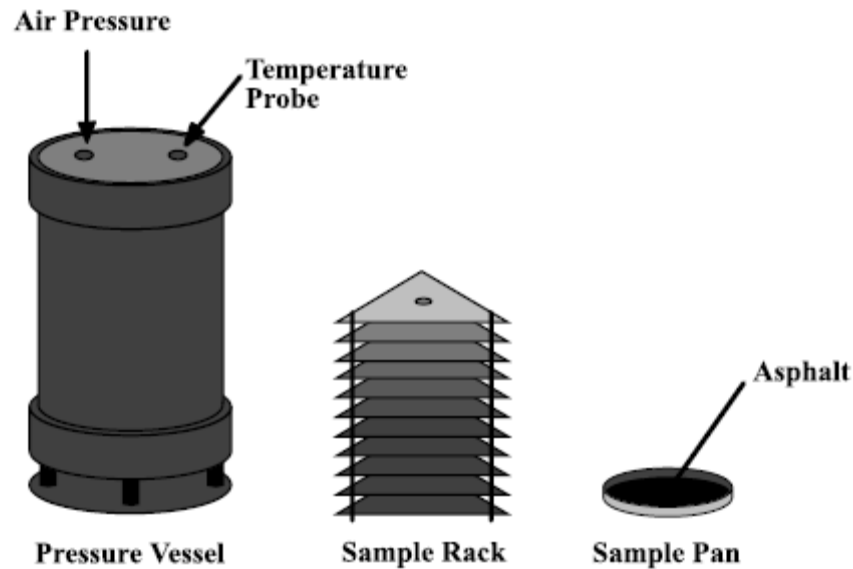


Figure 3.7. Pressure Aging Vessel (20).

Engineering properties of the blended binders were obtained through Dynamic Shear Rheometer (DSR) and Bending Beam Rheometer (BBR) testing. The DSR test was used in accordance with AASHTO TP 5 to measure the complex shear modulus (G^*) and phase angle (δ) of the blended binders at high and intermediate temperatures. The test uses a thin asphalt binder sample placed between two plates. The lower plate is fixed while the upper plate oscillates back and forth across the sample at 1.59 Hz to create a shearing action. These oscillations at 1.59 Hz (10 radians/sec) are meant to simulate the shearing action corresponding to a traffic speed of about 90 km/hr (55 mph).

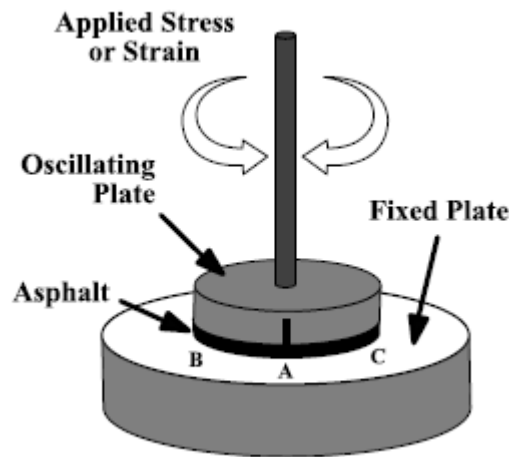


Figure 3.8. Basics of Dynamic Shear Rheometer (20).

The physical properties measured with the DSR allow obtaining the rutting and fatigue parameters, which are used to quantify the asphalt binder's contribution in resisting those types of distresses. Rutting is considered a stress controlled, cyclic loading phenomenon. Each traffic loading cycle does work that contributes to deform the HMA pavement surface. A part of this work is recovered by elastic rebound of the surface while some is dissipated in the form of permanent deformation and heat. The work dissipated per loading cycle at a constant stress can be expressed as:

$$W_c = \pi \times \sigma_o^2 \left[\frac{1}{G^* / \sin \delta} \right] \quad \text{Equation 3.1 (21)}$$

Where:

W_c = work dissipated per load cycle

σ_o = stress applied during the load cycle

G^* = complex modulus

δ = phase angle

The amount of work dissipated per loading cycle is inversely proportional to $G^*/\sin\delta$, called the rutting parameter. In order to minimize permanent deformation, W_c must be minimized as well. This indicates that higher values of $G^*/\sin\delta$ correspond to binders with better rutting resistance

In the case of fatigue cracking, this distress is considered a strain controlled phenomenon. The work dissipated per loading cycle at a constant strain can be expressed as:

$$W_c = \pi \times \epsilon_o^2 [G^* \sin \delta] \quad \text{Equation 3.2 (21)}$$

where ϵ is the strain and the other variables are as previously described. Fatigue cracking is minimized by decreasing the term $G^* \sin\delta$ (fatigue parameter).

The BBR test was performed according to AASHTO TP 1 to determine the binder's propensity to thermal cracking. The BBR basically subjects a simple asphalt beam to a small (1,000 mN) load over 240 seconds. Then, using basic beam theory, the BBR calculates the flexural creep stiffness (S) and logarithmic creep rate (m) of the asphalt binder. The creep stiffness of the asphalt binder beam at 60 seconds loading time is given by:

$$S(t) = \frac{PL^3}{4bh^3 \delta(t)} \quad \text{Equation 3.3 (21)}$$

Where:

S(t) = creep stiffness at time, t = 60 seconds

P = applied constant load, 100 g

L = distance between beam supports, 102 mm

b = beam width, 12.5 mm

h = beam thickness, 6.25 mm

$\delta(t)$ = deflection at time, $t = 60$ seconds

The m -value is the rate of change of the stiffness, $S(t)$, with loading time and is used to describe how the asphalt binder relaxes under load.

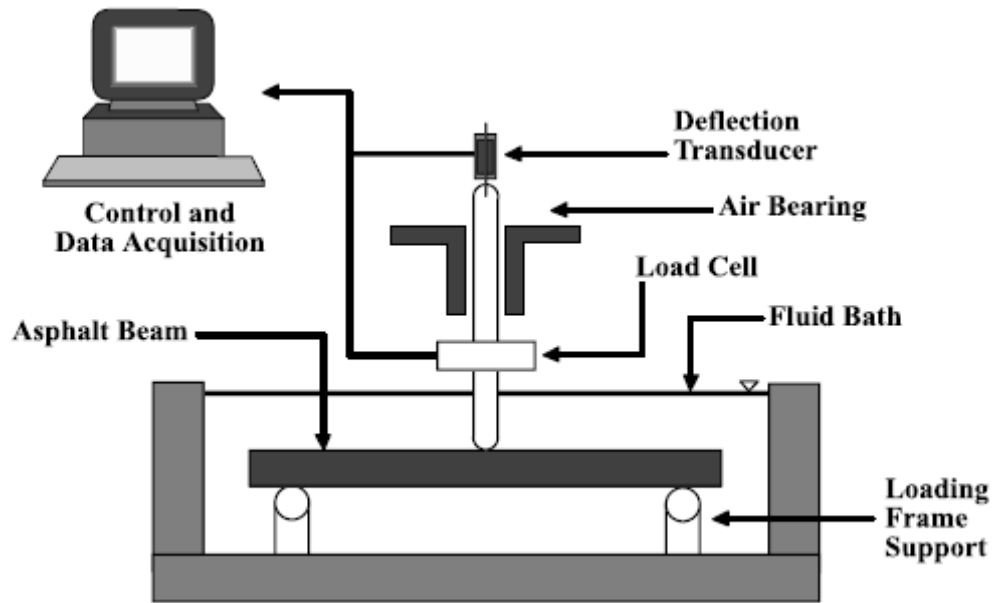


Figure 3.9. Schematic of Bending Beam Rheometer (20).

Creep stiffness is related to thermal stresses in an HMA pavement due to shrinking while the m -value is related to the ability of an HMA pavement to relieve these stresses. Therefore, asphalt binders with minimum creep stiffness and maximum creep rate are desired in order to resist thermal cracking.

The Superpave asphalt binder specification (AASHTO MP1) is intended to control permanent deformation, low temperature cracking and fatigue cracking in asphalt pavements. The specification accomplishes this by controlling the various physical

properties described previously ($G^*/\sin\delta$, $G^*\sin\delta$, $S(t)$ and m -value). The physical properties remain constant for all performance grades (PG), but the temperatures at which these properties must be achieved vary depending on the climate in which the binder is expected to serve (Figure 3.10).

Performance Grade	PG 52							PG 58		
	-10	-16	-22	-28	-34	-40	-46	-16	-22	-28
Average 7-day Maximum Pavement Design Temperature, C	<52							<58		
Minimum Pavement Design Temperature, C	>-10	>-16	>-22	>-28	>-34	>-40	>-46	>16	>-22	>-28
Flash Point Temp. T48: Minimum, C								Original Binder		
Flash Point Temp. T48: Minimum, C								230		
Viscosity, ASTM D 4402: ^b Maximum, 3 Pa-s (3000 cP) Test Temperature, C								135		
Dynamic Shear, TP5: ^c $G^* / \sin \delta$. Minimum, 1.00 kPa Test Temperature @ 10rad/sec, C	52							58		

**Spec Requirement
Remains Constant**

**Test Temperature
Changes**

Figure 3.10. Superpave Binder Specification Example (20).

3.2 PART 2 – MIX DESIGNS

RAP material, virgin asphalt and virgin aggregate were proportioned to produce 12.5 mm SMA mix designs. The 50-blow Marshall procedure, which is used by GDOT, was used for asphalt mixture compaction and PG 76-22 was used as the standard performance grade asphalt. RAP was blended at four proportions (0%, 10%, 20%, and 30%) to determine the effect of RAP over the ranges of anticipated use. A blend with no RAP was

used as a baseline for the study for comparisons of mix performance. A RAP content of 10% represented the least amount that can feasibly be utilized, and a maximum RAP content of 30% was used because it is improbable that blends with greater contents of RAP would be able to meet gradation and volumetric requirements of the mix design. The gradations for the control and recycled mixes are shown in Tables 3.9 through 3.13 and Figures 3.11 through 3.15.

Table 3.9. Gradations for Control Mixes.

Sieve Size	Percent Passing			
	Mt. View	Lithia Springs	Camak	Ruby
1"	100.0	100.0	100.0	100.0
3/4"	100.0	100.0	100.0	100.0
1/2"	98.0	90.0	95.0	96.9
3/8"	64.6	66.5	55.2	65.4
#4	24.6	25.8	18.5	24.4
#8	20.3	16.7	16.0	20.5
#16	17.2	14.4	14.0	16.9
#30	15.5	13.1	12.8	14.6
#50	13.3	11.4	11.4	12.4
#100	10.0	10.4	10.2	10.6
#200	8.0	8.5	8.4	8.6

Table 3.10. Gradations of Recycled SMA Mix Using DG1 RAP.

Sieve Size	Percent Passing		
	10% RAP	20% RAP	30% RAP
1"	100.0	100.0	100.0
3/4"	100.0	100.0	100.0
1/2"	89.1	97.0	95.8
3/8"	63.4	67.1	62.5
#4	27.7	25.9	27.6
#8	20.6	21.4	22.4
#16	17.2	18.1	19.1
#30	15.2	15.7	16.4
#50	12.6	13.3	13.7
#100	10.7	10.7	10.6
#200	8.1	8.4	8.0

Table 3.11. Gradations of Recycled SMA Mix Using DG2 RAP.

Sieve Size	Percent Passing		
	10% RAP	20% RAP	30% RAP
1"	100.0	100.0	100.0
3/4"	100.0	100.0	100.0
1/2"	95.6	98.0	90.1
3/8"	60.1	64.1	65.6
#4	25.9	24.9	31.2
#8	21.8	20.4	23.7
#16	18.5	17.3	19.7
#30	16.3	15.7	17.3
#50	13.8	13.6	14.2
#100	11.2	10.4	10.5
#200	8.6	8.4	7.8

Table 3.12. Gradations of Recycled SMA Mix Using -4 RAP.

Sieve Size	Percent Passing		
	10% RAP	20% RAP	30% RAP
1"	100.0	100.0	100.0
3/4"	100.0	100.0	100.0
1/2"	97.7	95.5	97.3
3/8"	60.0	59.4	70.0
#4	25.2	26.4	34.6
#8	22.2	21.9	28.3
#16	18.7	18.7	23.5
#30	16.6	16.3	19.9
#50	14.1	13.7	16.0
#100	10.4	10.6	11.5
#200	8.2	8.3	8.3

Table 3.13. Gradations of Recycled SMA Mix Using +4 RAP.

Sieve Size	Percent Passing		
	10% RAP	20% RAP	30% RAP
1"	100.0	100.0	100.0
3/4"	99.9	99.8	99.7
1/2"	96.8	89.9	97.0
3/8"	66.9	65.9	64.6
#4	24.9	27.2	23.8
#8	20.4	19.7	19.3
#16	17.0	16.8	16.7
#30	14.8	15.1	15.1
#50	12.7	12.9	13.4
#100	10.6	11.0	10.2
#200	8.5	8.5	8.1

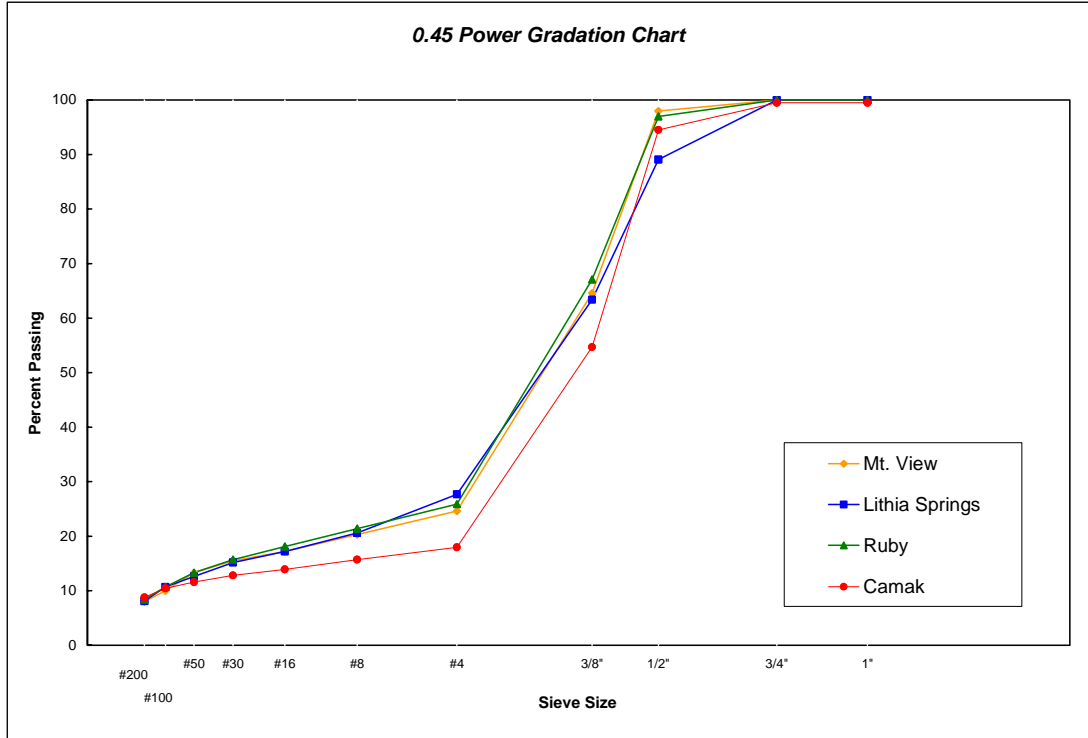


Figure 3.11. Gradations for Control Mixes.

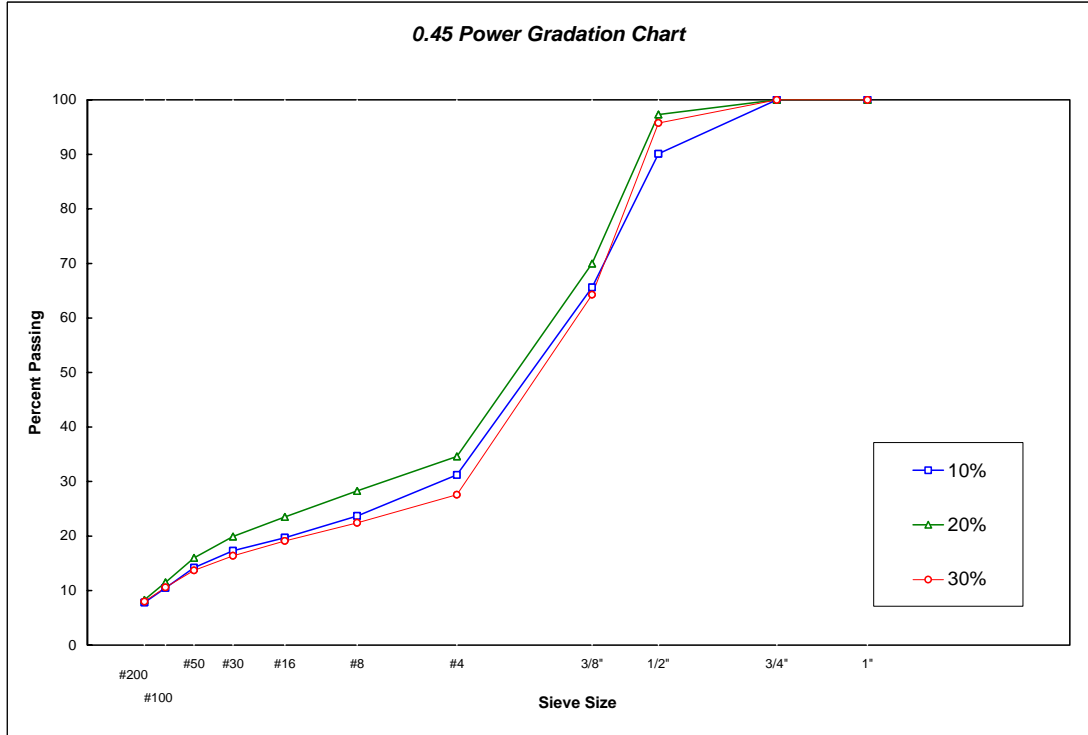


Figure 3.12. Gradations of Recycled SMA Mix Using DG1 RAP.

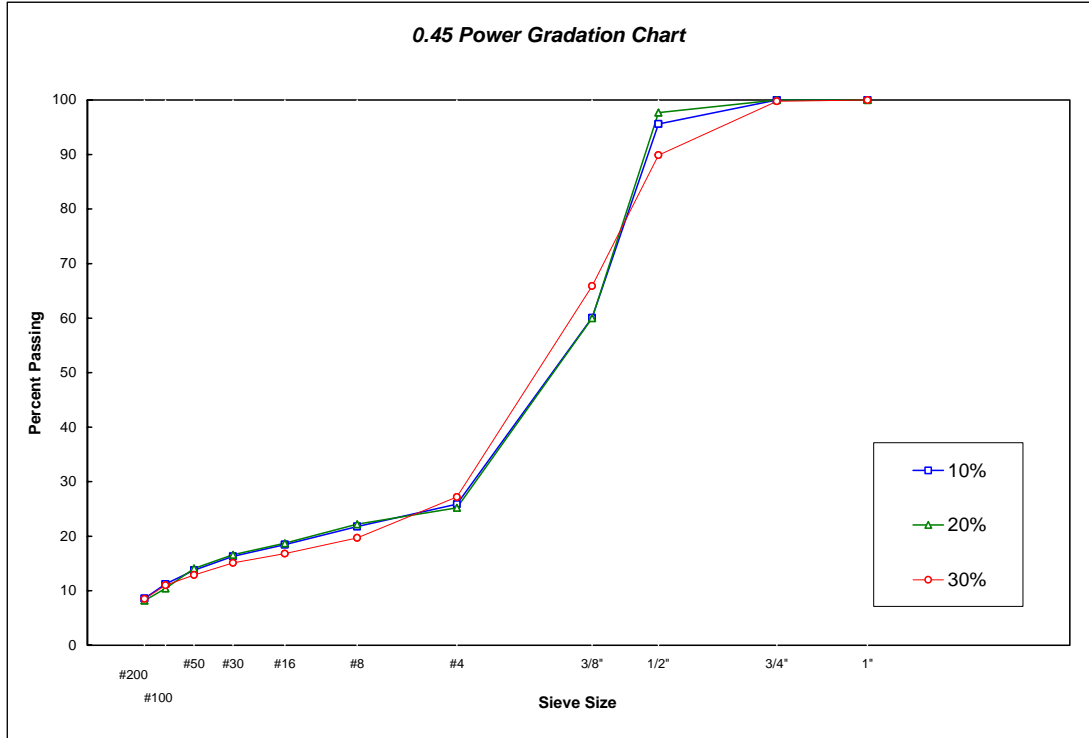


Figure 3.13. Gradations of Recycled SMA Mix Using DG2 RAP.

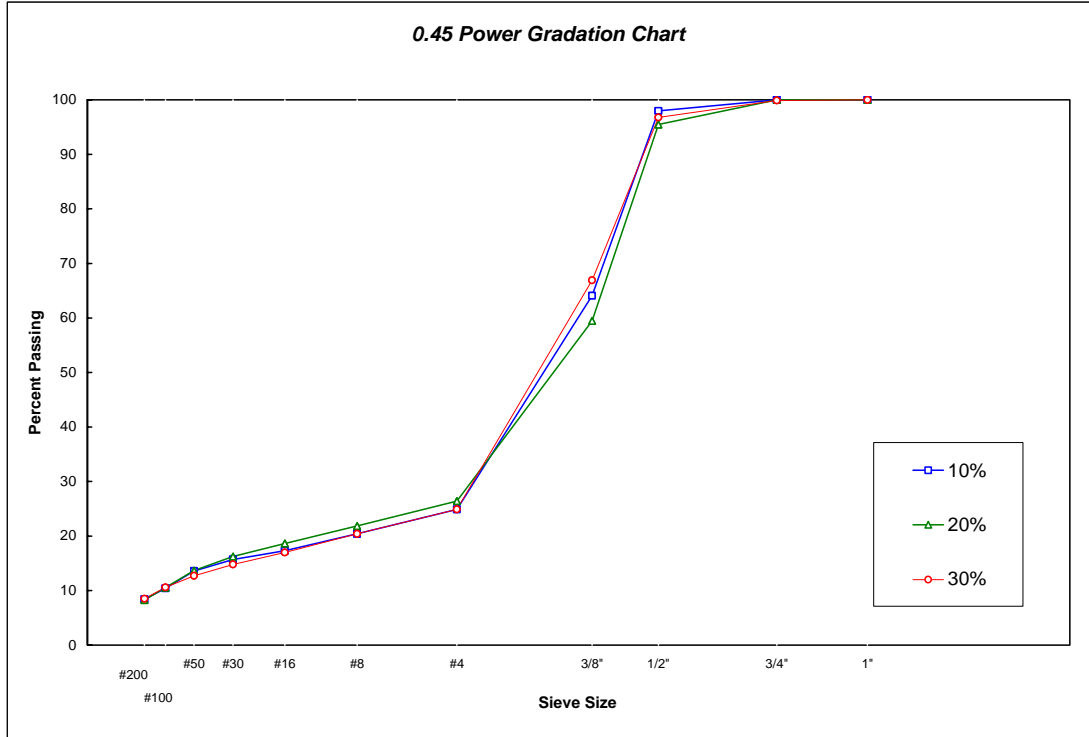


Figure 3.14. Gradations of Recycled SMA Mix Using -4 RAP.

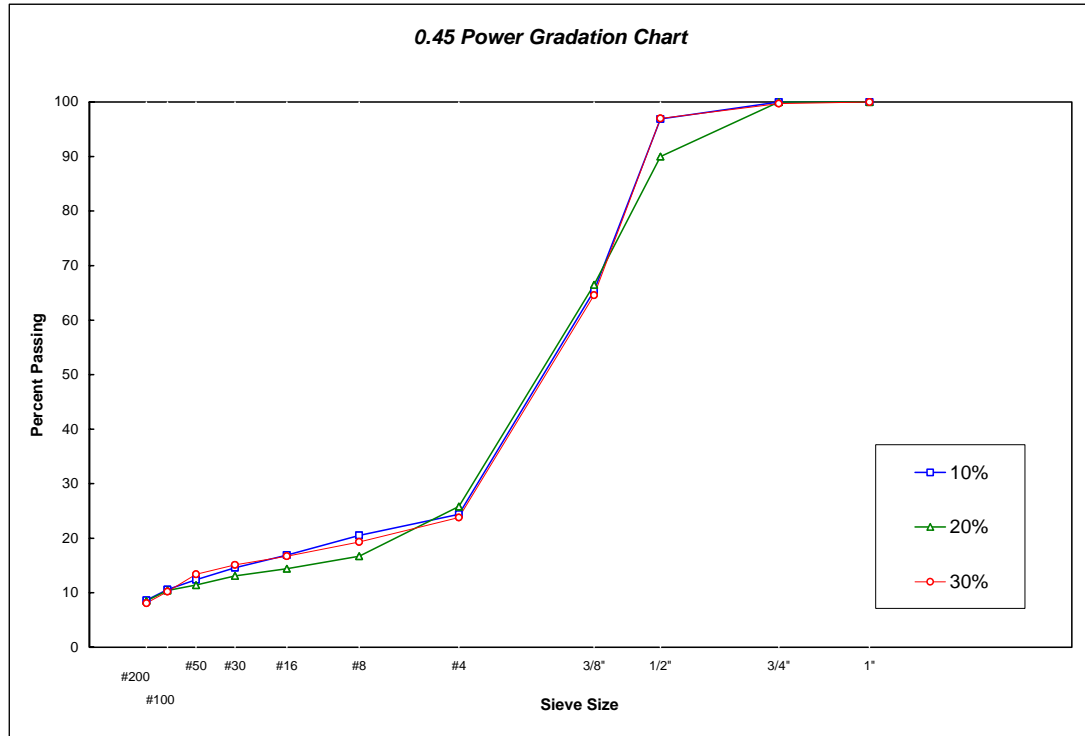


Figure 3.15. Gradations of Recycled SMA Mix Using +4 RAP.

In the mix design, the gradations of the SMA mixtures were kept as close as possible to each other to provide a proper comparison among the different aggregate sources and RAP types. The gradation charts in Figures 3.11 through 3.15 show that there is little variation in the percent passing each sieve size among the different mixtures (in most cases under 5%). Fiber stabilizing additive (cellulose fiber) and mineral filler (marble dust) were included in the mixture as specified by GDOT.

Once the blends for each type of aggregate were determined, an initial asphalt content was estimated for each mixture. Replicate samples prepared for each blend were mixed at three different asphalt contents and conditioned in accordance with AASHTO R30. Specimens were compacted using a Marshall hammer, following procedures in AASHTO T-245. The bulk specific gravity of each specimen was determined by

AASHTO T 166. The theoretical maximum specific gravity of the loose HMA mix samples was measured in accordance with AASHTO T 209. Percent of air voids in the mix, voids in mineral aggregate (VMA) and voids filled with asphalt (VFA) were calculated for each mixture.

3.3 PART 3 – PERFORMANCE TESTS

The performance of the bituminous concrete test mixes was evaluated by subjecting specimens to diametral tensile strength, moisture susceptibility, flexural beam fatigue, APA rutting, and indirect tensile creep compliance tests.

3.3.1 Moisture Susceptibility

The effect of RAP addition on the moisture susceptibility of the mixtures was evaluated by determining the diametral tensile strength on dry and wet specimens according to GDT-66, *Evaluating the Moisture Susceptibility of Bituminous Mixtures by Diametral Tensile Splitting*. In this test, internal water pressures in the mixtures are produced by vacuum saturation followed by a freeze and a warm-water soaking cycle.

Six Marshall specimens were prepared using optimum asphalt content and compacted to 7.0 ± 1.0 percent air voids. A subset of three specimens remained unconditioned and was used as the control group. The other subset was partially vacuum saturated with water for 30 minutes and then subjected to a freeze (-18°C for 15 hours) and thaw (60°C for 24 hours) cycle. Both subsets were then tested for indirect tensile

strength at a load rate of 0.065 in/minute. The diametral tensile strength of each specimen was determined by Equation 3.4.

$$S = \frac{2P}{\pi tD} \quad \text{Equation 3.4}$$

Where:

S = tensile strength, psi (kPa)

P = maximum load, pounds (N)

t = specimen height immediately before tensile test, inches (millimeters)

D = specimen diameter, inches (millimeters)

The percentage of retained strength (TSR) was calculated by comparing the properties of dry specimens with water-conditioned specimens.

$$TSR = \frac{S_a}{S_c} \times 100 \quad \text{Equation 3.5}$$

Where:

TSR = percent retained strength

S_a = average tensile strength of conditioned subset, psi (kPa)

S_c = average tensile strength of control subset, psi (kPa)

3.3.2 Rutting Susceptibility

Rutting susceptibility of the mixtures was tested with the Asphalt Pavement Analyzer (APA), according to GDT-115, *Determining Rutting Susceptibility Using the Loaded Wheel Tester*. The APA is a modification of the Georgia Loaded Wheel Tester (GLWT),

and it follows a similar rut-testing procedure. A wheel is loaded onto a pressurized linear hose and tracked back and forth over a testing sample to induce rutting. Six samples for each mix type were compacted with a gyratory compactor to 5.0 ± 1 percent air voids and tested at 64°C using a vertical load of 100 lbs. and hose pressure of 100 psi for 8,000 cycles.

3.3.3 Creep Compliance

The creep compliance of the mixtures was evaluated according to AASHTO T 322, *Determining the Creep Compliance and Strength of Hot-Mix Asphalt Using the Indirect Tensile Test Device*, in order to determine if the addition of RAP affected the resistance of the mixtures to thermal cracking. Three replicate specimens for each mixture were compacted with a gyratory compactor to approximately 7% air voids and cut to dimensions of 150 mm diameter by 50 mm height. The tensile creep compliance was determined by applying a static compressive load of fixed magnitude along the diametral axis of each specimen for 100 s. Each specimen was tested at temperatures of -20 , -10 and 0°C . The horizontal and vertical deformations measured near the center of the specimen were used to calculate the tensile creep compliance as a function of time, given by the following relationship:

$$D(t) = \frac{\varepsilon(t)}{\sigma_0} \quad \text{Equation 3.5}$$

where $\varepsilon(t)$ is the strain and σ_0 is the stress.

Compliance is a way of characterizing the stiffness of a material. Another term frequently used is creep stiffness, $S(t)$, which is the inverse of creep compliance as determined from a creep test:

$$S(t) = \frac{1}{D(t)} = \frac{\sigma_0}{\varepsilon(t)} \quad \text{Equation 3.6}$$

An example of creep compliance curves measured at multiple temperatures using the indirect tensile test at low temperature is presented in Figure 3.16. A nonlinear regression routine is used to determine the master creep compliance curve from the creep compliance curves measured at multiple temperatures. The regression is performed in two steps. First, a regression is performed to simultaneously determine the temperature shift factors (a_t) and the parameters for the following Prony series (Maxwell model) representation of the master creep compliance curve:

$$D(\xi) = D(0) + \sum_{i=1}^N D_i \left(1 - e^{-\xi/\tau_i}\right) + \frac{\xi}{\eta_v} \quad \text{Equation 3.7}$$

Where:

$D(\xi)$ = creep compliance at reduced time ξ

ξ = reduced time (= t/a_t)

a_t = temperature shift factor

$D(0)$, D_i , τ_i , η_v = Prony series parameters

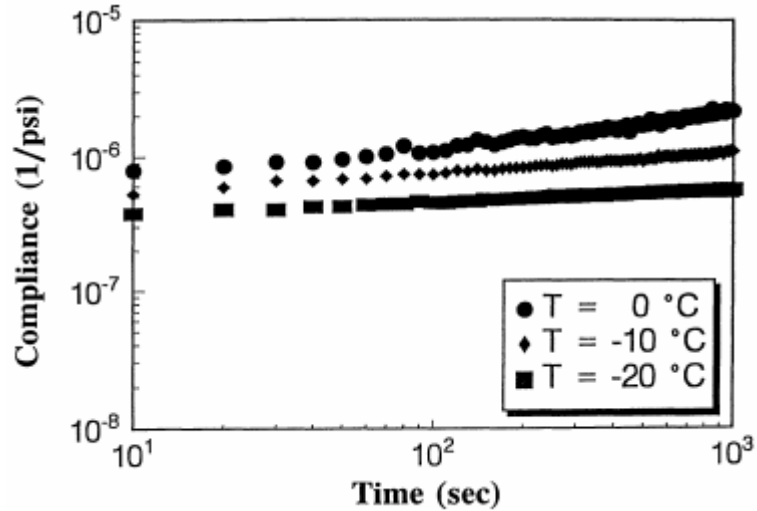


Figure 3.16. Indirect Tension Test Creep Compliance Curves (23).

In essence, the regression finds the best shift factors and Prony series parameters to fit the measured data based upon a least-squares criterion. One of the temperatures is selected as the reference temperature for the master curve (typically -20°C), and thus the creep compliance curve at this temperature is fixed in time ($a_t = 1$). The regression determines the amount of time (horizontal) shift required for the curves at the remaining temperatures to result in a smooth master curve. Each of these remaining creep compliance curves will thus have a shift factor (a_t) associated with it. Figure 3.17 shows the shifted creep compliance data.

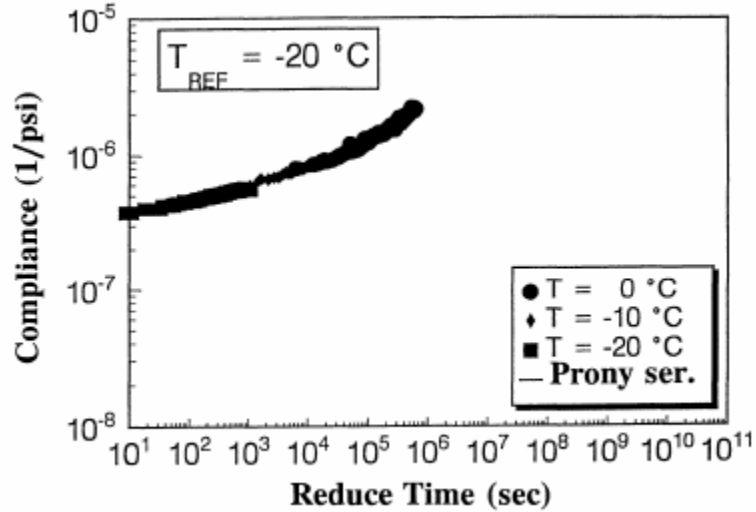


Figure 3.17. Prony Series Fit to Master Creep Compliance Curve (23).

The second step in the regression routine is to fit a second functional form to the master creep compliance information. This second functional form is the following power law:

$$D(\xi) = D(0) + D_1 \xi^m \quad \text{Equation 3.8}$$

where $D(\xi)$ and ξ are as defined previously, and $D(0)$, D_1 , and m are the coefficients of the functional form. The primary purpose for fitting this functional form is to determine the parameter m . This parameter is essentially the slope of the linear portion of the master creep compliance curve on a log-log plot (Figure 3.18). It has been found to be an important parameter in distinguishing between the thermal cracking performance of different materials.

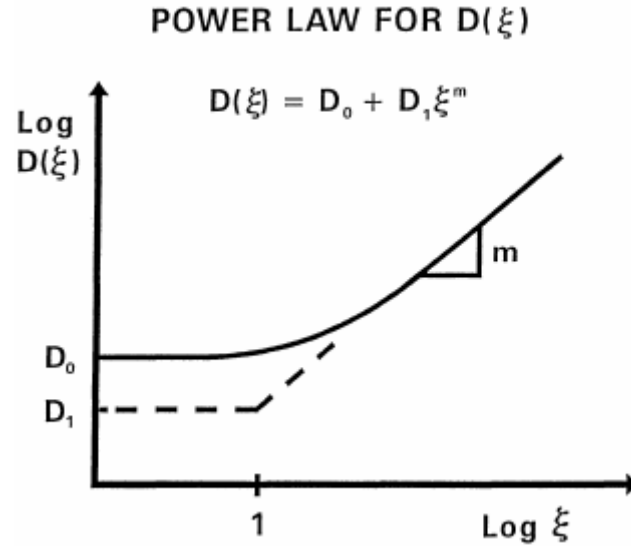


Figure 3.18. Determination of m , the Slope of the Log Creep Compliance Curve (23).

3.3.4 Flexural Beam Fatigue

Fatigue tests were conducted according to AASHTO TP 8, *Determining the Fatigue Life of Compacted Hot-Mix Asphalt Subjected to Repeated Flexural Bending*, to evaluate the stiffening effect of RAP on the mixture and its impact on the long-term fatigue life of the pavement. Three replicate beams were compacted with a kneading compactor to 6.0 ± 1.0 percent air voids and cut to dimensions of 380 mm long by 50 mm thick by 63 mm wide. The beams were placed in four-point loading and subjected to repeated haversine loads. The deflection caused by the load was measured at the center of the beam. The tests were performed under a constant-strain condition, at strain levels of 400 and 800 micro-strain and at a temperature of 20°C.

The variables measured include the number of cycles to failure, initial and final stiffnesses, and dissipated energy. The flexural stiffness is defined as:

$$S = \frac{1000 \times \sigma_t}{\varepsilon_t} \quad \text{Equation 3.9}$$

Where:

S = flexural stiffness, MPa

σ_t = maximum tensile stress, kPa

ε_t = maximum tensile microstrain

The initial stiffness is defined as the measured flexural stiffness after 50 cycles. The number of cycles to failure (N_f) is the load cycle at which the specimen exhibits a 50 percent reduction in stiffness relative to the initial stiffness. The dissipated energy is calculated by determining the area within the stress-strain hysteresis loop for each captured data pulse. The cumulative dissipated energy is the summation of the dissipated energy per cycle.

CHAPTER 4. TEST RESULTS AND ANALYSIS

4.1 MATERIAL PROPERTIES

4.1.1. Aggregates

Properties of the virgin and recycled SMA mixes used in Part 1 of the study are shown in Table 4.1. These data were used to perform an analysis of variance (shown in Table 4.2), which indicated that combined blend properties such as LA abrasion and flat and elongated particle content are mainly influenced by the aggregate source (p-values < 0.001). At 95% confidence level, RAP content and RAP type did not have a significant effect on percent loss or F/E particle content. As Table 4.3 shows, there is little variation in the aggregate properties of the RAP materials (3.0% difference for % loss and 0.8% difference for F/E particle content), which is the reason why RAP type is not significant in this data.

Table 4.1. Aggregate Properties for Combined Blends.

Aggregate	% RAP	RAP Type	LA Abrasion, % loss	F/E particles, % (3:1 ratio)
Mt. View	0	DG1	48.0	8.6
	10	-4	48.0*	4.0
	20	DG2	46.7	5.4
	30	+4	47.7	4.0
Lithia Springs	0	-4	39.6	11.3
	10	DG1	40.4	11.8
	20	+4	41.1	13.1
	30	DG2	41.0	17.5
Camak	0	+4	37.3	9.3
	10	DG2	38.7	7.9
	20	-4	37.3*	9.3
	30	DG1	40.3	12.9
Ruby	0	DG2	21.1	6.4
	10	+4	23.8	4.7
	20	DG1	26.4	5.7
	30	-4	21.1*	6.4

*Same as virgin blend because coarse recycled material was not added.

Table 4.2. Analysis of Variance for Aggregate Properties.

Factor	LA Abrasion		F/E Particles	
	F-statistic	p-value	F-statistic	p-value
Agg. Source	763.25	0.000	25.05	0.000
RAP Content	2.55	0.082	2.89	0.058
RAP Type	7.24	0.001	1.85	0.167

Table 4.3. Aggregate Properties for RAP Material.

RAP Type	LA Abrasion, % loss	F/E particles, % (3:1 ratio)
DG1	47.2	6.8
DG2	44.2	6.0
-4	N/A	N/A
+4	47.2	6.8

The effect of RAP addition on aggregate properties depended on the quality of the virgin and recycled materials contained in the blend. As mentioned above, the differences among aggregate sources were significant (Table 4.4), and they determined the results for

the combined blend. If a virgin aggregate is combined with RAP aggregates that have higher percent loss values, increasing the RAP content will increase the percent loss of the blend. Likewise, if a virgin aggregate is combined with RAP aggregates that have lower percent loss values, increasing the RAP content will decrease the percent loss of the blend. However, the differences produced by the increase in RAP content were very small (less than 1.5%, as Table 4.5 shows) and were not significant for these data. The results for the F/E particles had a maximum difference of 3.1% among RAP contents, which was not significant.

Table 4.4. Average Results for Aggregate Sources.

Aggregate Source	LA Abrasion, % Loss	F/E Particles, % (3:1 ratio)
Mt. View	47.6	5.5
Lithia Springs	40.5	13.4
Camak	38.2	9.8
Ruby	23.1	5.8

Table 4.5. Average Results for RAP Contents.

RAP Content, %	LA Abrasion, % Loss	F/E Particles, % (3:1 ratio)
0	36.5	8.9
10	37.5	7.1
20	37.9	8.4
30	37.5	10.2

4.1.2 Asphalt Binder

The single type of virgin asphalt cement was PG 76-22, which is a polymer-modified asphalt. The results for the virgin and recovered RAP asphalts are presented in Table 4.6.

The critical high temperatures for the extracted RAP binders were obtained by testing the recovered RAP binder as if it had been RTFO aged.

Table 4.6. Critical Temperatures and Performance Grades of Virgin and Recovered RAP Binders.

Aging	Property	Virgin Binder	Recovered RAP Binders			
			+4	-4	DG1	DG2
Original	G*/sin δ, kPa	78.9	---	---	---	---
RTFO	G*/sin δ, kPa	79.2	87.4	89.0	89.0	94.2
RTFO+PAV	G* sin δ, kPa	21.1	26.0	26.5	27.6	28.5
	BBR S, MPa	-27.2	-27.9	-28.1	-30.2	-25.1
	BBR m-value	-24.4	-25.5	-20.1	-23.9	-18.4
PG	Actual	78.9-24.4	87.4-25.5	89.0-20.1	89.0-23.9	94.2-18.4
	MP1	76-22	82-22	88-16	88-22	94-16

The actual binder properties of the blends are shown in Tables 4.7 through 4.10. It can be observed that among RAP types, blends that contain DG2 RAP had higher values of $G^*/\sin\delta$ at a given RAP content for both original (1.96 kPa and higher at passing temperatures) and RTFO aged samples (3.5 kPa and higher at passing temperatures), which indicates better resistance of the resulting binder blends to rutting. Blends containing DG2 RAP also had lower values of $G^*\sin\delta$ than the corresponding blends containing other RAP binder types (maximum 3,847 kPa at passing temperature). This is indicative of a higher fatigue cracking resistance for these binder blends.

Finally, the properties obtained with the BBR test (creep stiffness and creep rate) also had more favorable results for blends using DG2 RAP binder. These blends had lower stiffness (maximum 151 MPa at passing temperature) and higher creep rate (0.322 and higher at passing temperatures) than the corresponding blends containing other RAP binder types. Low creep stiffness values are desired in order to minimize thermal stresses, while the m-value must be high to maximize the ability of the HMA pavement to relieve

those stresses; therefore, mixtures that contain DG2 RAP have a binder blend that is more resistant to thermal cracking.

Table 4.7. Measured Binder Properties of +4 RAP Blends.

Aging	Property	Critical Property	Temp. °C	+4 RAP		
				10%	20%	30%
Original	G*/sin δ, kPa	≥ 1.00 kPa	76	1.290	1.634	2.521
			82	0.762	0.967	1.354
RTFO	G*/sin δ, kPa	≥ 2.20 kPa	76	2.695	2.802	3.312
			82	1.570	1.559	1.968
RTFO+PAV	G* sin δ, kPa	≤ 5,000 kPa	25	3,427	3,614	4,413
			22	4,915	5,190	6,233
	BBR S, MPa	≤ 300 MPa	-12	148	157	167
			-18	273	270	264
	BBR m-value	≥ 0.300	-12	0.332	0.324	0.304
			-18	0.276	0.223	0.266

Table 4.8. Measured Binder Properties of -4 RAP Blends.

Aging	Property	Critical Property	Temp. °C	-4 RAP		
				10%	20%	30%
Original	G*/sin δ, kPa	≥ 1.00 kPa	76	1.578	1.657	1.849
			82	0.884	0.956	1.036
RTFO	G*/sin δ, kPa	≥ 2.20 kPa	76	3.018	3.318	3.964
			82	1.760	1.818	2.087
RTFO+PAV	G* sin δ, kPa	≤ 5,000 kPa	25	4,370	4,153	4,690
			22	6,227	5,915	6,520
	BBR S, MPa	≤ 300 MPa	-12	176	179	182
			-18	287	297	297
	BBR m-value	≥ 0.300	-12	0.304	0.306	0.291
			-18	0.261	0.263	0.266

Table 4.9. Measured Binder Properties of DG1 RAP Blends.

Aging	Property	Critical Property	Temp. °C	DG1 RAP		
				10%	20%	30%
Original	G*/sin δ, kPa	≥ 1.00 kPa	76	1.518	1.593	
			82	0.877	0.885	1.112
			88			0.603
RTFO	G*/sin δ, kPa	≥ 2.20 kPa	76	3.032	3.183	
			82	1.736	1.843	2.243
			88			1.217
RTFO+PAV	G* sin δ, kPa	≤ 5,000 kPa	25	3,688	3,997	4,149
			22	5,297	5,715	5,854
	BBR S, MPa	≤ 300 MPa	-12	164	164	168
			-18	308	344	345
	BBR m-value	≥ 0.300	-12	0.313	0.311	0.304
			-18	0.326	0.254	0.271

Table 4.10. Measured Binder Properties of DG2 RAP Blends.

Aging	Property	Critical Property	Temp. °C	DG2 RAP		
				10%	20%	30%
Original	G*/sin δ, kPa	≥ 1.00 kPa	76	2.039	1.965	
			82	1.150	1.101	2.676
			88			0.652
RTFO	G*/sin δ, kPa	≥ 2.20 kPa	76	3.488	4.038	4.213
			82	2.042	2.274	2.676
RTFO+PAV	G* sin δ, kPa	≤ 5,000 kPa	25	3,030	3,416	3,847
			22	4,374	4,876	5,438
	BBR S, MPa	≤ 300 MPa	-12	142	127	151
			-18	317	299	317
	BBR m-value	≥ 0.300	-12	0.334	0.329	0.322
			-18	0.281	0.271	0.260

Table 4.6 showed that the critical high temperatures of the RAP binders are higher than that of the virgin binder, which suggests that the combined blends of the recycled mixture should be more resistant to rutting. The intermediate temperatures were also higher for the RAP binders, meaning that the fatigue resistance of the asphalt blends may be affected by the addition of RAP binder. The ability of the combined blends to resist thermal cracking could also be affected, since three of the RAP binders had critical low

temperatures higher than that of the virgin binder and this could cause the combined blends to have higher critical low temperatures as well.

DG2 RAP binder has a higher critical high temperature (Table 4.6), which caused the DG2 RAP binder blends to have critical high temperatures at least 1.7°C higher than the other blends (Figure 4.1). It can also be observed that blends containing -4 RAP always had a higher critical high temperature than blends containing +4 RAP. This could be due to the higher asphalt content in -4 RAP, which results in a lower demand of virgin asphalt in the mix. The resulting asphalt blends are therefore stiffer and have higher values of critical high temperatures.

Even though the recovered DG2 RAP binder had the highest temperatures in both cases, in general, the combined DG2 RAP blends had critical intermediate temperatures between 0.5°C and 3.0°C lower than the other blends, as shown in Figure 4.2. The DG2 RAP blends also had most critical low temperatures between 0.1°C and 4.3°C lower than the other blends, and only in one case was the critical temperature exceeded by that of the blend containing +4 RAP (Figure 4.3).

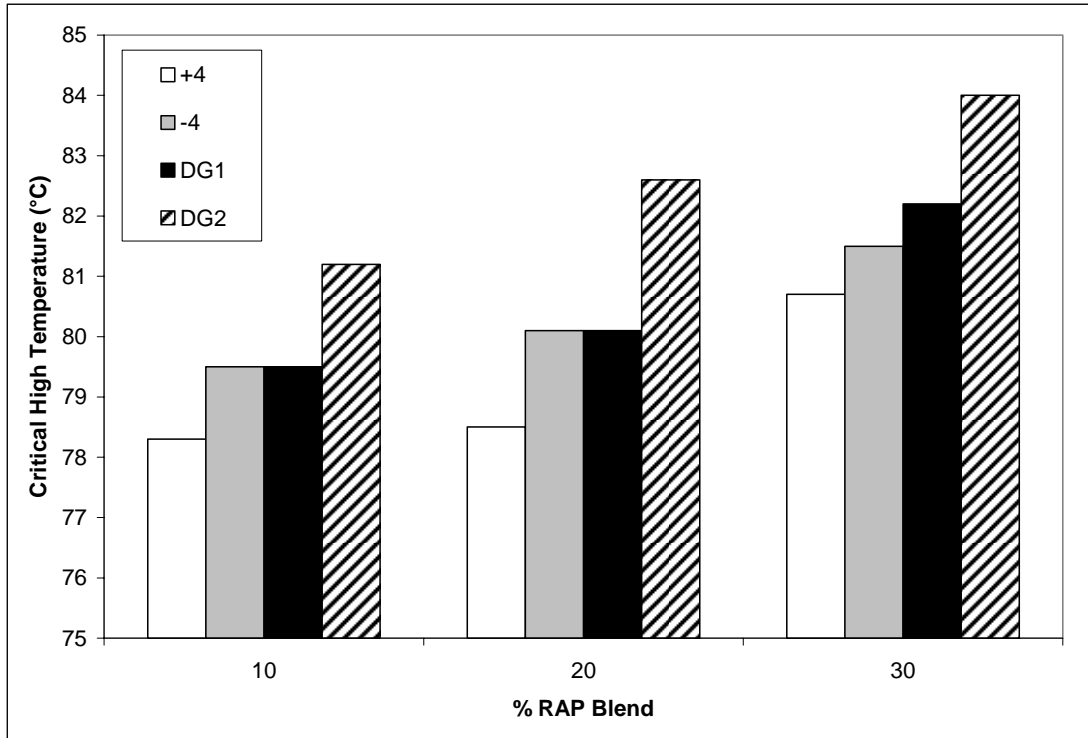


Figure 4.1. Critical High Temperatures for Binder Blends.

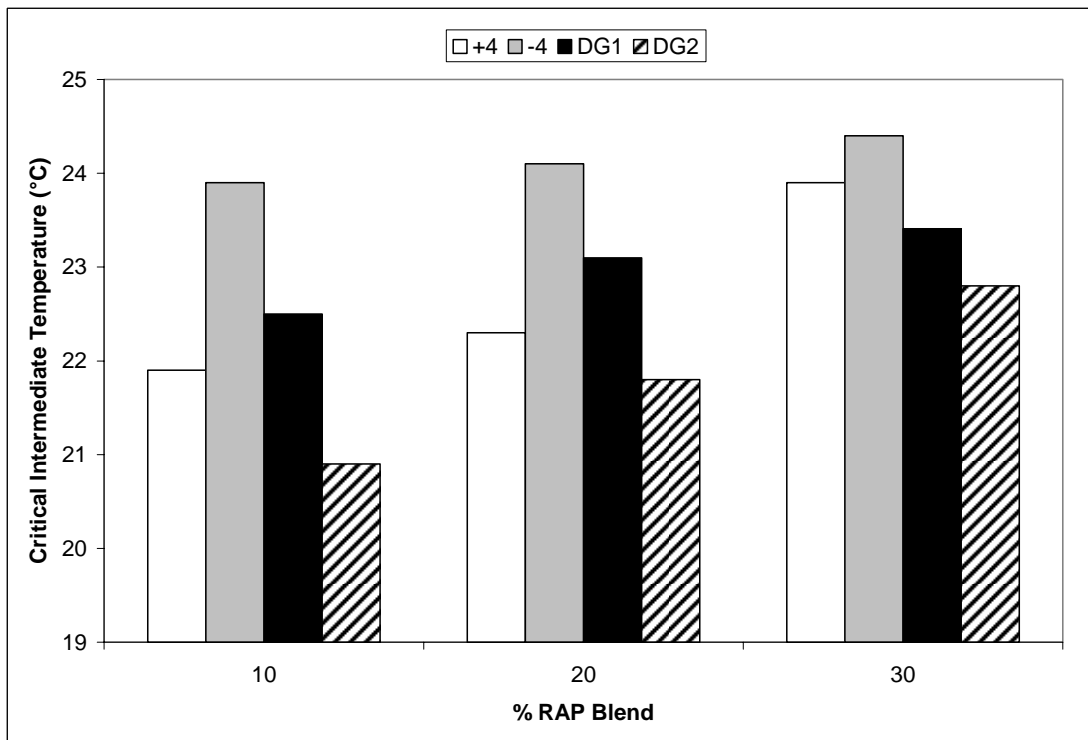


Figure 4.2. Critical Intermediate Temperatures for Binder Blends.

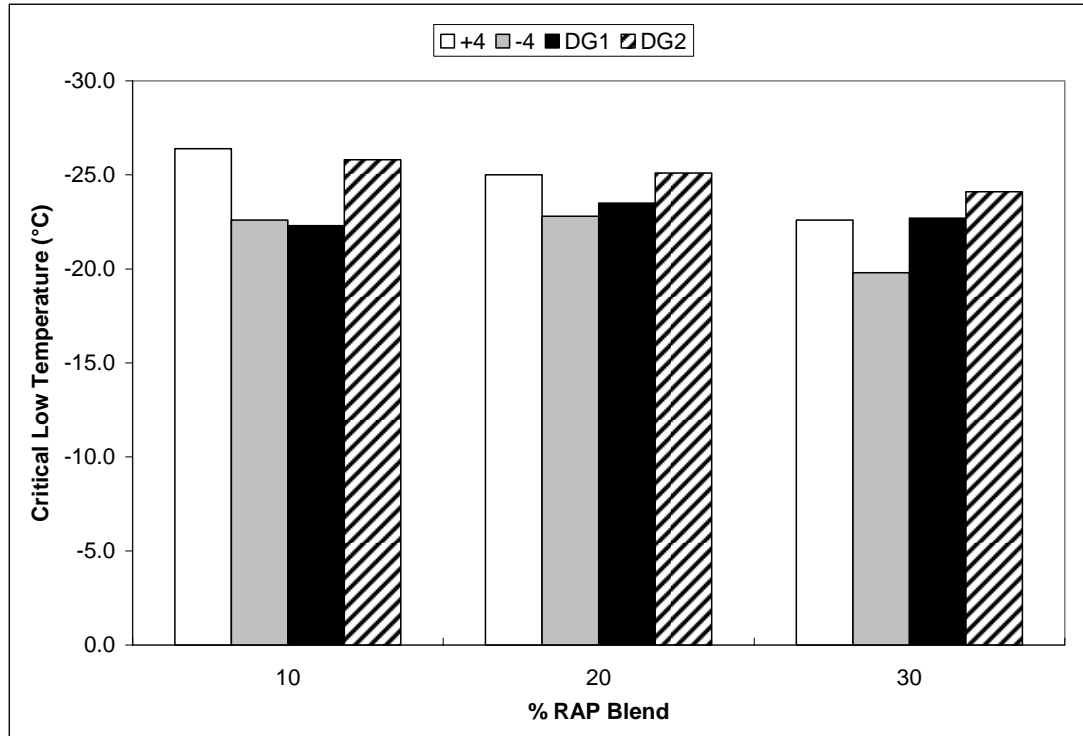


Figure 4.3. Critical Low Temperatures for Binder Blends.

Table 4.11 shows the results for the performance grades of the binder blends. The addition of 10% RAP binder did not change the performance grade of the binder blends. Increasing the RAP binder content to 20% only affected the DG2 blend by raising the high-temperature grade by one grade. The low temperature performance grade remained the same as the virgin asphalt binder. Finally, the use of 30% RAP binder reduced the low-temperature grade of the -4 blend by one grade, raised the high-temperature grade of the DG1 blend by one grade, and had no further effect on the DG2 and +4 blends.

These results support the ETG design guidelines (8), where no PG grade change in the virgin binder is necessary for mixtures containing less than 15% RAP; mixtures containing 16 to 25% RAP require the new asphalt binder to be one grade lower than the

grade required for a virgin asphalt binder, and mixtures with over 25% RAP need to select the new asphalt binder using a blending chart.

Table 4.11. Performance Grades of RAP Blends.

RAP Source	% RAP blend	Performance Grade	
		Actual	MP 1
+4	0	PG 78.9-24.4	PG 76-22
	10	PG 78.3-26.4	PG 76-22
	20	PG 78.5-25.0	PG 76-22
	30	PG 80.7-22.6	PG 76-22
-4	0	PG 78.9-24.4	PG 76-22
	10	PG 79.5-22.6	PG 76-22
	20	PG 80.1-22.8	PG 76-22
	30	PG 81.5-19.8	PG 76-16
DG1	0	PG 78.9-24.4	PG 76-22
	10	PG 79.5-23.5	PG 76-22
	20	PG 80.1-23.5	PG 76-22
	30	PG 82.2-22.7	PG 82-22
DG2	0	PG 78.9-24.4	PG 76-22
	10	PG 81.2-25.8	PG 76-22
	20	PG 82.6-25.1	PG 82-22
	30	PG 83.8-24.1	PG 82-22

The trends of binder properties obtained with the DSR and BBR tests in the range of 0% to 30% RAP binder in the blend were analyzed for the different mixtures in this study. The rates of change of the properties in that range were calculated to assess the impact of the RAP asphalt content in the blends. These rates were computed as the change in the binder property divided by the change in RAP content, for the entire range studied. The results are discussed below.

DSR Results

Results for the rutting and fatigue parameters were analyzed for original (unaged) blends, RTFO-aged and RTFO+PAV aged blends at failing and passing temperatures. Estimated and actual critical temperatures were compared for original and aged blends.

Figure 4.4 shows that, as expected, the rutting parameter $G^*/\sin\delta$ in the original blends was higher at the low temperature and increased with the addition of RAP binder because the old binder makes the resulting blends stiffer. The rates of increase were also higher at the low temperature (Table 4.12), with the biggest rates being that of +4 and DG2 RAP mixtures, but they were not significant for the range of RAP binder percentages used in this study (0-30%).

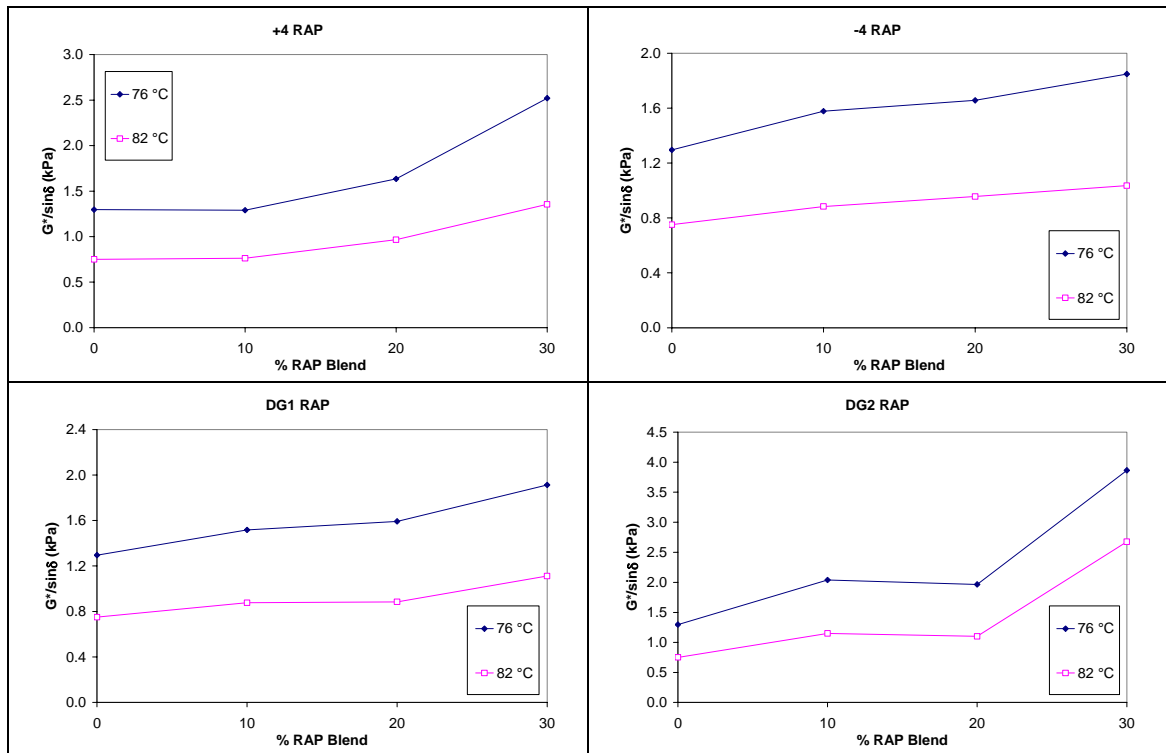


Figure 4.4. $G^*/\sin\delta$ Trends for Unaged RAP Blends.

Table 4.12. Rate of Increase in $G^*/\sin\delta$ for Unaged Blends.

RAP Type	Increase Rate (kPa/%RAP)	
	76°C	82°C
+4	0.041	0.020
-4	0.018	0.010
DG1	0.021	0.012
DG2	0.086	0.064

The results for RFTO-aged blends, shown in Figure 4.5 were similar to those of unaged blends. Lower temperature and higher RAP binder percentages increased $G^*/\sin\delta$, but not at a high rate, as shown in Table 4.13 (increase rates smaller than 0.05kPa/%RAP). This suggests that even though the rutting parameter increases with the addition of RAP for both original and RTFO-aged blends, the rates of change are so small that the rutting resistance of the mixes is not likely to be significantly improved.

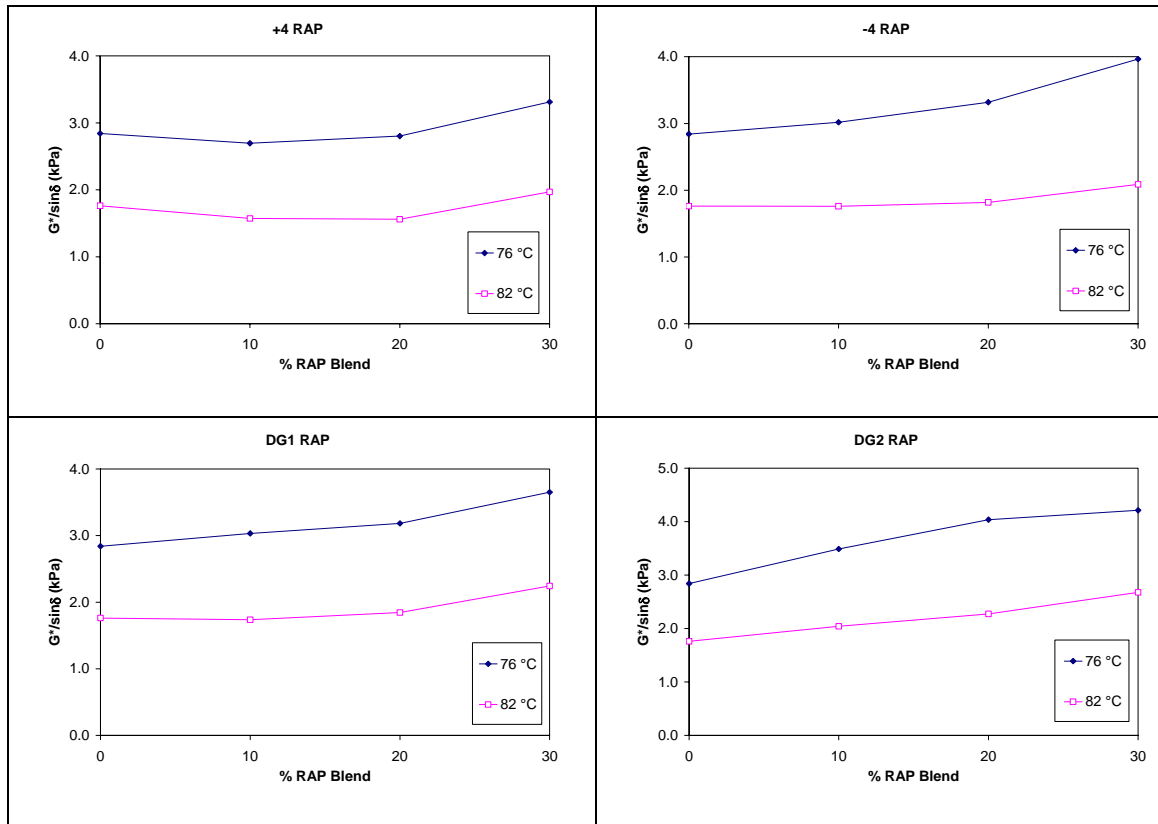


Figure 4.5. $G^*/\sin\delta$ Trends for RTFO-Aged RAP Blends.

Table 4.13. Rate of Increase in $G^*/\sin\delta$ for RTFO-Aged Blends.

RAP Type	Increase Rate (kPa/%RAP)	
	76 °C	82 °C
+4	0.016	0.007
-4	0.037	0.011
DG1	0.027	0.016
DG2	0.046	0.031

For the RTFO and PAV residues, the fatigue parameter $G^*/\sin\delta$ increased with the addition of RAP binder (Figure 4.6). The results were considerably higher the lower temperature. Unlike the trends for the unaged and RTFO-aged blends, the rate of increase was much more significant in this case (over 25 kPa/%RAP), especially for the +4 and -4 RAP blends, where the rate of increase is as high as 68.4 kPa/%RAP (Table 4.14).

These results indicate that the fatigue resistance of the binder blends is highly influenced by temperature and RAP content. Addition of RAP binder may result in mixes more susceptible to fatigue cracking, especially at high temperatures.

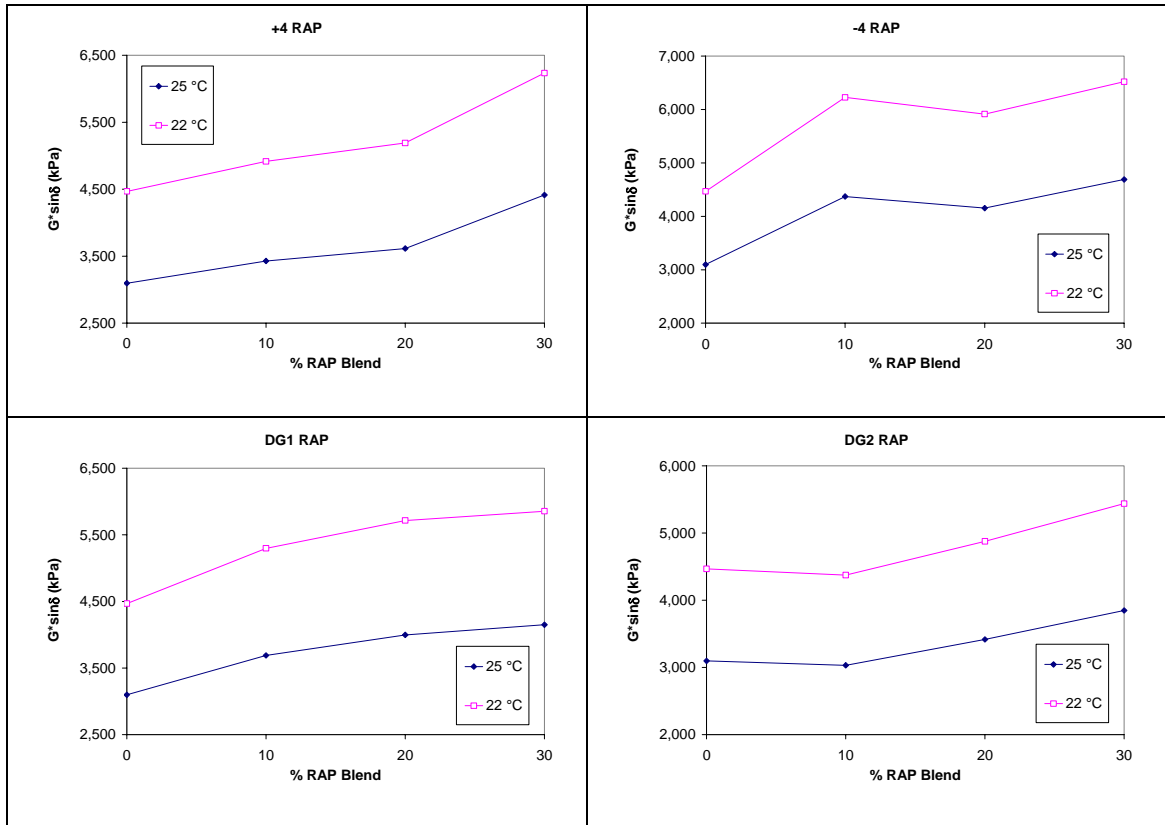


Figure 4.6. $G^* \sin \delta$ Trends for RTFO+PAV-Aged RAP Blends.

Table 4.14. Rate of Increase in $G^* \sin \delta$ for RTFO and PAV-Aged Blends.

RAP Type	Increase Rate (kPa/%RAP)	
	22°C	25°C
+4	58.9	43.9
-4	68.4	53.1
DG1	46.2	35.1
DG2	32.4	25.0

BBR Results

Results for creep stiffness and creep rate obtained with the bending beam rheometer were analyzed for the asphalt blends at failing and passing temperatures. Figure 4.7 shows that the creep stiffness of the blends increased with lower temperature and addition of RAP binder, although it did it at a slow rate, as seen in Table 4.15 (maximum 2.85 MPa/%RAP). In most cases, the increase rate was higher at the lower temperature (Table 4.15). The results suggest that addition of RAP is not highly influential for the creep stiffness of the binder blend at the temperatures studied (low rates of increase), but could become more significant at lower temperatures.

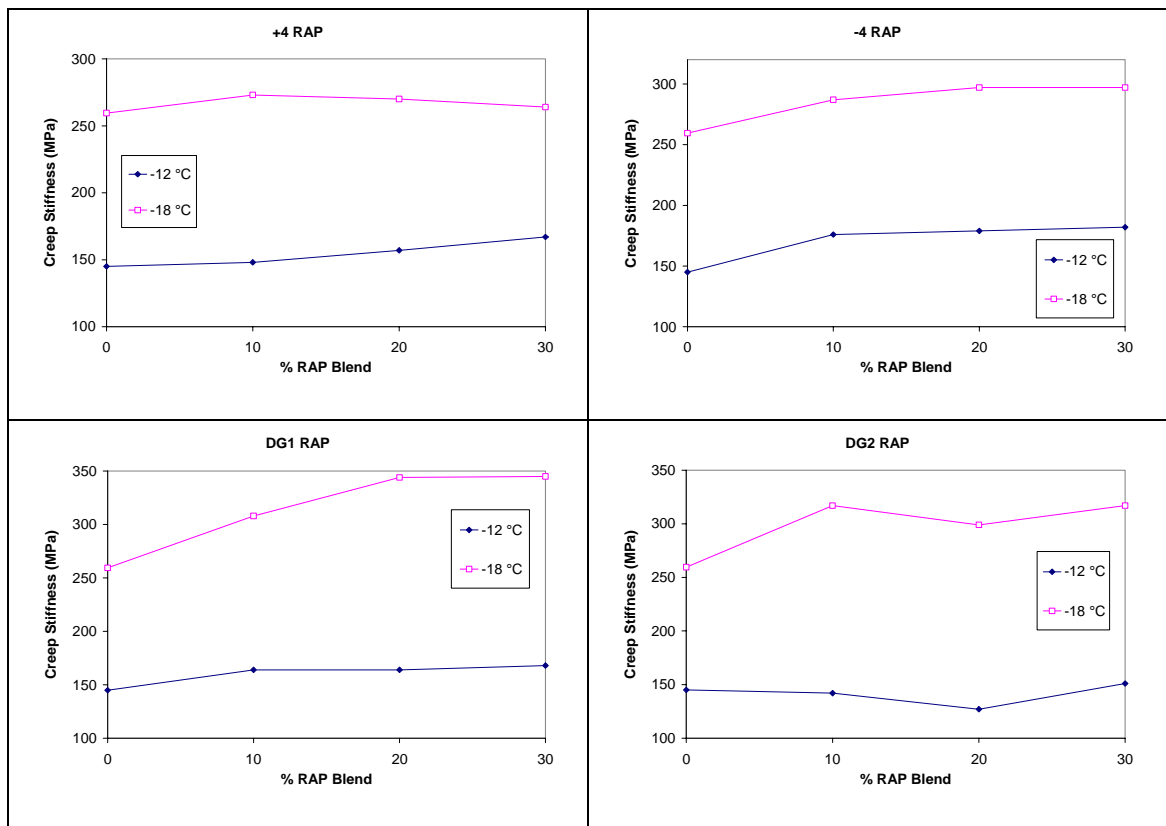


Figure 4.7. Creep Stiffness Trends for RAP Blends.

Table 4.15. Rate of Increase in Creep Stiffness.

RAP Type	Increase Rate (MPa/%RAP)	
	-18°C	-12°C
+4	0.150	0.733
-4	1.250	1.233
DG1	2.850	0.767
DG2	1.917	0.200

Figure 4.8 shows that, as expected, higher RAP binder percentages and low temperature resulted in lower creep rates. The decrease rate for these values was very small (less than 0.0011 MPa/%RAP) and had a maximum variation of 0.008 MPa/%RAP between temperatures (Table 4.16). As with creep stiffness, the small rates of change suggest that increasing RAP content does not decrease the creep rate significantly, and that the thermal cracking resistance of the recycled binder blends will not be affected.

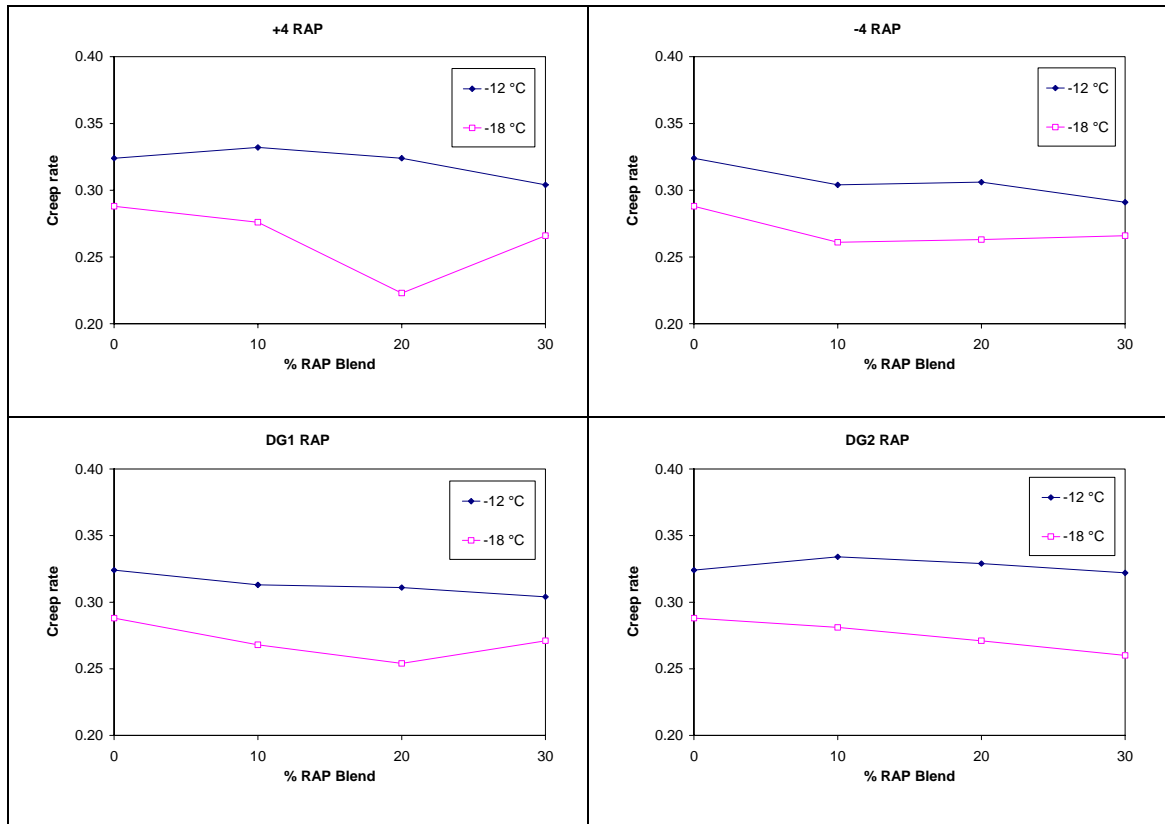


Figure 4.8. Creep Rate Trends for RAP Blends.

Table 4.16. Rate of Decrease in Creep Rate.

RAP Type	Decrease Rate (MPa/%RAP)	
	-18°C	-12°C
+4	-0.0007	-0.0007
-4	-0.0007	-0.0011
DG1	-0.0006	-0.0007
DG2	-0.0009	-0.0001

4.2 MIX DESIGNS

Table 4.17 shows the virgin asphalt content, total asphalt content (virgin binder plus RAP binder), voids in the mineral aggregate (VMA), and voids filled with asphalt (VFA). The mix design information for all mixtures is presented in Appendix A. The VMA values

were calculated using the effective specific gravity (G_{se}) of the aggregate blends, as specified by GDOT. It can be observed that the results for VMA and VFA do not change significantly with the addition of RAP or with the types of RAP used.

Table 4.17. Volumetric Properties of RAP Mixtures.

Aggregate Source	% RAP	RAP Type	Total AC, %	VMA, %	VFA, %
Mt. View	0	+4	6.2	18.3	74.6
	10	DG2	6.1	18.2	77.2
	20	-4	6.8	19.3	80.3
	30	DG1	6.3	18.3	78.9
Lithia Springs	0	-4	6.2	18.1	76.5
	10	DG1	6.0	17.6	76.8
	20	+4	6.4	18.0	79.4
	30	DG2	6.0	17.3	77.1
Camak	0	DG1	6.9	19.6	78.8
	10	-4	6.4	18.9	76.4
	20	DG2	6.9	19.4	79.0
	30	+4	7.3	19.8	82.8
Ruby	0	DG2	6.2	18.5	76.7
	10	+4	5.9	18.0	76.4
	20	DG1	6.6	18.9	79.8
	30	-4	5.8	17.6	76.5

One parameter that can be useful to evaluate the impact of RAP addition on mixture performance is the ratio of old binder to virgin binder, shown in Table 4.18. Figure 4.9 shows that as RAP content increases, the ratio of old binder to virgin binder increases as well. When grouped by RAP type, mixes that contained -4 RAP had the highest ratio (0.19) due to the higher asphalt content present in -4 RAP (6.2%). For aggregate sources, mixes that contained Ruby aggregates had the highest ratio (0.18). Figure 4.10 shows the virgin and RAP asphalt binder contents for each mixture.

Table 4.18. Virgin and RAP Binder Contents for SMA Mixes.

RAP Type	% RAP	Agg. Source	Virgin AC, %	Old AC, %	Old AC/Virgin AC
+4	0	Camak	6.9	0.0	0.00
	10	Ruby	5.5	0.4	0.08
	20	Lithia Springs	5.5	0.9	0.16
	30	Mt. View	5.0	1.3	0.26
-4	0	Lithia Springs	6.2	0.0	0.00
	10	Mt. View	5.5	0.6	0.11
	20	Camak	5.7	1.2	0.21
	30	Ruby	4.0	1.8	0.45
DG1	0	Mt. View	6.2	0.0	0.00
	10	Lithia Springs	5.5	0.5	0.10
	20	Ruby	5.5	1.1	0.19
	30	Camak	5.7	1.6	0.28
DG2	0	Ruby	6.2	0.0	0.00
	10	Camak	6.0	0.4	0.07
	20	Mt. View	6.0	0.8	0.14
	30	Lithia Springs	4.7	1.3	0.27

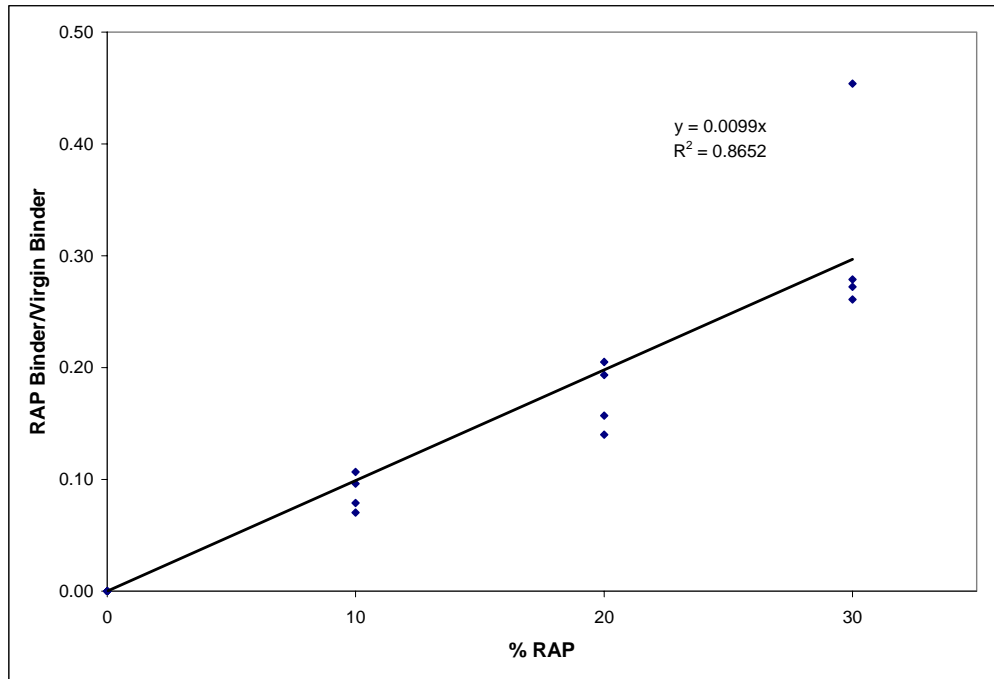


Figure 4.9. Old to New Asphalt Ratio vs RAP Content.

Table 4.19 illustrates the savings in virgin binder content for all RAP types. These savings were calculated as a percent of reduction on virgin binder compared to the control mix. Since there are four different mixes with 0% RAP (one for each aggregate source), these percentages were computed by matching the recycled SMA mix with the control mix that contained the same aggregate source. For example, the mix that contains 10% -4 RAP and Camak aggregates was compared to the control mix that contains Camak aggregates; while the mix that contains 20% -4 RAP and Mt. View aggregates was compared to the control mix that contains Mt. View aggregates, and so on.

At 10% and 20% RAP, the reduction in the required virgin binder is very similar (averages of 11.7% and 10.8%, respectively). Normally, the required amount of virgin binder will decrease with RAP content, and these results can be attributed to variability in mix design. At 30% RAP the savings increase dramatically to an average of 24.1%, which would represent an important economical benefit, since asphalt cement is the most expensive component of an HMA mix. This benefit is particularly important for mixtures containing -4 RAP, where the virgin binder required is reduced in up to 35.5%.

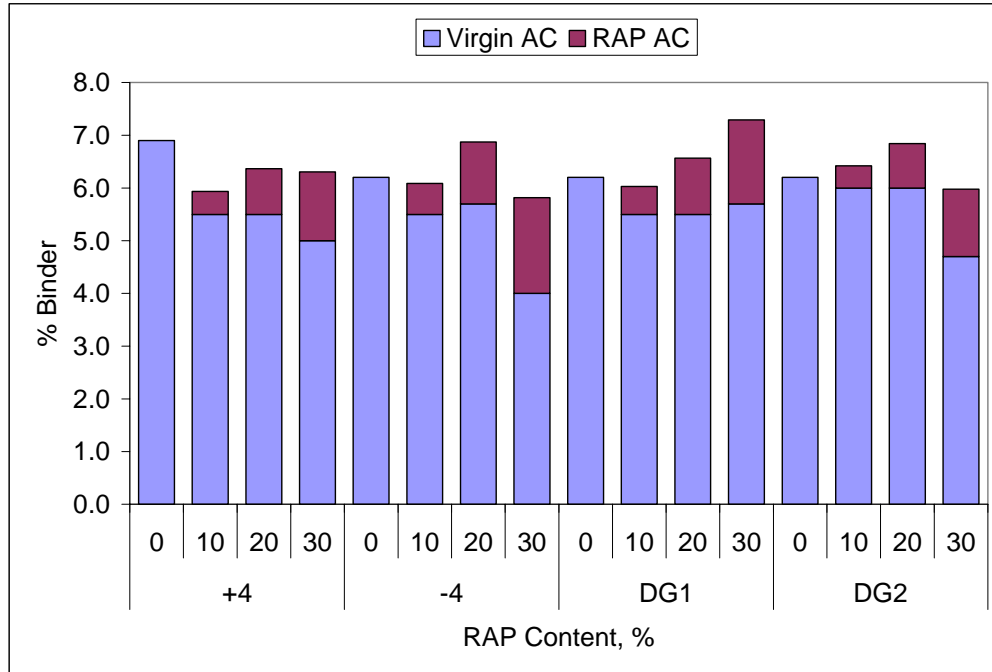


Figure 4.10. Asphalt Contents for SMA Mixtures.

Table 4.19. Savings in Virgin Binder (%) for RAP Mixtures.

% RAP	RAP Type				Average
	DG1	DG2	-4	+4	
10	11.3	13.0	11.3	11.3	11.7
20	11.3	3.2	17.4	11.3	10.8
30	17.4	24.2	35.5	19.4	24.1

4.3 PERFORMANCE TESTS

4.3.1 Moisture Susceptibility

Table 4.20 and Figure 4.11 show the wet (conditioned) and dry (unconditioned) strength values for the SMA mixes with recycled material. An analysis of variance (shown in Table 4.21) indicated that at 95% confidence level, the amount of RAP significantly influences the tensile strength (p-values < 0.001), while type of RAP has a significant effect (p-value = 0.015 for dry strength and 0.019 for wet strength). This was expected

because increasing the RAP content increases the amount of old binder (binder from RAP) and makes the mixture stiffer, which has an effect on the tensile strength and bond to the aggregates. The analysis of variance also indicated that the interaction between aggregate source and RAP type is significant for both conditioned and unconditioned tensile strengths (p-values < 0.001).

Table 4.20. Tensile Strengths for SMA Mixtures.

RAP Type	% RAP	Agg. Source	Unconditioned Tensile Strength (psi)	Conditioned Tensile Strength (psi)
+4	0	Camak	87.7	78.7
	10	Ruby	103.6	92.3
	20	Lithia Springs	87.0	90.8
	30	Mt. View	105.7	99.8
-4	0	Lithia Springs	89.0	70.9
	10	Mt. View	87.2	88.2
	20	Camak	98.5	85.7
	30	Ruby	144.7	141.7
DG1	0	Mt. View	71.6	71.6
	10	Lithia Springs	83.6	79.7
	20	Ruby	83.1	83.6
	30	Camak	124.8	118.1
DG2	0	Ruby	69.7	70.2
	10	Camak	85.1	72.3
	20	Mt. View	101.9	91.9
	30	Lithia Springs	94.8	95.8

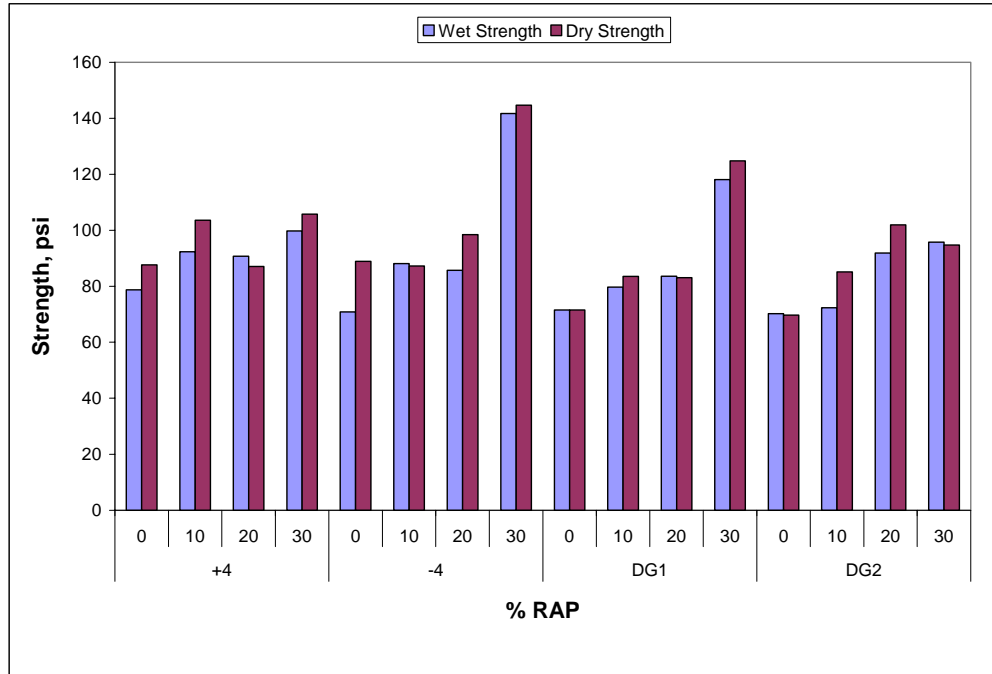


Figure 4.11. Strength Values from Moisture Susceptibility Test.

Table 4.21. Analysis of Variance for Tensile Strengths.

Factor	Unconditioned		Conditioned	
	F-statistic	p-value	F-statistic	p-value
Agg. Source	2.24	0.099	3.18	0.035
RAP Content	18.21	0.000	33.61	0.000
RAP Type	3.96	0.015	3.73	0.019
Agg. Source x RAP Type	16.33	0.000	33.90	0.000

Figure 4.12 shows that strength increased as the percentage of RAP increased. This is not surprising since recycled SMA mixtures contain RAP binder that would be expected to have an effect on the mixture properties of the samples, such as increased stiffness. Table 4.22 shows the differences in tensile strengths for various RAP contents and confirms that the higher the RAP content, the more significant those differences become. This can be attributed to the higher old to new binder ratio for mixtures with higher RAP contents.

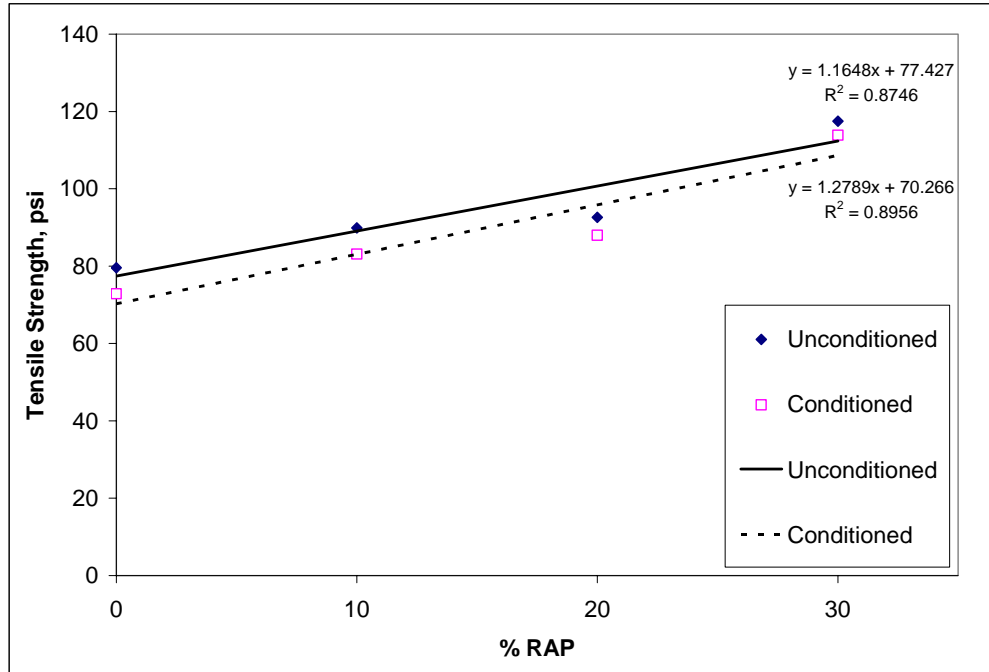


Figure 4.12. Effect of RAP Percentage on Tensile Strength.

Table 4.22. Tensile Strength Comparisons for SMA Mixes with Various RAP Contents.

% RAP	Unconditioned		Conditioned	
	Difference of Means (psi)	Are differences significant at 95% confidence level?	Difference of Means (psi)	Are differences significant at 95% confidence level?
0 – 10	10.30	No	10.28	No
0 – 20	13.03	No	15.16	Yes
0 – 30	37.91	Yes	41.01	Yes
10 – 20	2.74	No	4.88	No
10 – 30	27.62	Yes	30.72	Yes
20 – 30	24.88	Yes	25.85	Yes

The pairwise comparisons for tensile strengths among RAP types are shown in Table 4.23, where it can be observed that the differences among RAP types are not significant, except between mixes containing -4 RAP and mixes containing DG2 RAP. Figure 4.13 shows that recycled mixtures using -4 RAP had the highest tensile strengths (96.6 psi for conditioned and 104.9 psi for unconditioned specimens), which was

expected because as mentioned earlier, these mixtures have the highest old to new binder ratio (an average of 0.19), and this increases stiffness. Recycled mixtures using DG2 RAP, have the lowest old to new binder ratio (an average of 0.12) which produces a softer binder blend, and this caused them to have the lowest tensile strengths (82.6 psi for conditioned and 87.9 psi for unconditioned specimens).

Table 4.23. Tensile Strength Comparisons for SMA Mixes with Various RAP Types.

RAP Type	Unconditioned		Conditioned	
	Difference of Means (psi)	Are differences significant at 95% confidence level?	Difference of Means (psi)	Are differences significant at 95% confidence level?
DG1 – DG2	-2.89	No	-5.69	No
DG1 – -4	14.18	No	8.38	No
DG1 – +4	5.26	No	2.14	No
DG2 – -4	17.07	Yes	14.07	Yes
DG2 – +4	8.16	No	7.83	No
-4 – +4	-8.92	No	-6.24	No

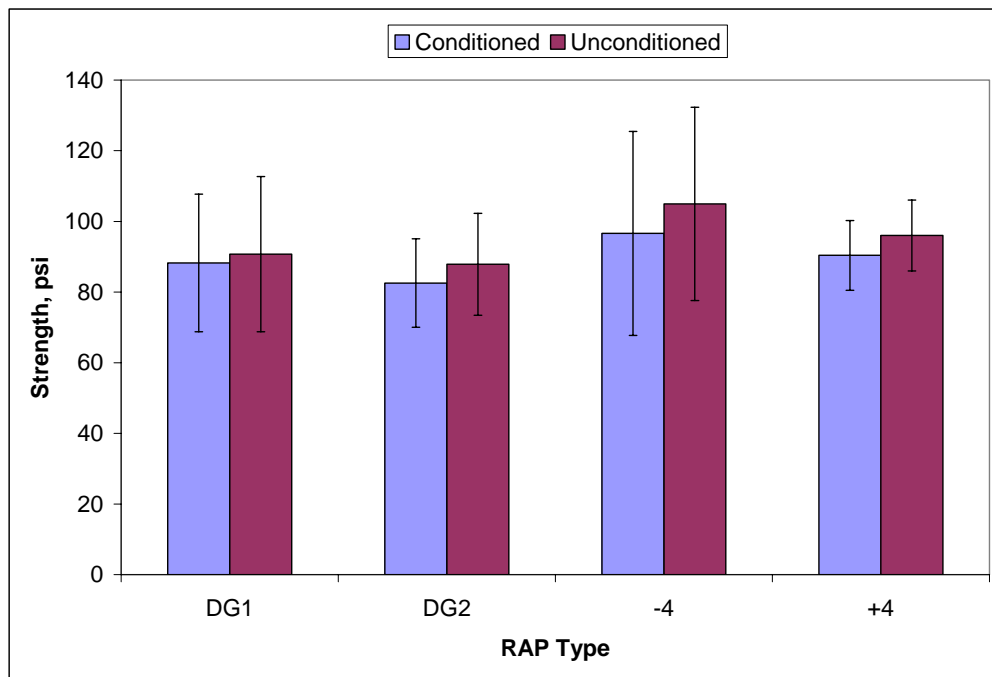


Figure 4.13. Strength Values for RAP Types.

Tables 4.24 and 4.25 show the difference of mean tensile strengths for the interaction term for conditioned and unconditioned specimens. The results are consistent with the trend observed for the individual factors: mixtures with higher old to new binder ratio had higher tensile strengths, such as mixtures containing Ruby aggregates and -4 RAP, which had an average ratio of 0.45 and tensile strengths up to 75.0 psi higher for unconditioned and 71.5 psi higher for conditioned specimens.

Table 4.24. Unconditioned Tensile Strengths Comparisons for Aggregate Source – RAP Type Interaction.

RAP Type	Difference of Means (psi)			
	Mt. View	Lithia Spr.	Camak	Ruby
DG1 – DG2	30.3	11.2	-39.7	-13.4
DG1 – -4	15.6	5.5	-26.3	61.6
DG1 – +4	34.2	3.5	-37.1	20.5
DG2 – -4	-14.7	-5.4	13.3	75.0
DG2 – +4	3.8	-7.7	2.6	33.9
-4 – +4	18.5	-2.4	-10.8	-41.4

Significant differences at 95% confidence level are in bold.

Table 4.25. Conditioned Tensile Strengths Comparisons for Aggregate Source – RAP Type Interaction.

RAP Type	Difference of Means (psi)			
	Mt. View	Lithia Spr.	Camak	Ruby
DG1 – DG2	20.3	16.1	-45.8	-13.4
DG1 – -4	16.6	-8.8	-32.4	58.1
DG1 – +4	28.2	11.1	-39.4	8.7
DG2 – -4	-3.7	-24.9	13.4	71.5
DG2 – +4	7.9	-5.0	6.3	22.1
-4 – +4	11.7	19.9	-7.0	-49.4

Significant differences at 95% confidence level are in bold.

Tables 4.26 through 4.30 summarize the moisture susceptibility results. All mixtures contained between 0.8 and 1.0 percent of lime by total weight of mix. A minimum TSR of 0.80 is generally required by GDOT for SMA mixtures. However, a

TSR of 0.7 may be acceptable so long as all individual test values exceed 100 psi. All mixtures met or exceeded the 0.8 minimum retained strength.

Table 4.26. Moisture Susceptibility Results for Control Mixes.

Measurement	Mt. View	Lithia Springs	Camak	Ruby
Unconditioned Samples				
% Air voids	7.2	7.1	7.1	6.5
Load, lbs	1,124	1,397	1,377	1,094
Dry S, psi	71.6	89.4	87.7	69.7
Conditioned Samples				
% Air voids	7.2	7.7	7.7	6.9
Load, lbs	1,124	1,114	1,236	1,103
Wet S, psi	71.6	70.9	78.7	70.2
% Saturation	77.4	75.0	54.2	64.4
TSR	1.00	0.80	0.90	1.01

Table 4.27. Moisture Susceptibility Results for SMA Mixes Using +4 RAP.

Measurement	+4 RAP		
	10% Ruby	20% Lithia Springs	30% Mt. View
Unconditioned Samples			
% Air voids	6.8	7.3	6.9
Load, lbs	1,628	1,367	1,661
Dry S, psi	103.6	87.0	105.7
Conditioned Samples			
% Air voids	6.8	7.3	6.8
Load, lbs	1,450	1,426	1,568
Wet S, psi	92.3	90.8	99.8
% Saturation	85.6	86.0	71.7
TSR	0.89	1.04	0.94

Table 4.28. Moisture Susceptibility Results for SMA Mixes Using -4 RAP.

Measurement	-4 RAP		
	10% Mt. View	20% Camak	30% Ruby
Unconditioned Samples			
% Air voids	6.9	6.6	6.5
Load, lbs	1,370	1,547	2,273
Dry S, psi	87.2	98.5	144.7
Conditioned Samples			
% Air voids	6.9	7.0	6.4
Load, lbs	1,385	1,346	2,226
Wet S, psi	88.2	85.7	141.7
% Saturation	78.4	76.0	82.6
TSR	1.01	0.87	0.98

Table 4.29. Moisture Susceptibility Results for SMA Mixes Using DG1 RAP.

Measurement	DG1 RAP		
	10% Lithia Springs	20% Ruby	30% Camak
Unconditioned Samples			
% Air voids	7.1	6.2	6.6
Load, lbs	1,313	1,305	1,960
Dry S, psi	83.6	83.1	124.8
Conditioned Samples			
% Air voids	7.1	6.2	6.6
Load, lbs	1,252	1,314	1,855
Wet S, psi	79.7	83.6	118.1
% Saturation	75.1	90.0	61.4
TSR	0.95	1.01	0.95

Table 4.30. Moisture Susceptibility Results for SMA Mixes Using DG2 RAP.

Measurement	DG2 RAP		
	10% Camak	20% Mt. View	30% Lithia Springs
Unconditioned Samples			
% Air voids	6.9	6.7	6.9
Load, lbs	1,337	1,601	1,488
Dry S, psi	85.1	101.9	94.8
Conditioned Samples			
% Air voids	6.9	6.8	6.9
Load, lbs	1,136	1,443	1,504
Wet S, psi	72.3	91.9	95.8
% Saturation	90.8	75.2	79.9
TSR	0.85	0.90	1.01

The results for the analysis of variance shown in Table 4.31 indicated that the TSR values do not change significantly with the variations in RAP content (p-value = 0.682). The analysis of variance indicated that none of the main factors had a significant effect on TSR. Table 4.32 shows that the average TSR values range from 0.93 for control mixes to 0.97 for mixes with 30% RAP content, all well above the minimum specified by GDOT. The differences in TSR are shown in Table 4.33, where it can be seen that the increase is not significant (less than 0.05).

Table 4.31. Analysis of Variance for TSR.

Factor	F-statistic	p-value
Agg. Source	1.38	0.265
RAP Content	0.50	0.682
RAP Type	0.62	0.605
$R^2 = 16.49\%$		

Table 4.32. Average TSR Values for Various RAP Contents.

RAP Content, %	TSR
0	0.93
10	0.93
20	0.96
30	0.97

Table 4.33. Tensile Strength Ratios Comparisons for RAP Contents.

RAP Content, %	Difference of Means	Are differences significant at 95% confidence level?
0 – 10	0.002	No
0 – 20	0.033	No
0 – 30	0.044	No
10 – 20	0.031	No
10 – 30	0.042	No
20 – 30	0.011	No

4.3.2 Rutting Susceptibility

Table 4.34 shows the APA results. An analysis of variance (Table 4.35) indicated that aggregate source, RAP type and the interaction between RAP content and RAP type were significant factors, while RAP content did not have an effect on rutting susceptibility (p-value = 0.720). Table 4.36 shows that the average rut depths for different RAP contents range from 3.1 mm to 3.4 mm, all below the maximum 5 mm criteria specified by GDOT. It is probable that because the rut depths were already low, RAP content did not have a significant impact on rutting performance.

Table 4.34. Rutting Susceptibility Results for RAP Mixtures.

Aggregate Source	RAP Type	% RAP	Rut depth, mm
Mt. View	DG1	0	3.11
	-4	10	3.23
	DG2	20	4.41
	+4	30	1.70
Lithia Springs	-4	0	2.37
	DG1	10	2.00
	+4	20	2.44
	DG2	30	4.50
Camak	+4	0	3.67
	DG2	10	1.96
	-4	20	1.48
	DG1	30	3.25
Ruby	DG2	0	3.58
	+4	10	5.16
	DG1	20	5.38
	-4	30	3.85

Table 4.35. Analysis of Variance for Rut Depths.

Factor	F-statistic	p-value
Agg. Source	14.36	0.000
RAP Content	0.45	0.720
RAP Type	2.86	0.038
RAP Content x RAP Type	15.24	0.000

Table 4.36. Average Rut Depths for Various RAP Contents.

RAP Content, %	Rut Depth, mm
0	3.18
10	3.09
20	3.43
30	3.32

The analysis of variance (Table 4.35) suggests that rutting is highly affected by the aggregate source and the interaction between RAP content and RAP type (p-values < 0.001). RAP type also has a significant impact on rutting performance (p-value = 0.038). Figure 4.14 and Table 4.37 show that mixtures that contained Ruby aggregates had higher rut depths than the rest of the mixtures (up to 1.9 mm higher), but these results still met the design criteria and therefore there is not a practical difference in terms of rutting performance.

Table 4.37. Differences in Rut Depth for Aggregate Sources.

Aggregate Source	Difference of Means (mm)	Are differences significant at 95% confidence level?
Mt. View – Lithia Springs	-0.285	No
Mt. View – Camak	-0.522	No
Mt. View – Ruby	1.381	Yes
Lithia Springs – Camak	-0.237	No
Lithia Springs – Ruby	1.665	Yes
Camak – Ruby	1.902	Yes

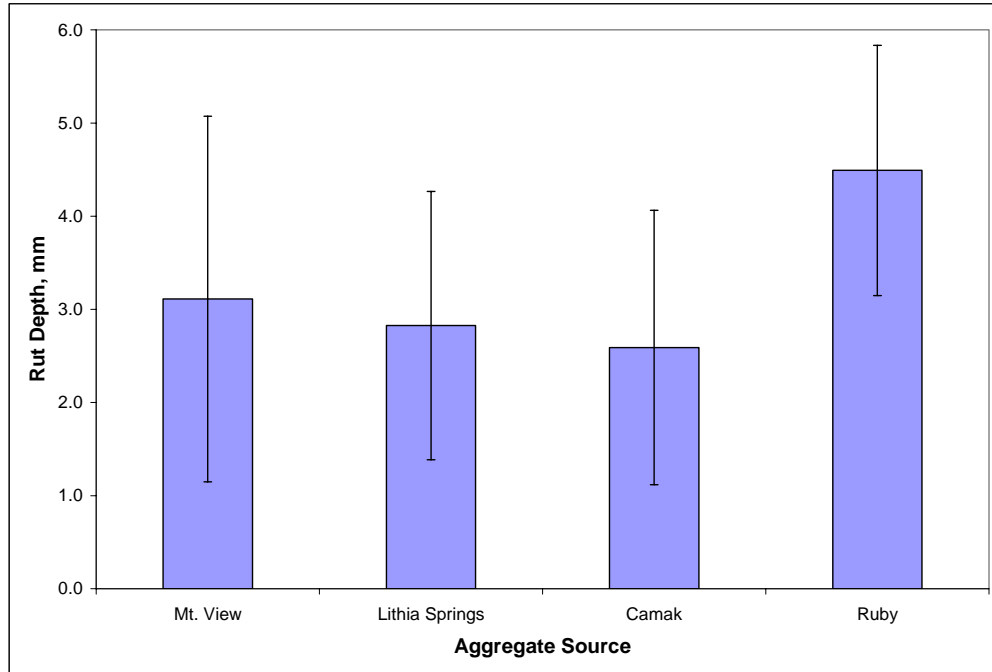


Figure 4.14. Effect of Aggregate Source on Rut Depth.

Figure 4.15 shows the average rut depths for various RAP types. There is no significant difference in the results among RAP types, except between mixtures with -4 RAP and mixtures with DG2 RAP (Table 4.38), which would be expected because of the difference in old to new binder ratio (0.07 higher for mixes containing -4 RAP). However, all mixtures had average rut depths below 5 mm, which means that rutting performance was not really affected by changing the RAP type.

Table 4.38. Rut Depth Comparisons for RAP Types.

RAP Type	Difference of Means (mm)	Are differences significant at 95% confidence level?
DG1 – DG2	0.178	No
DG1 – -4	-0.702	No
DG1 – +4	-0.192	No
DG2 – -4	-0.880	Yes
DG2 – +4	-0.370	No
-4 – +4	0.510	No

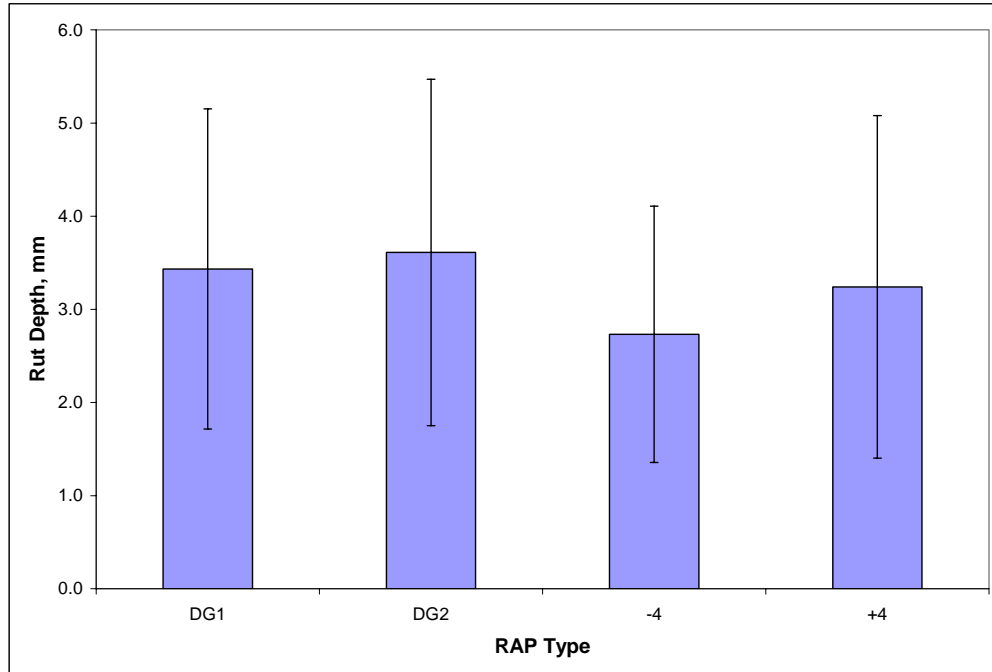


Figure 4.15. Average Rut Depths for Various RAP Types.

Table 4.39 shows the differences in rut depth for the interaction between RAP content and RAP type. In general, specimens that contained RAP had no significant differences in rut depth when compared to the control mixtures (0% RAP). Two mixtures, one containing 20% DG1 RAP and one containing 10% +4 RAP, exhibited rut depths significantly higher (up to 3.5 mm higher than other mixtures) that also exceeded the 5 mm maximum criteria (Table 4.34). The fact that mixes with these RAP types only affected rutting performance at a particular RAP content can be attributed to test variability.

Table 4.39. Rut Depths for RAP Content – RAP Type Interaction.

% RAP	Difference of Means (mm)			
	DG1	DG2	-4	+4
0 – 10	-1.11	-1.62	0.86	1.49
0 – 20	2.26	0.82	-0.89	-1.23
0 – 30	0.14	0.91	1.48	-1.97
10 – 20	3.38	2.45	-1.75	-2.72
10 – 30	1.25	2.54	0.62	-3.46
20 – 30	-2.13	0.09	2.37	-0.74

Significant differences at 95% confidence level are in bold.

4.3.3 Indirect Tensile Creep Compliance

As mentioned in Section 3.3.4, the creep compliance test is used to evaluate thermal cracking resistance of the mixtures. Figures 4.16 through 4.19 show the creep compliance results at 50 seconds. It is clear that, as expected, creep compliance increases with temperature. However, there is not a clear relationship between creep compliance and RAP content in these data. Addition of RAP does not clearly change the stiffness of the mix, as characterized by the IDT creep test, suggesting that the low temperature performance would not be affected by the higher RAP content.

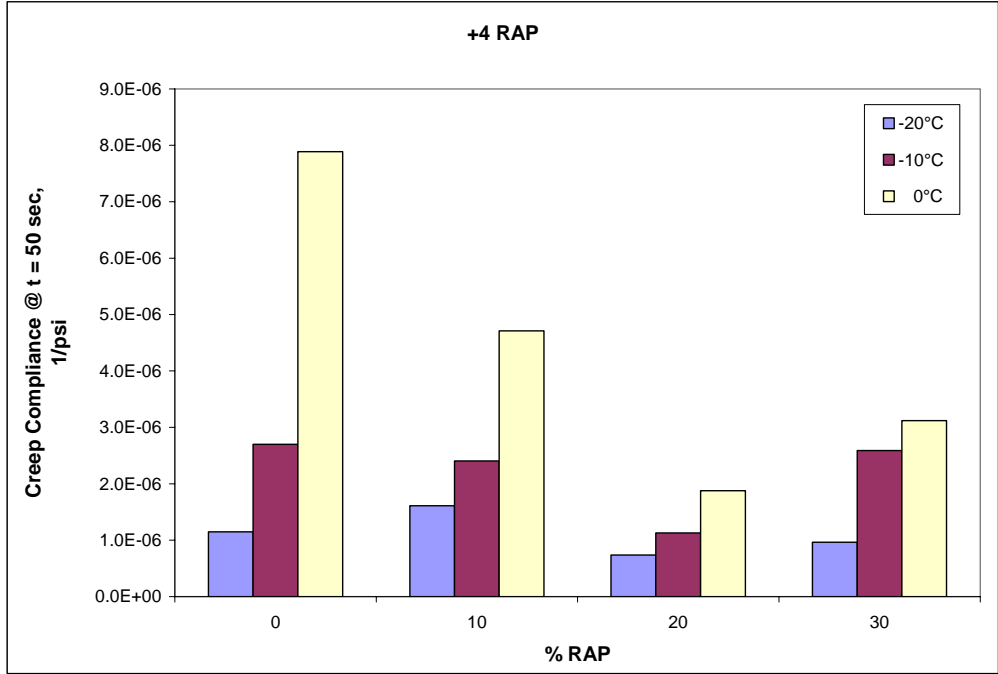


Figure 4.16. Effect of RAP Content on Creep Compliance for Recycled Mixes Using +4 RAP.

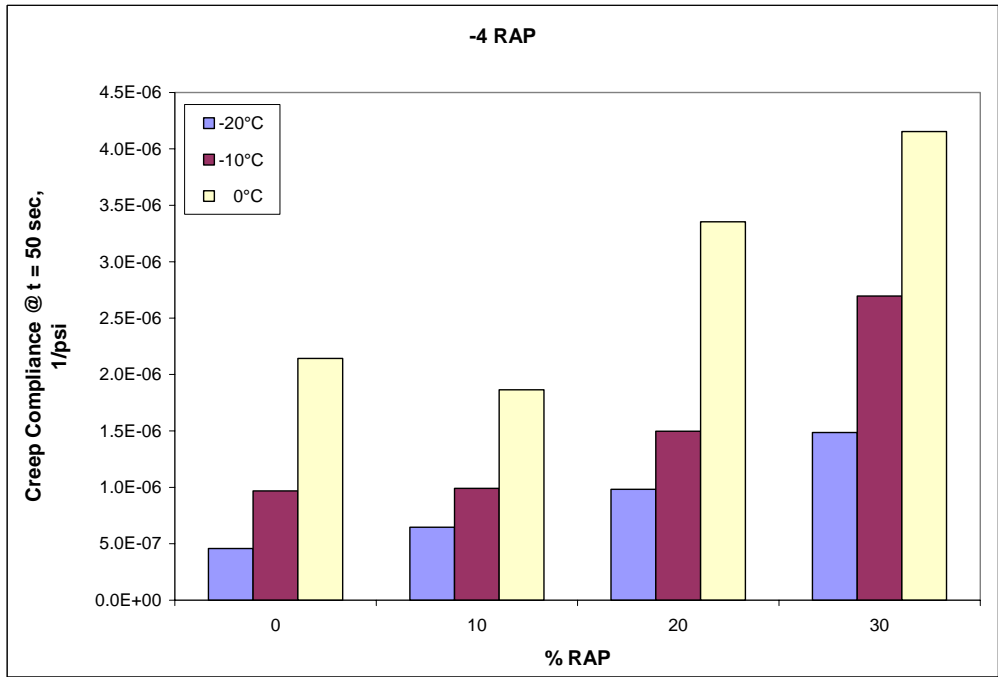


Figure 4.17. Effect of RAP Content on Creep Compliance for Recycled Mixes Using -4 RAP .

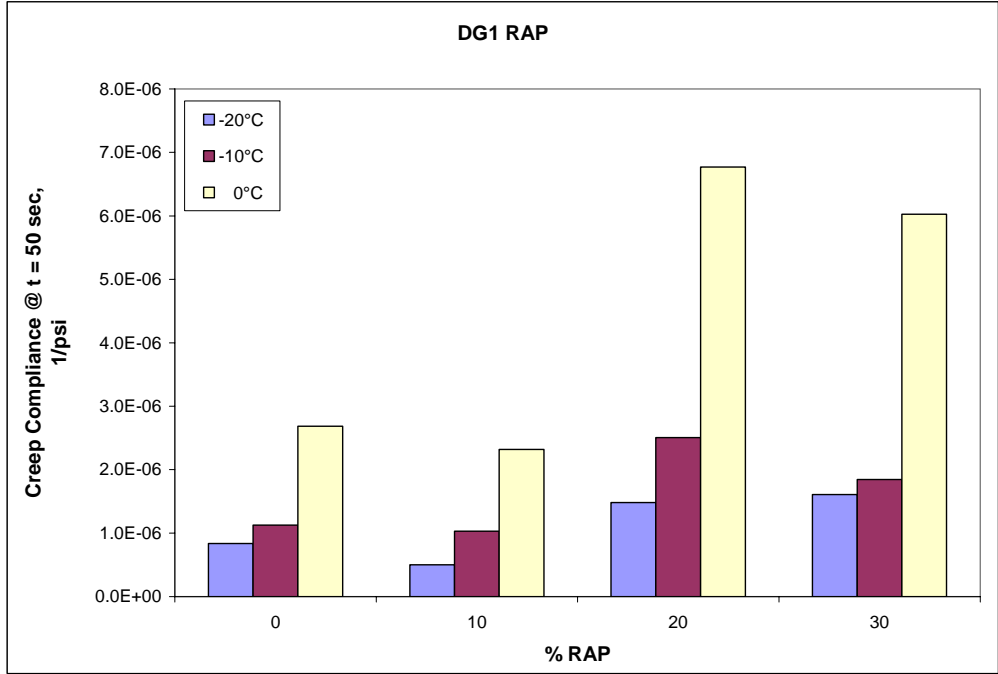


Figure 4.18. Effect of RAP Content on Creep Compliance for Recycled Mixes Using DG1 RAP.

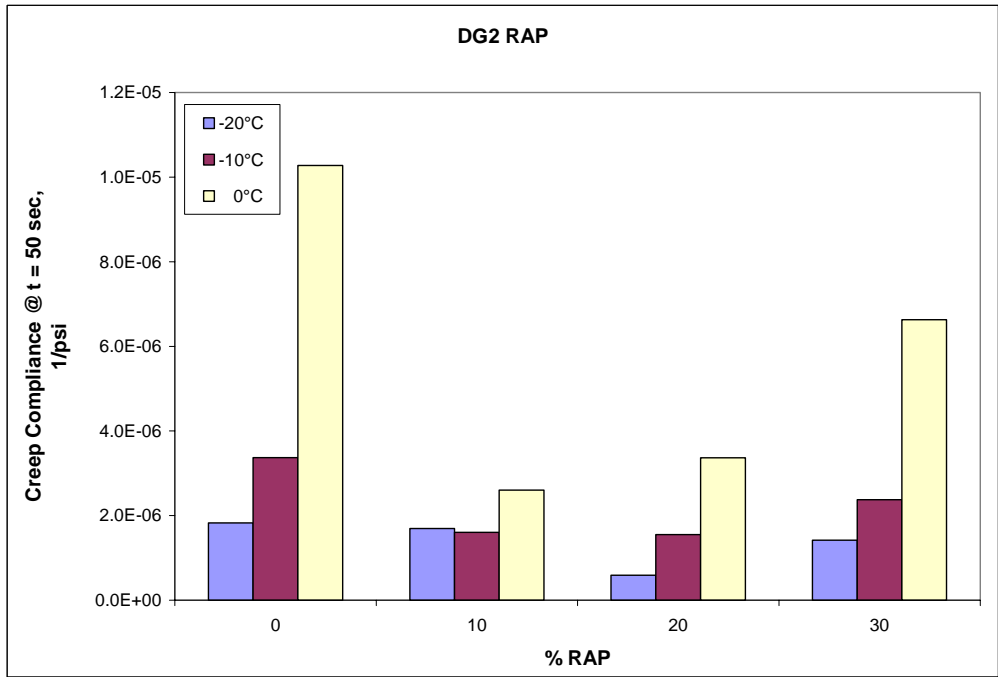


Figure 4.19. Effect of RAP Content on Creep Compliance for Recycled Mixes Using DG2 RAP.

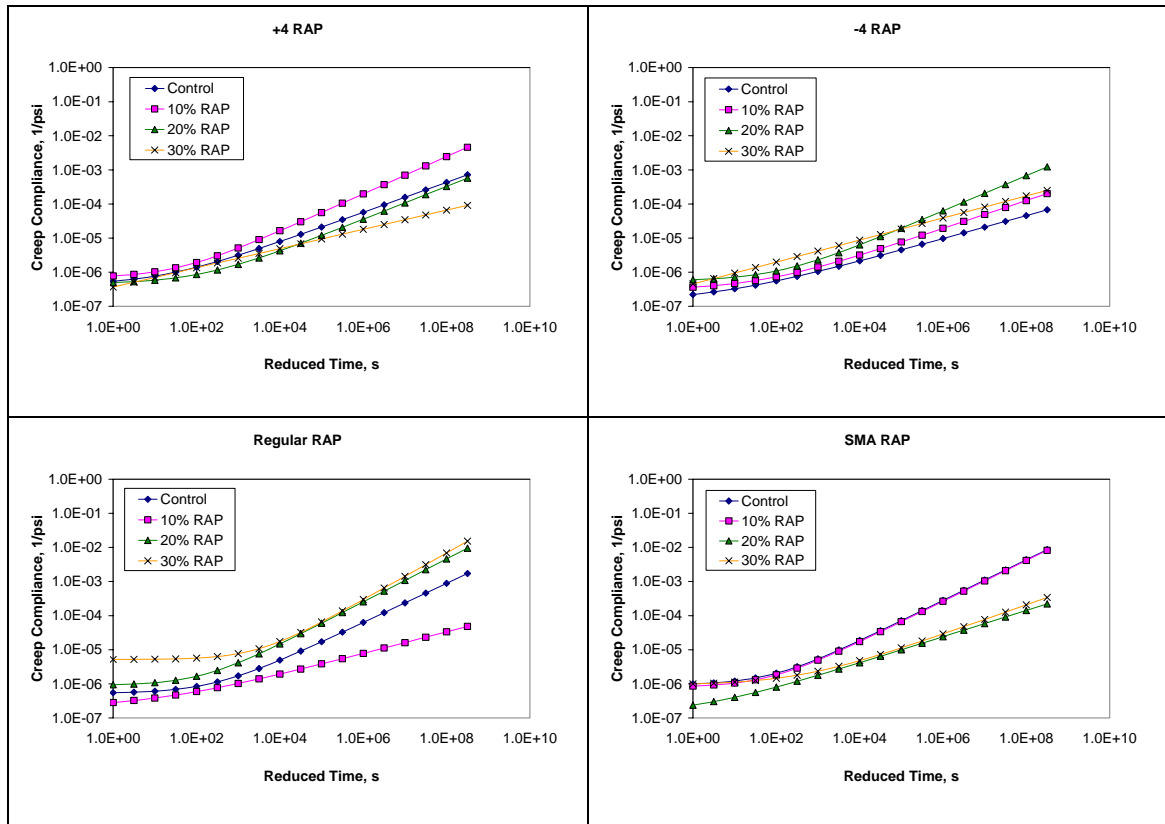


Figure 4.20. Creep Compliance Master Curves for RAP Mixtures.

The other parameter that measures thermal cracking resistance is the m-value. Figure 4.20 shows the creep compliance master curves used to calculate the m-value for each mix (Table 4.40). The m-value is obtained by fitting a power law through the master creep compliance curve obtained from the indirect tensile creep tests, following the procedure described in Section 3.3.4. Mixtures with higher m-values tend to have greater resistance to thermal cracking.

Table 4.40. m-values for SMA Mixes.

RAP Type	% RAP	Agg. Source	m-value
+4	0	Camak	0.440
	10	Ruby	0.548
	20	Lithia Springs	0.484
	30	Mt. View	0.372
-4	0	Lithia Springs	0.339
	10	Mt. View	0.410
	20	Camak	0.518
	30	Ruby	0.331
DG1	0	Mt. View	0.574
	10	Lithia Springs	0.320
	20	Ruby	0.630
	30	Camak	0.687
DG2	0	Ruby	0.598
	10	Camak	0.599
	20	Mt. View	0.386
	30	Lithia Springs	0.432

Table 4.41 shows that the m-value is not influenced by RAP content (p-value = 0.552) but is significantly affected by the aggregate source and RAP type. The influence of aggregate source is somewhat unexpected because thermal cracking resistance is not really defined by the aggregate properties, and is instead dictated by the binder properties. This may be attributed to the difference in mean old to new binder ratios among mixtures with different aggregate sources. Figure 4.21 shows the m-values as a function of RAP content and confirms that there is not a strong relationship between the two ($R^2 = 0.29$). Even though the m-value appears to decrease with RAP content (higher old to new binder ratios), the poor correlation between the two variables is not sufficient to conclude that addition of RAP would affect thermal cracking potential significantly.

Table 4.41. Analysis of Variance for m-value.

Factor	F-statistic	p-value
Agg. Source	5.16	0.004
RAP Content	0.71	0.552
RAP Type	3.49	0.025

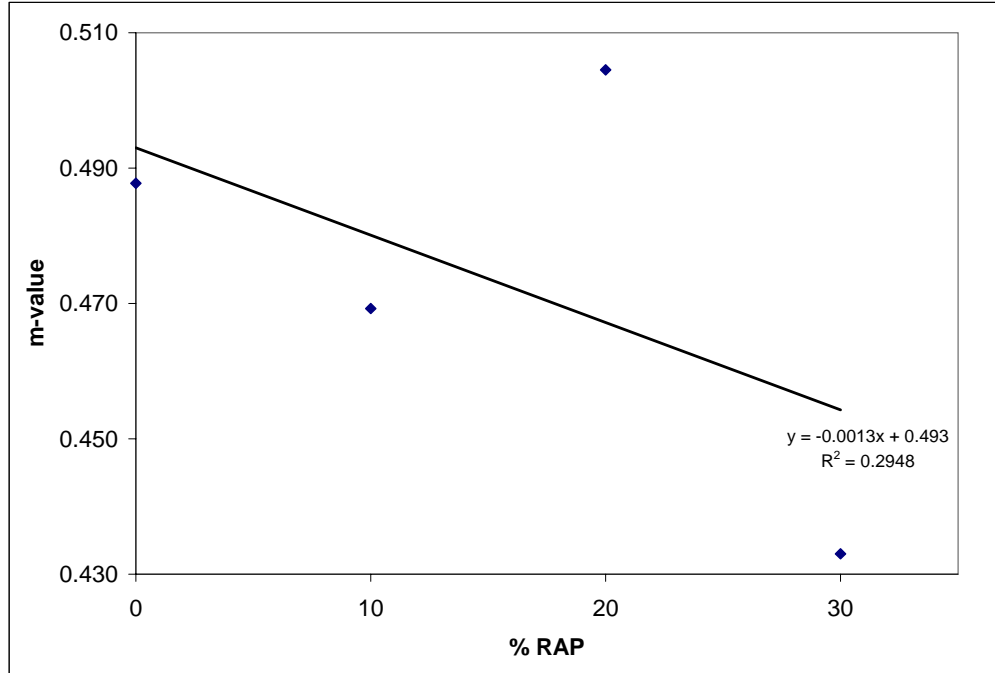


Figure 4.21. Average m-values for RAP Mixtures.

Tables 4.42 and 4.43 show all pairwise comparisons among levels for aggregate source and RAP type, and the effect of these variables on the m-value is shown in Figures 4.22 and 4.23. It can be observed that in general, Camak and Ruby mixtures had m-values up to 0.17 higher than Mt. View and Lithia Springs mixtures. Mixtures containing DG1 RAP performed better than only -4 RAP mixtures (Table 4.43). This may be attributed to the higher amount of RAP binder present in -4 RAP mixtures and its rheological properties, which as noted earlier, indicated these binder blends were more sensitive to thermal cracking.

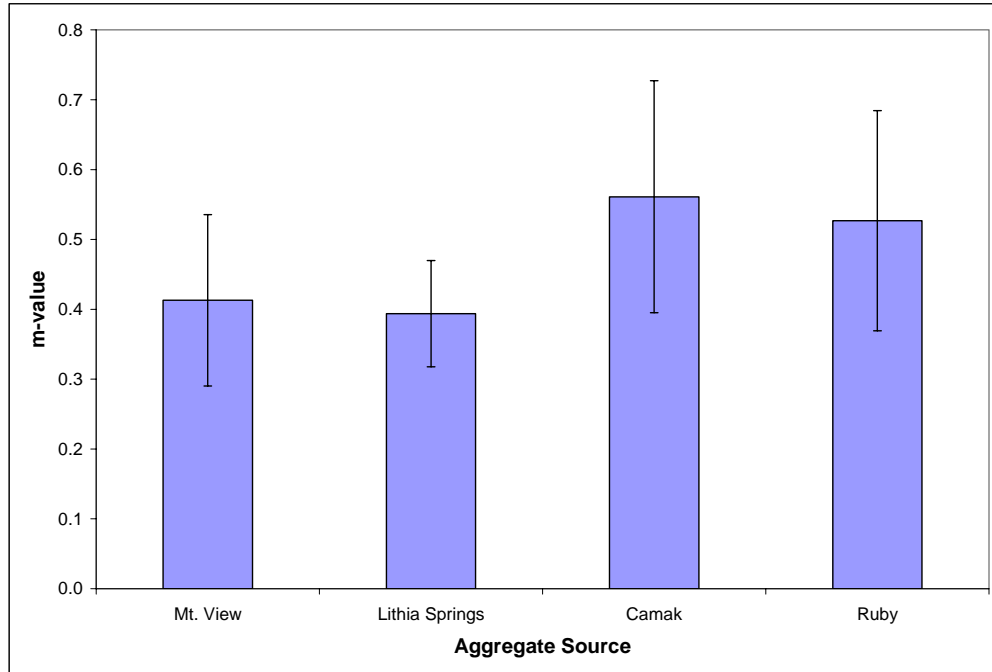


Figure 4.22. Effect of Aggregate Source on m-value.

Table 4.42. m-value Comparisons for Aggregate Sources.

Aggregate Source	Difference of Means	Are differences significant at 95% confidence level?
Mt. View – Lithia Springs	-0.019	No
Mt. View – Camak	0.148	Yes
Mt. View – Ruby	0.114	No
Lithia Springs – Camak	0.167	Yes
Lithia Springs – Ruby	0.133	Yes
Camak – Ruby	-0.034	No

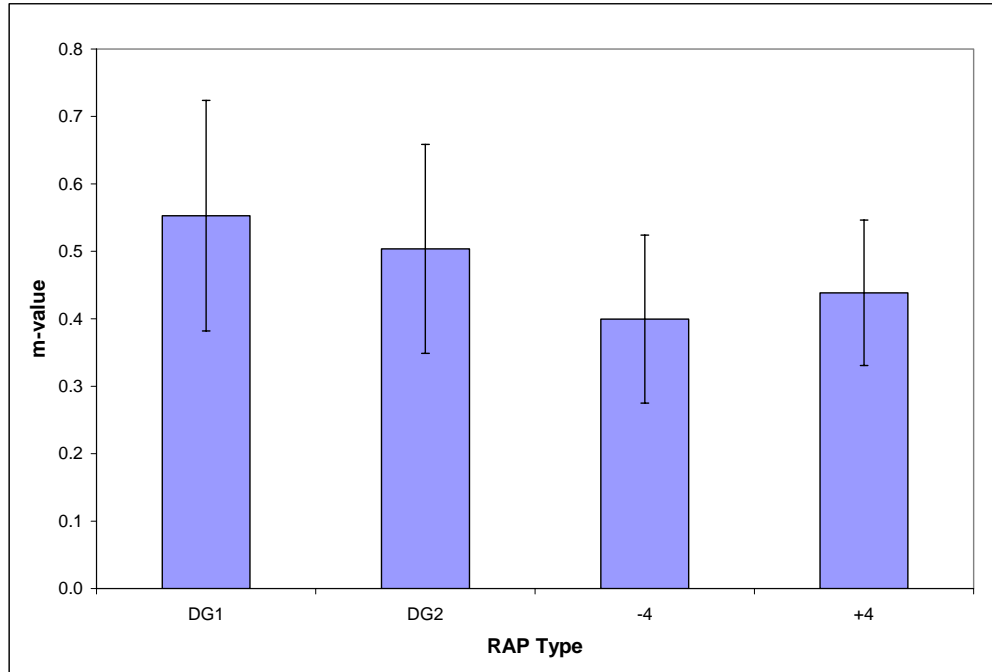


Figure 4.23. Average m-values for RAP Types.

Table 4.43. m-value Comparisons for RAP Types.

RAP Type	Difference of Means	Are differences significant at 95% confidence level?
DG1 – DG2	-0.049	No
DG1 – -4	-0.153	Yes
DG1 – +4	-0.114	No
DG2 – -4	-0.104	No
DG2 – +4	-0.065	No
-4 – +4	0.039	No

4.3.4 Flexural Beam Fatigue

As described in the previous chapter, beams were tested at two strain levels to simulate different pavement structures. The high strain level (800 $\mu\epsilon$) simulates a thin pavement with weak structure or poor subgrade, while the low strain level (400 $\mu\epsilon$) simulates a thick pavement with adequate subgrade (6). Because low strain beams typically do not reach the termination stiffness in a reasonable amount of time, it was necessary to

establish a cut off point of 1,000,000 cycles, which allowed the test to be completed in a maximum time of nearly 28 hours.

High Strain Results

Table 4.44 shows the results for the high strain beams. An analysis of variance indicated that the number of cycles to failure is affected by the aggregate source and RAP content (p-values < 0.001) and the interaction of the two (p-value = 0.023). Figure 4.24 shows that as the amount of RAP increases, the number of cycles to failure decreases. As shown in Table 4.45, the fatigue life of the mixes is reduced as soon as RAP is added. This was expected because as the old to new binder ratio increases mixes become stiffer and tend to fail sooner in a constant strain test (Table 4.46).

Table 4.44. Test Results for High Strain Beams (800 $\mu\epsilon$).

Aggregate Source	% RAP	RAP Type	Cycles to Failure	Initial Stiffness (MPa)	Final Stiffness (MPa)	Initial Dissipated Energy (kPa)
Mt. View	0	DG1	45,800	2,952	1,473	0.985
	10	-4	50,143	3,169	1,577	1.069
	20	DG2	31,013	4,325	2,148	1.105
	30	+4	19,880	4,315	2,150	0.964
Lithia Springs	0	-4	58,703	3,090	1,532	1.039
	10	DG1	44,877	3,411	1,690	0.937
	20	+4	57,940	3,179	1,583	0.965
	30	DG2	16,753	4,949	2,469	0.662
Camak	0	+4	92,070	3,220	1,607	0.985
	10	DG2	40,947	3,221	1,600	1.055
	20	-4	71,070	3,380	1,677	1.028
	30	DG1	74,760	3,433	1,710	0.717
Ruby	0	DG2	72,680	3,028	1,510	0.862
	10	+4	40,933	3,141	1,566	1.034
	20	DG1	21,123	3,348	1,671	0.894
	30	-4	4,273	4,798	2,382	0.542

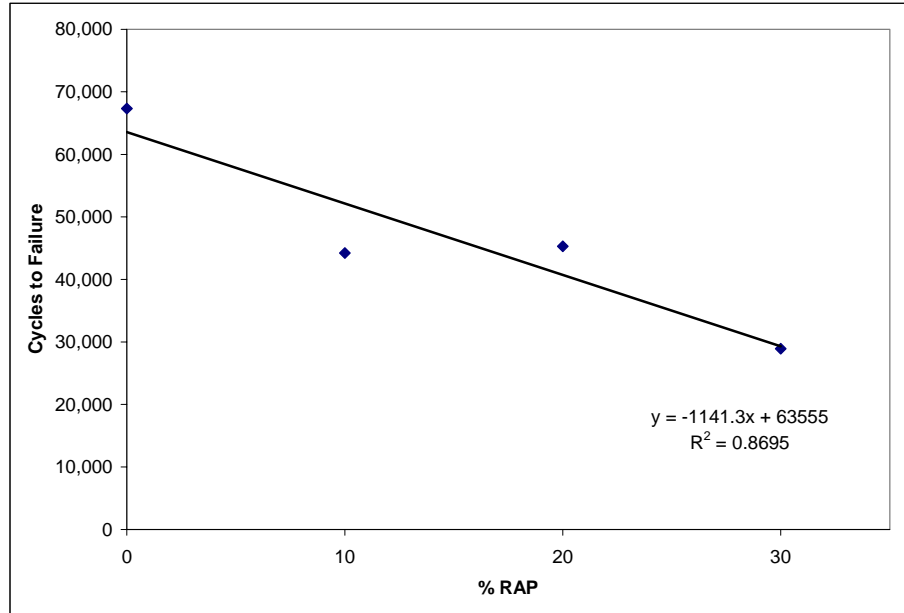


Figure 4.24. Number of Cycles to Failure for RAP Mixtures (800 $\mu\epsilon$).

Table 4.45. N_f Comparisons for RAP Contents (800 $\mu\epsilon$).

RAP Content (%)	Difference of Means (Cycles)	Are differences significant at 5% confidence level?
0 – 10	-23,088	Yes
0 – 20	-22,027	Yes
0 – 30	-38,397	Yes
10 – 20	1,062	No
10 – 30	-15,308	No
20 – 30	-16,370	Yes

Table 4.46. Effect of RAP Binder on Fatigue Life (800 $\mu\epsilon$).

% RAP	Old binder/ New binder	Cycles to Failure	Initial Stiffness (MPa)
0	0.00	67,313	3,073
10	0.09	44,225	3,236
20	0.17	45,287	3,558
30	0.32	28,917	4,374

Figure 4.25 shows the effect of aggregate source on fatigue life. Table 4.47 indicates that Camak mixtures reached a higher number of cycles to failure than the rest.

Camak blends did not have aggregate properties that would seem to significantly improve the fatigue resistance of the mixture; however, they had a low old to new binder ratio (an average of 0.12) and the specimens tested had lower air voids than the other beams (0.6 percent lower on average). Both properties are desirable to obtain greater fatigue life in HMA mixtures.

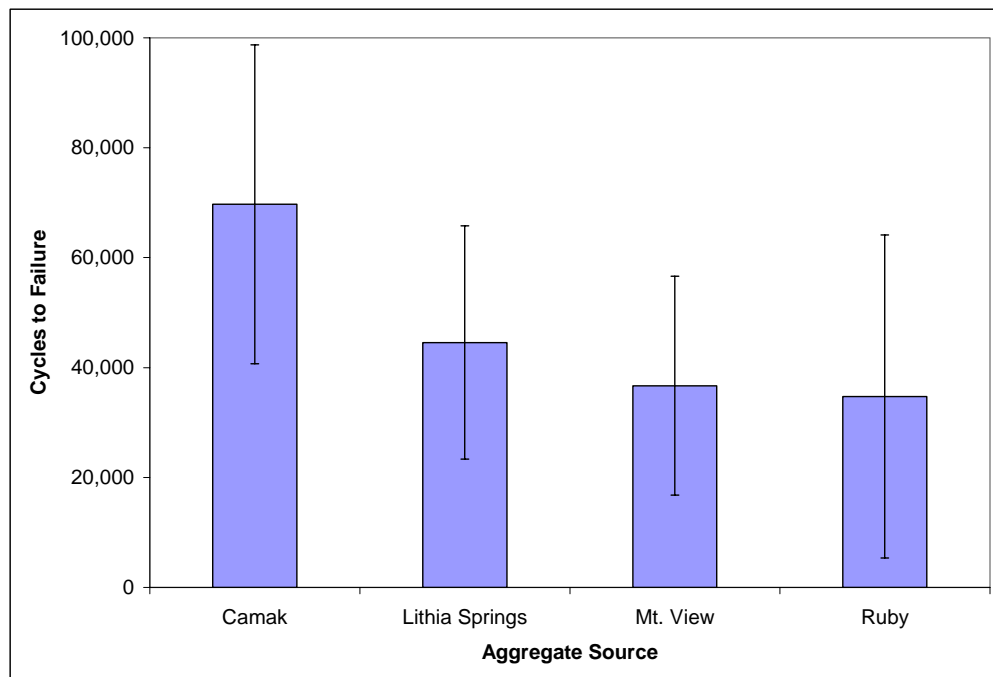


Figure 4.25. Effect of Aggregate Source on N_f (800 $\mu\epsilon$).

Table 4.47. N_f Comparisons for Aggregate Sources (800 $\mu\epsilon$).

Aggregate Source	Difference of Means (Cycles)	Are differences significant at 5% confidence level?
Mt. View – Lithia Springs	7,859	No
Mt. View – Camak	33,002	Yes
Mt. View – Ruby	-1,957	No
Lithia Springs – Camak	25,143	Yes
Lithia Springs – Ruby	-9,816	No
Camak – Ruby	-34,959	Yes

Table 4.48 shows the difference of mean N_f for the interaction between aggregate source and RAP content. It is important to note that the number of cycles to failure only changes significantly with RAP content for Ruby mixtures, and only at the 30% RAP level, which is expected because these mixtures have the highest old to new binder ratio (0.45).

Table 4.48. N_f Comparisons for RAP Content – Aggregate Source Interaction (800 $\mu\epsilon$).

% RAP	Difference of Means (Cycles)			
	Mt. View	Lithia Spr.	Camak	Ruby
0 – 10	4,343	-13,827	-51,123	-31,747
0 – 20	-14,787	-763	-21,000	-51,557
0 – 30	-25,920	-41,950	-17,310	-68,407
10 – 20	-19,130	13,063	30,123	-19,810
10 – 30	-30,263	-28,123	33,813	-36,660
20 – 30	-11,133	-41,187	3,690	-16,850

Significant differences at 95% confidence level are in bold.

As mentioned earlier, in a controlled-strain test, stiffer mixes are expected to fail earlier (lower number of cycles to failure). It can be observed that the results in Figure 4.26 followed the expected trend, and that the higher initial stiffnesses are related to higher RAP contents and higher old to new asphalt ratios (up to 0.32 on average, as previously shown in Table 4.46). An analysis of variance confirmed that the initial stiffness of the mixtures is influenced by RAP content (p-value < 0.001). Table 4.49 shows that the increase in initial stiffness becomes more significant at higher RAP contents due to the higher amount of old binder present (up to 1.5 percent by total weight of mix higher).

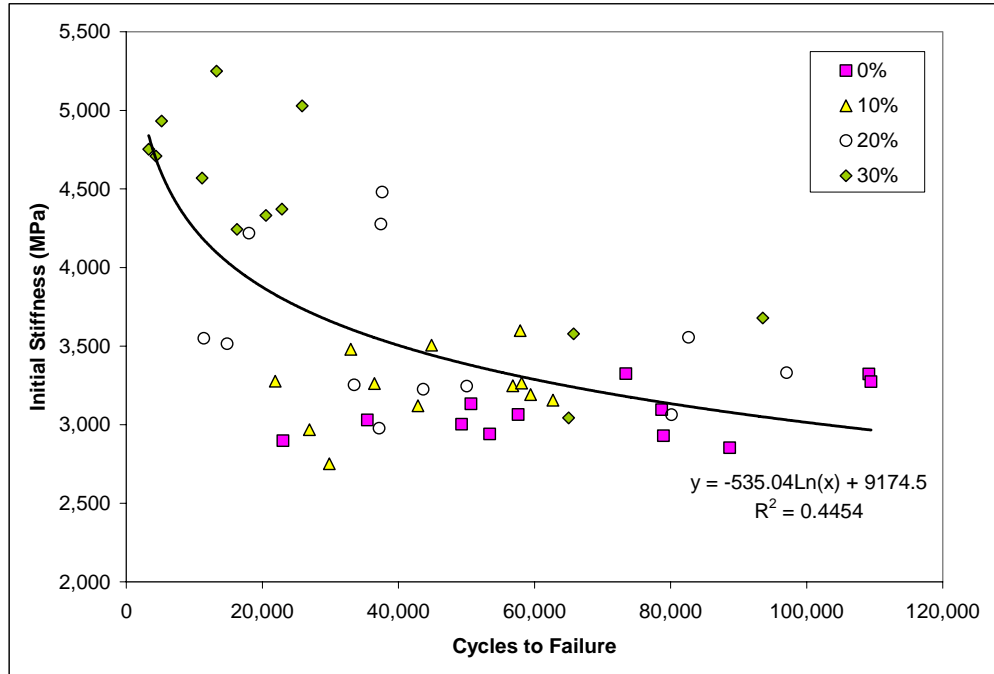


Figure 4.26. Relationship between Initial Stiffness and Number of Cycles to Failure (800 $\mu\epsilon$).

Table 4.49. Initial Stiffness Comparisons for Recycled SMA with Various RAP Contents (800 $\mu\epsilon$).

RAP Content (%)	Difference of Means (MPa)	Are differences significant at 95% confidence level?
0 – 10	163.1	No
0 – 20	485.4	Yes
0 – 30	1301.6	Yes
10 – 20	322.3	Yes
10 – 30	1,138.5	Yes
20 – 30	816.2	Yes

The initial dissipated energy is the energy required at the beginning of the test to deflect the beam, and is an indication of the susceptibility of the mixture to fatigue damage. Mixtures that are more resistant to fatigue cracking would require a higher amount of energy to produce this damage. An analysis of variance showed that RAP content significantly affects the initial dissipated energy (p -value < 0.001). However, the

only significant difference was found for 30% RAP mixes, in which the dissipated energy was up to 0.37 MPa lower (Table 4.50). This is also related to the high old to new binder ratio (an average of 0.32) that stiffens the mix and makes it more easily damaged.

Table 4.50. Initial Dissipated Energy Comparisons for RAP Contents (800 $\mu\epsilon$).

RAP Content (%)	Difference of Means (kPa)	Are differences significant at 95% confidence level?
0 – 10	0.088	No
0 – 20	0.063	No
0 – 30	-0.282	Yes
10 – 20	-0.026	No
10 – 30	-0.371	Yes
20 – 30	-0.345	Yes

Fatigue cracking is a distress that initiates at the bottom of the HMA layer where the tensile stress is the highest then propagates to the surface as one or more longitudinal cracks. Since SMA mixes are typically placed at or near the surface of the pavement, fatigue cracking may not be a major concern.

Low Strain Results

The results for the low strain beams are shown in Table 4.49. Most tests were stopped at the cutoff point of 1,000,000 cycles, and only a few specimens reached 50% of the initial stiffness before that. The number of cycles to failure shown in Table 4.51 corresponds to the extrapolated value from the best fit curve of the N_f vs stiffness plot at 50% of the initial stiffness. Because data extrapolation can be a source of error, the percent drop in initial stiffness at the end of the test (1,000,000 cycles maximum) was also included in the results. Low percentages indicate that the specimen had experienced

less damage at the end of the test and it was likely to withstand a higher number of cycles before reaching the failure point. As shown in Figure 4.27, there is a good correlation between the percent drop in stiffness and estimated N_f ($R^2 = 0.66$).

Table 4.51. Average Test Results for Low Strain Beams.

Aggregate Source	% RAP	RAP Type	Cycles to Failure *	Initial Stiffness (MPa)	% Drop in Stiffness **	Initial Dissipated Energy (kPa)
Mt. View	0	DG1	3,601,543	3,369	38.4	0.271
	10	-4	5,153,700	3,450	37.6	0.267
	20	DG2	2,338,070	3,485	35.9	0.279
	30	+4	1,332,883	4,715	46.6	0.199
Lithia Springs	0	-4	5,526,153	3,653	36.5	0.290
	10	DG1	3,686,010	3,845	39.6	0.292
	20	+4	4,791,923	3,547	38.6	0.279
	30	DG2	1,532,050	4,166	45.2	0.485
Camak	0	+4	4,353,263	3,187	38.3	0.267
	10	DG2	4,686,913	3,571	34.7	0.438
	20	-4	2,689,257	3,139	41.8	0.245
	30	DG1	3,857,159	3,285	33.3	0.251
Ruby	0	DG2	5,405,080	3,502	38.6	0.223
	10	+4	4,552,187	3,570	39.1	0.294
	20	DG1	4,460,207	3,395	39.3	0.274
	30	-4	759,820	4,621	49.9	0.317

*Extrapolated values for specimens that did not reach 50% of the initial stiffness after 1,000,000 cycles.

**Measured at 1,000,000 cycles.

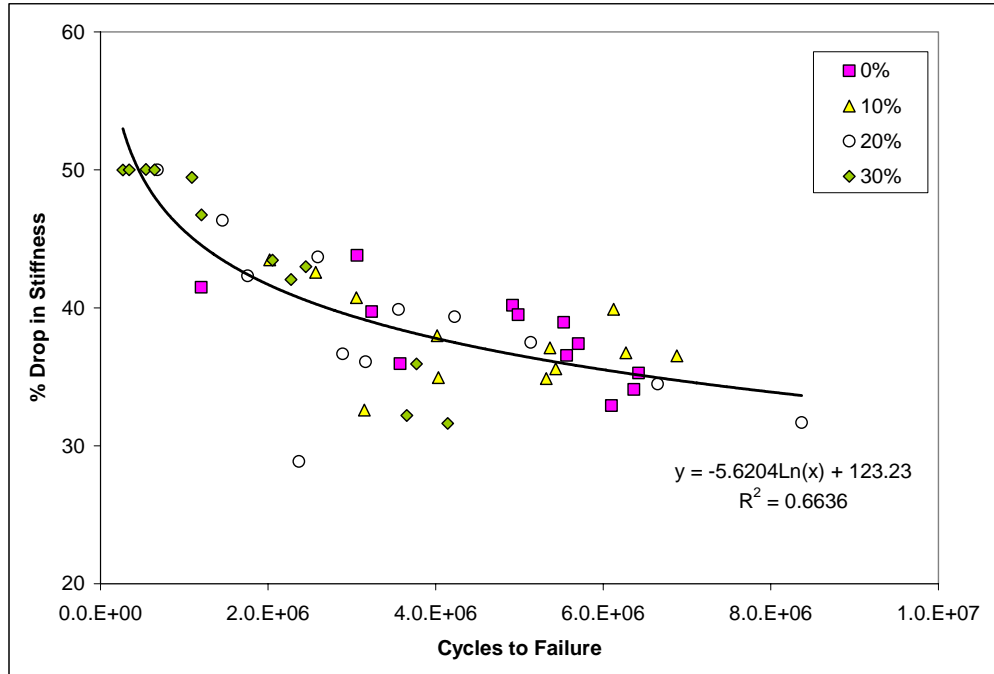


Figure 4.27. Relationship between Drop in Initial Stiffness at 1,000,000 Cycles and Estimated N_f (400 $\mu\epsilon$).

An analysis of variance indicated the main factor that influenced the number of cycles to failure was RAP content (p-value = 0.002). Again, this is related to the old to new binder ratio that increases with RAP content. Fatigue life is more affected at high ratios (over 0.3), where the number of cycles to failure was reduced by up to 2.8 million cycles (Table 4.52). Similar trends were obtained when using the percent drop in initial stiffness instead of N_f .

Table 4.52. N_f and Percent Drop Comparisons for RAP Contents (400 $\mu\epsilon$).

RAP Content (%)	Difference of Means (Cycles)	Difference of Means (%)	Are differences significant at 95% confidence level?
0 – 10	-201,808	-0.22	No
0 – 20	-1,151,646	0.94	No
0 – 30	-2,851,032	5.75	Yes
10 – 20	-949,838	1.17	No
10 – 30	-2,649,224	5.98	Yes
20 – 30	-1,699,386	4.81	No

As with the high strain results, N_f decreases with an increase in initial stiffness. Figure 4.28 shows that in general, mixtures with 30% RAP have higher initial stiffness and lower fatigue life. An analysis of variance confirmed that initial stiffness is highly influenced by RAP content (p-value < 0.001) and aggregate source (p-value = 0.001).

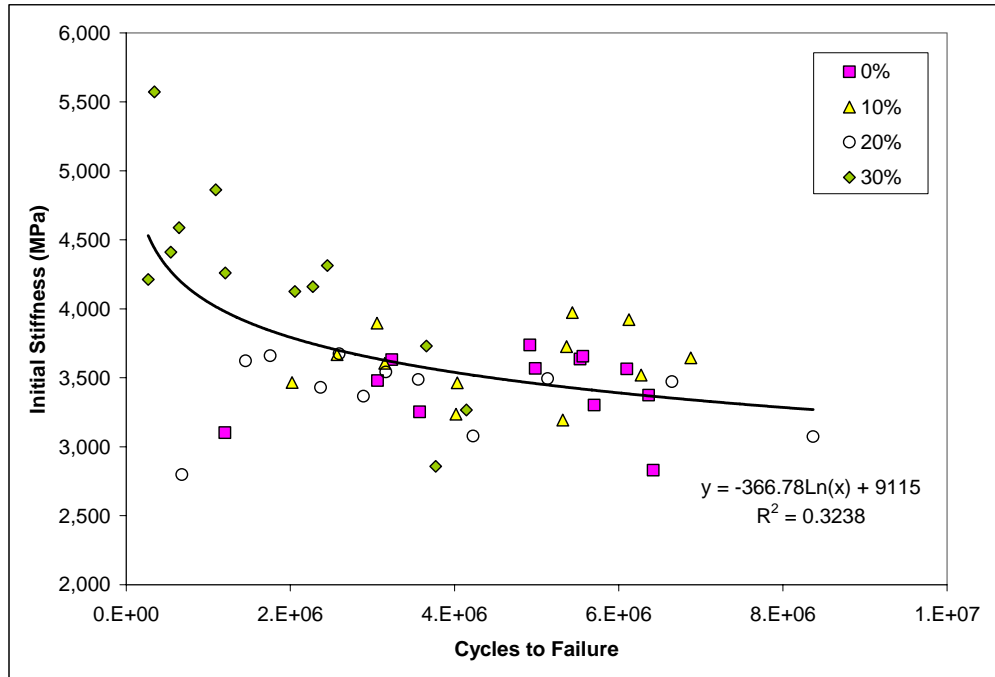


Figure 4.28. Relationship between Initial Stiffness and N_f (400 $\mu\epsilon$).

Figure 4.29 and Table 4.53 show that mixtures that contained Camak aggregates had the lower stiffness among aggregate sources. As mentioned earlier, these mixtures have more virgin binder content (old to new asphalt ratio = 0.13), which is likely the cause of this result. Table 4.54 shows the difference of means for the initial stiffness for the interaction between RAP content and aggregate source. It was found that specimens that contained Lithia Springs and Camak aggregates (both with old to new asphalt ratios

= 0.13, lowest among aggregate sources) did not change their initial stiffness significantly with an increase in RAP content.

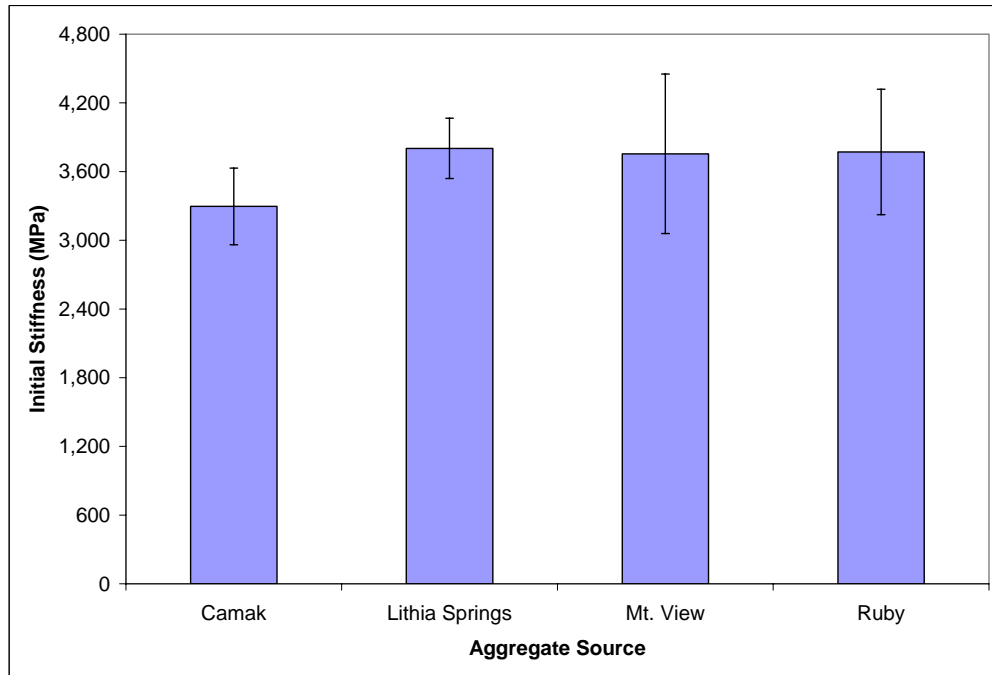


Figure 4.29. Effect of Aggregate Source on Initial Stiffness (400 $\mu\epsilon$).

Table 4.53. Initial Stiffness Comparisons for Aggregate Sources (400 $\mu\epsilon$).

Aggregate Source	Difference of Means (MPa)	Are differences significant at 5% confidence level?
Mt. View – Lithia Springs	47.6	No
Mt. View – Camak	-459.6	Yes
Mt. View – Ruby	16.9	No
Lithia Springs – Camak	-507.2	Yes
Lithia Springs – Ruby	-30.7	No
Camak – Ruby	476.5	Yes

Table 4.54. Initial Stiffness Comparisons for RAP Content – Aggregate Source Interaction (400 $\mu\epsilon$).

% RAP	Difference of Means (MPa)			
	Mt. View	Lithia Spr.	Camak	Ruby
0 – 10	81	192	383	68
0 – 20	116	-106	-48	-107
0 – 30	1,346	514	98	1,119
10 – 20	35	-298	-432	-175
10 – 30	1,265	321	-286	1,050
20 – 30	1,230	620	146	1,226

Significant differences at 5% confidence level are in bold.

For low strain specimens, the analysis of variance indicated that the dissipated energy was not influenced by any of the main factors or interaction terms at the 95% significance level.

High Strain and Low Strain Comparison

As expected, the average number of cycles to failure was higher for low strain samples than for high strain samples (in the order of millions of cycles higher, as shown in Figure 4.30). Mixtures with no RAP showed the best performance (N_f up to 2.5 times higher than recycled mixtures, as seen in Table 4.55) because they only contain virgin binder that is less stiff. As the RAP content is increased and more old binder goes into the mix, the fatigue life of the specimens is significantly reduced for both strain levels. This is associated with an increase in initial stiffness that causes earlier failure in controlled-strain specimens. However, this increase in stiffness may not affect performance when the mixes are placed near the top of the pavement, since fatigue cracking originates at the bottom of the HMA layer.

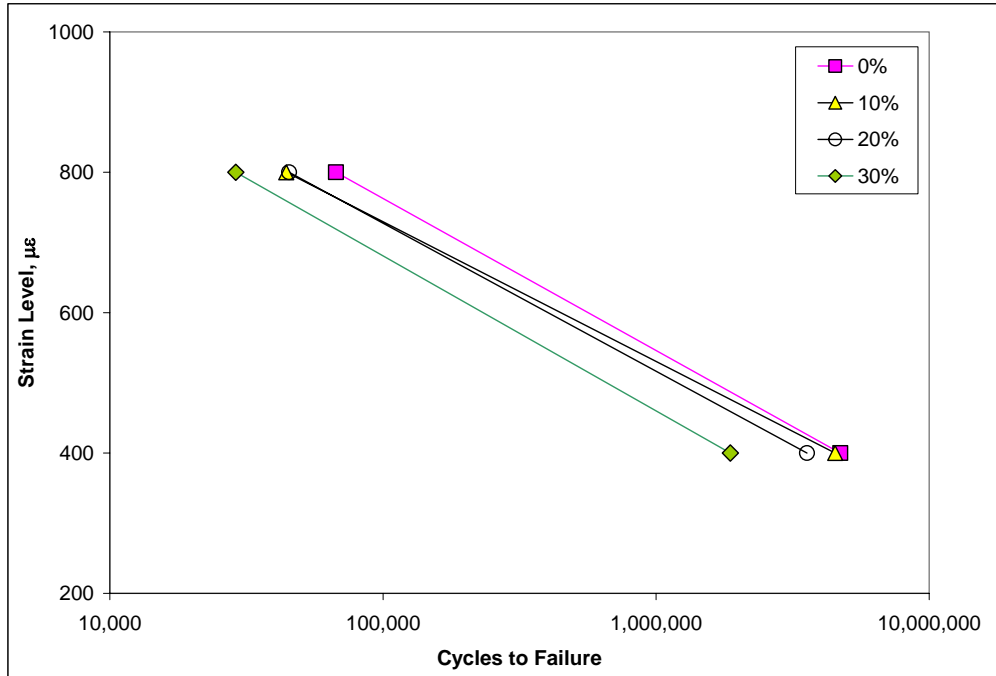


Figure 4.30. Number of Cycles to Failure for High and Low Strain Levels.

Table 4.55. Fatigue Life Comparisons for Strain Levels.

% RAP	Old binder/ New binder	N_f (400 $\mu\epsilon$)	N_f (800 $\mu\epsilon$)
0	0.00	67,313	4,721,510
10	0.09	44,225	4,519,703
20	0.17	45,287	3,569,864
30	0.32	28,917	1,870,478

4.3.5 Summary

The results of this study have shown that adding RAP to an SMA mix has an impact in the sense that a portion of the total binder content corresponds to old (aged) binder. As the RAP content increases, this portion of binder increases as well. The main implication is that the stiffness of the resulting asphalt blend is higher than that of the virgin binder, and therefore mixture stiffness increases with RAP content. For RAPs with high asphalt content, such as the fine-graded portion of screened RAP, the old to new binder ratio is

higher and the effect is greater. The magnitude of the effect also depends on the properties of the RAP binder compared to the virgin binder.

For the performance tests conducted in this study, the increase in stiffness caused by higher old to new asphalt ratios did not have a significant effect in most cases. Figure 4.31 shows that there is a poor correlation between old to new binder ratio and TSR ($R^2 = 0.08$). However, all mixtures were above the minimum requirement and the TSR values increased slightly as RAP content increased; therefore moisture susceptibility was not an issue for recycled SMA mixes.

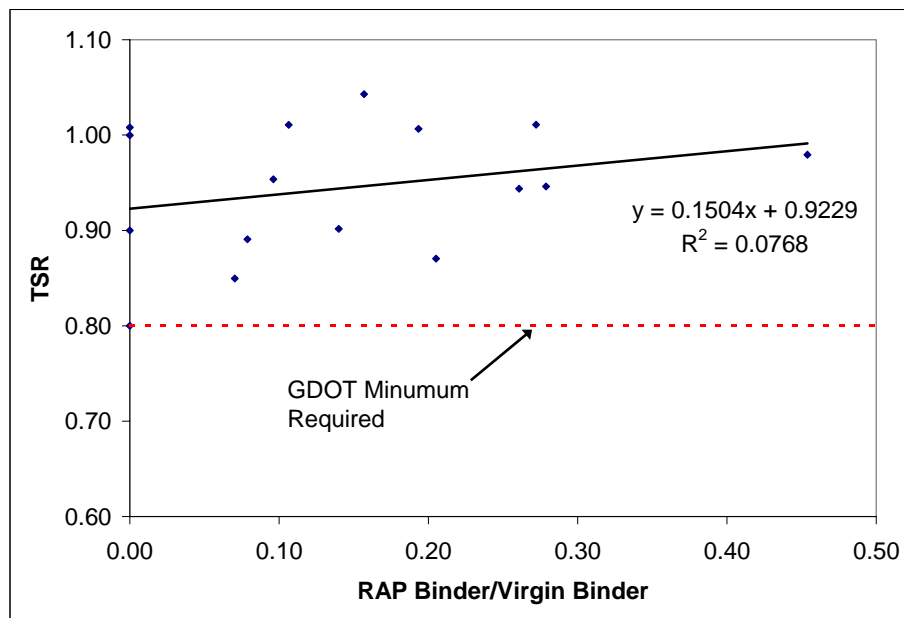


Figure 4.31. Effect of RAP Binder on TSR.

Figure 4.32 shows that the rut depths were not correlated to the old to new binder ratio either ($R^2 = 0.01$). Still, most mixtures had average rut depths below the maximum specified by GDOT. Two recycled mixtures had results that exceeded the design criteria by no more than 0.4 mm, which could be attributed to test variability. In general,

mixtures had good rutting performance that was not significantly changed by the presence of old binder.

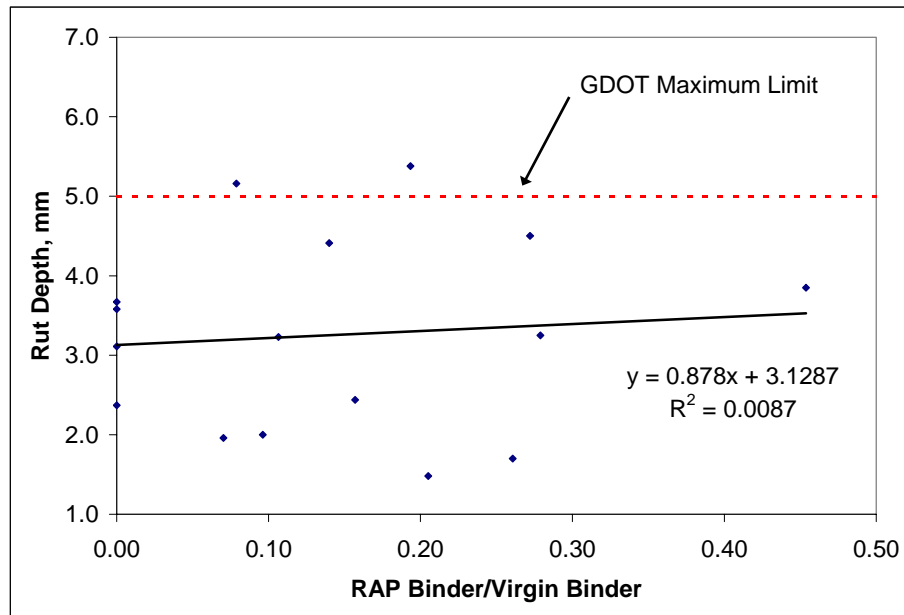


Figure 4.32. Effect of RAP binder on Rutting Performance.

Susceptibility of the mixes to thermal cracking was poorly correlated to the old to new binder ratio ($R^2 = 0.02$), as shown in Figure 4.33. This could be due to the fact that even though the old binder content increases, there was not a significant change in the combined binder blend properties that control thermal cracking (creep stiffness and creep rate, shown in Figure 4.34).

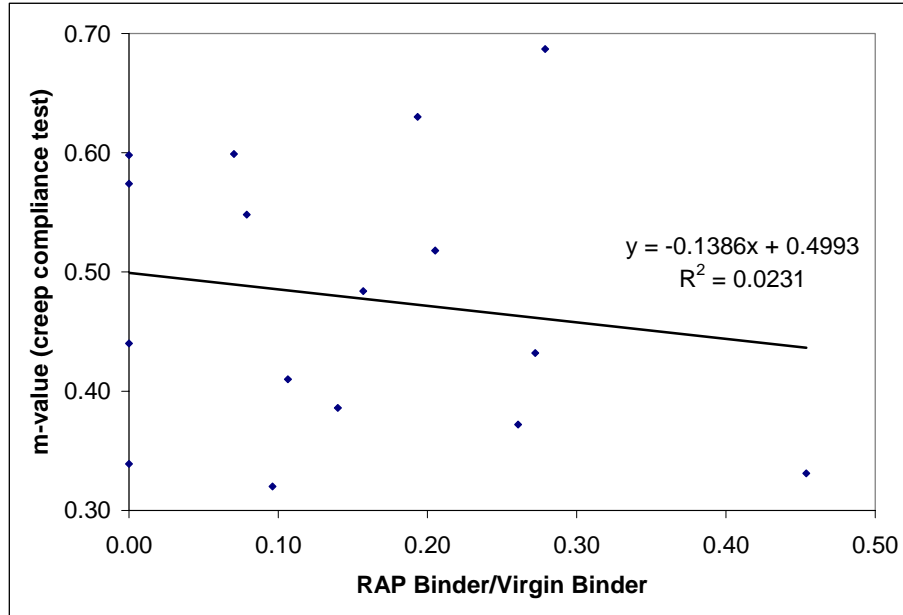


Figure 4.33. Effect of RAP Binder on Thermal Cracking.

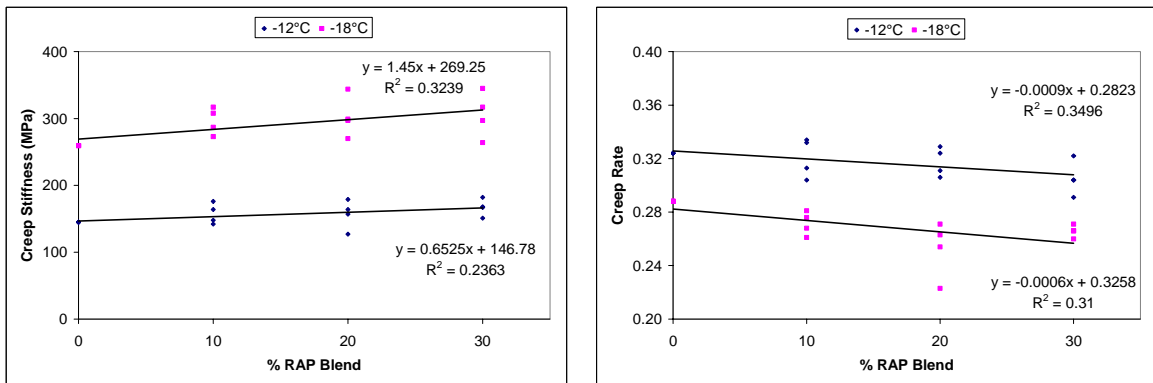


Figure 4.34. Effect of RAP on Low Temperature Binder Properties.

One result that was affected by the increase in the old to new binder ratio was the fatigue life of the mixes. Figure 4.34 shows that adding more RAP binder to the mixtures produces lower number of cycles to failure for specimens tested in controlled-strain mode. This occurs because the stiffness of the mix increases with higher old to new asphalt ratios.

It was observed that the fatigue life of the mixes was significantly reduced at high strain levels. However, recycled mixes are stiffer and will have less strain. Fatigue life may not be as affected unless the mixes are used in thin pavements. Also, SMA mixes are likely to be used as a surface layer, and because fatigue cracking originates at the bottom of the HMA pavement layers, it may not be a concern for this type of mixture.

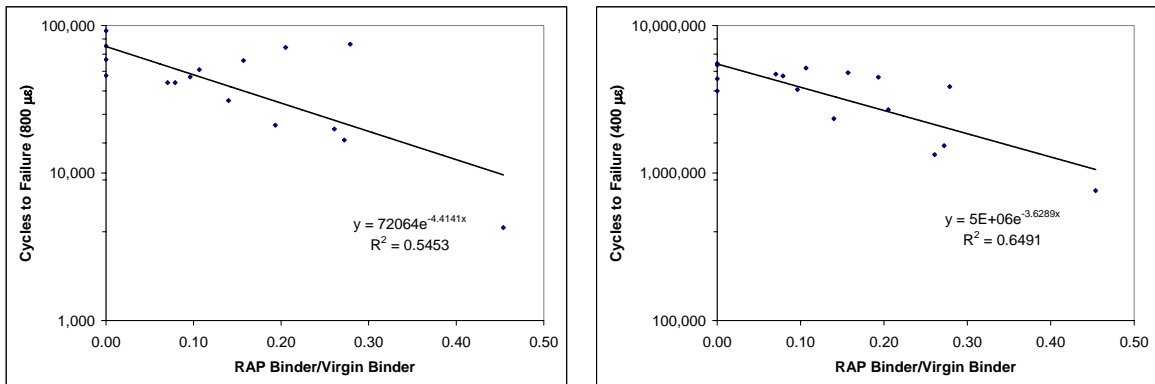


Figure 4.35. Effect of RAP Binder on Fatigue Life.

It is important to mention that the type of RAP used in recycled mixes can also have an important influence in performance. When the fine-graded portion of the RAP was used, the amount of old binder was increased because this portion of the RAP typically has a higher asphalt content than dense-graded or coarse graded RAP. As already discussed, this results in higher stiffness of the mix. It is expected that mixes that contain fine-graded RAP will have good resistance to moisture susceptibility and permanent deformation, but low fatigue life. Thermal cracking may not be a major concern for the reasons discussed above. One benefit of using fine-graded RAP is that the virgin binder requirement can be considerably reduced, lowering the cost of the mix.

Replacing a percentage of the No. 7 stone with coarse-graded aggregate did not affect the performance of the recycled mixes significantly. The low asphalt content characteristic of coarse-graded RAP produces asphalt blends with a low old to new asphalt ratio that did not increase the stiffness of the mixes in a way that would influence performance. Moisture susceptibility, permanent deformation and thermal cracking were not a concern for mixtures containing coarse-graded RAP. Fatigue life may be reduced depending on the RAP content used. The advantage of substituting virgin material with RAP aggregate is that recycled aggregates could be used if quarries were faced with a critical supply shortage of No. 7 stone due to its high demand, and still obtain a mix with characteristics similar to those of a virgin SMA mix.

The feasibility of using RAP from reclaimed SMA could not be evaluated conclusively. The SMA RAP received for this project did not match some of the characteristics of an SMA mix (asphalt content, percent passing the No. 4 sieve). This has been partially attributed to circumstances that occurred during the milling process and the fact that the material was crushed to have 100 percent passing the 12.5 mm sieve. The resulting RAP was more similar to a dense-graded mix with low asphalt content. No general conclusions can be made unless it is assured that the same conditions would be repeated as part of a standard procedure for this type of RAP.

CHAPTER 5. CONCLUSIONS AND RECOMMENDATIONS

The following general conclusions and recommendations were obtained from this research:

- Tests on the aggregate properties of the combined blends indicated that addition of RAP changes the LA abrasion and F/E particle content depending on the properties of the RAP aggregates in relation to the virgin aggregates. However, for the aggregates and RAPs tested the change was not significant up to 30% RAP.
- Use of RAP changed the engineering properties of the resulting binder blends due to the increased old to new binder ratio. The stiffness of the binder blend ($G^*/\sin\delta$, $G^*\sin\delta$ and creep stiffness) increases with RAP content, particularly increasing the fatigue cracking potential.
- The volumetric properties of the mix (air voids, VMA and VFA) were met with all of the RAP stockpiles and various RAP contents.
- RAP content influenced only the tensile strength and fatigue life (N_f) of the mixtures. Increasing RAP content resulted in higher tensile strengths (conditioned and unconditioned) and lower number of cycles to failure. It can be concluded that RAP content significantly affects only the fatigue performance of the mixtures, especially at high strain levels.

- Separating the RAP into fine and coarse-graded fractions produced two stockpiles with different properties. The fine-graded portion had a high asphalt content and therefore, produced mixes with high old to new binder ratios. Additionally, fine-graded RAP contains more material passing the No. 200 sieve, which must be accounted for during mix design. The coarse-graded portion had lower asphalt content, which indicates that mixtures containing this material will have a lower amount of old binder and less increase in stiffness.
- Use of fine-graded RAP reduced the virgin binder requirements due its high asphalt content, which translates into increased economic benefits. However, mixes that contain fine-graded graded RAP are stiffer because they have higher old to new binder ratios and are more susceptible to fatigue cracking.
- Use of coarse-graded RAP allowed reducing the No. 7 stone requirement without affecting the performance of the mixes. This may be beneficial in the case that quarries were faced with a shortage due to the high demand of this material.
- It is uncertain whether SMA pavement material can be successfully recycled back into an SMA mixture. The reclaimed asphalt used in this study had a mix gradation resembled a dense-graded mix and it had low asphalt content. Unless the same conditions are always repeated as part of a standard procedure for this material, it can not be assured that mixes containing recycled SMA will perform similar to other recycled mixes.
- Because fatigue cracking is the main concern for recycled mixtures and this distress originates at the bottom of the HMA layer, it is recommended that SMA

mixes containing RAP be used primarily in the top layers of the pavement. Also, a good bond between the SMA layer and the underlying material must be provided.

- Adding RAP up to 30% had little effect on the low temperature PG properties. The low temperature grade of the combined binder blends was raised by one grade on only one of the cases. This may indicate that the grade of virgin binder does not have to be adjusted to provide the desired properties.

REFERENCES

1. Beyond Roads, Questions and Answers. Asphalt Education Partnership.
<http://www.beyondroads.com/index.cfm?fuseaction=page&filename=asphaltQandA.html>. Accessed March 15th, 2006.
2. Summary of Georgia's Experience with Stone Matrix Asphalt Mixes. Georgia Department of Transportation.
<http://www.dot.state.ga.us/dot/construction/materials-research/b-admin/research/onlinereports%5Cr-SMA2002.pdf>. Accessed February 21st, 2006.
3. Brown, E.R., R.B. Mallick, J. E. Haddock and J. Bukowski. *Performance of Stone Matrix Asphalt (SMA) Mixtures in the United States*. National Center for Asphalt Technology, Report No. 97-01, Jan. 1997.
4. Watson, D. E. Updated Review of Stone Matrix Asphalt and Superpave Projects. In *Transportation Research Record 1832*, TRB, National Research Council, Washington, D.C., 2003, pp. 217-223.
5. Brown, E.R., R.B. Mallick, J. E. Haddock and T.A. Lynn. *Development of a Mixture Design Procedure for Stone Matrix Asphalt (SMA)*. National Center for Asphalt Technology, Report No. 97-03, March 1997.
6. McDaniel, R.S., H. Soleymani, R.M. Anderson, P. Turner, and R. Peterson. *Recommended Use of Reclaimed Asphalt Pavement in the Superpave Mix Design*

- Method. Contractor's Final Report. NCHRP Web Document 30 (Project D9-12). 2000.*
7. Huang, B., G. Li, D. Vukosavljevic, X. Shu, and B.K. Egan. Laboratory Investigation of Mixing Hot-Mix Asphalt with Reclaimed Asphalt Pavement. In *Transportation Research Record 1929*, TRB, National Research Council, Washington, D.C., 2005, pp. 37-45.
 8. Kandhal, P.S. and K.Y. Foo. *Designing Recycled Hot Mix Asphalt Mixtures Using Superpave Technology*. National Center for Asphalt Technology, Report No. 96-05, Jan. 1997.
 9. Bukowski, J. R., *Guidelines for the Design of Superpave Mixtures Containing Reclaimed Asphalt Pavement (RAP)*, Memorandum, ETG Meeting, FHWA Superpave Mixtures Expert Task Group, San Antonio, Texas, March, 1997.
 10. Kennedy T.W., W.O. Tam, and M. Solaimanian. *Effect of Reclaimed Asphalt Pavement on Binder Properties Using the Superpave System*. Center for Transportation Research, Bureau of Engineering Research, The University of Texas at Austin. Research Report 1250-1, September 1998.
 11. Abdulshafi, O., B. Kedzierki, and M.G. Fitch. *Determination of Recycled Asphalt Pavement (RAP) Content in Asphalt Mixes Based on Expected Mixture Durability*. Ohio State University. December, 2000.
 12. Li X., T.R. Clyne, and M.O. Marasteanu. *Recycled Asphalt Pavement (RAP) Effects on Binder and Mixture Quality*. Minnesota Department of Transportation. July, 2004.

13. Stroup-Gardiner M. and C. Wagner. Use of RAP in Superpave HMA Applications. In *Transportation Research Record 1681*, TRB, National Research Council, Washington, D.C., 1999, pp. 1-9.
14. Daniel, J.S., and A. Lachance. Mechanistic and Volumetric Properties of Asphalt Mixtures with Recycled Asphalt Pavement. In *Transportation Research Record 1929*, TRB, National Research Council, Washington, D.C., 2005, pp. 28-36.
15. Tam, K.K., P. Joseph, and D.F. Lynch. Five Year Experience of Low-Temperature Performance of Recycled Hot Mix. In *Transportation Research Record 1362*, TRB, National Research Council, Washington, D.C., 1992, pp. 56-65.
16. McDaniel, R.S., A. Sha, G.A. Huber, and V.L. Gallivan. Investigation of Properties of Plant-Produced RAP Mixtures. Transportation Research Board Annual Meeting 2007 Paper #07-2855.
17. Huang, B., W.R. Kingery, and Z. Zhang. Laboratory Study of Fatigue Characteristics of HMA Mixtures Containing RAP. Presented at the International Symposium on Design and Construction of Long Lasting Asphalt Pavements, Auburn, AL. June, 2004.
18. Puttagunta, R., S.Y. Oloo, and A.T. Bergan. A Comparison of the Predicted Performance of Virgin and Recycled Mixes. *Canadian Journal of Civil Engineering*. Vol. 24, National Research Council of Canada, Ottawa. 1997. pp. 115-121.

19. Sargious, M. and N. Mushule. Behaviour of Recycled Asphalt Pavements at Low Temperatures. *Canadian Journal of Civil Engineering*. Vol. 18, National Research Council of Canada, Ottawa. 1991. pp. 428-435.
20. McGennis, R.B., S. Shuler, and H.U. Bahia. *Background of Superpave Asphalt Binder Test Methods*. FHWA, Report No. FHWA-SA-94-069, July 1994.
21. Roberts, F.L., P.S. Kandhal, E.R. Brown, D.Y. Lee, T.W. Kennedy. Hot Mix Asphalt Materials, Mixture Design and Construction. National Asphalt Pavement Association Research and Education Foundation, 1996.
22. Kandhal, P.S. and F. Parker. *Aggregate Tests Related to Asphalt Concrete Performance in Pavements*. National Cooperative Highway Research Program NCHRP Report No. 405, 1998.
23. Strategic Highway Research Program Report SHRP-A-357. *Development and Validation of Performance Prediction Models and Specifications for Asphalt Binders and Paving Mixes*. Strategic Highway Research Program, National Research Council, Washington D.C., 1993.
24. Kandhal, P.S. *Accelerated Laboratory Rutting Tests: Evaluation of the Asphalt Pavement Analyzer*. National Cooperative Highway Research Program NCHRP Report No. 508, 2003.
25. Strategic Highway Research Program Report SHRP-A-404. *Fatigue Response of Asphalt-Aggregate Mixes*. Strategic Highway Research Program, National Research Council, Washington D.C., 1994.

26. Christensen, D. Analysis of Creep Data from Indirect Tension Test on Asphalt Concrete. *Asphalt Paving Technology*. Volume 67, Journal of the Association of Asphalt Paving Technologists, St. Paul, MN, 1998. pp. 458-492.

APPENDIX A

Laboratory Mix Designs

A.1 Mix Designs for Mt. View Mixtures

Mt. View 0% RAP

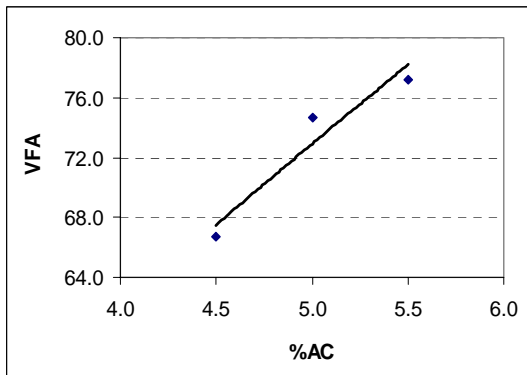
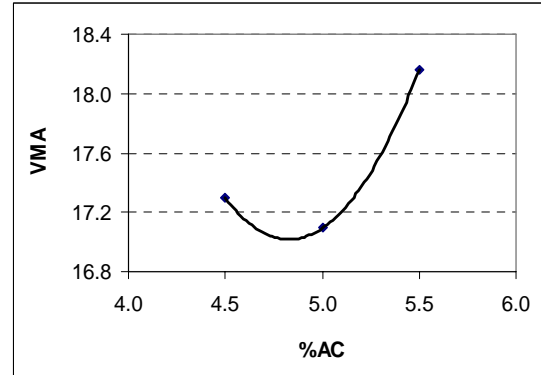
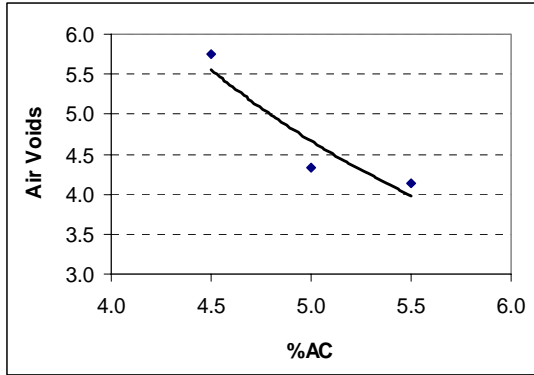
Sieve size	Aggregate Components					
	007	089	M10	Marble dust	Lime	Blend
Proportions	68.0%	12.0%	13.0%	6.0%	1.0%	100%
1"	100.0	100.0	100.0	100.0	100.0	100.0
3/4"	100.0	100.0	100.0	100.0	100.0	100.0
1/2"	97.0	100.0	100.0	100.0	100.0	98.0
3/8"	48.0	100.0	100.0	100.0	100.0	64.6
#4	3.0	22.0	99.0	100.0	100.0	24.6
#8	3.0	4.0	83.0	100.0	100.0	20.3
#16	2.0	2.0	66.0	100.0	100.0	17.2
#30	2.0	2.0	53.0	100.0	100.0	15.5
#50	2.0	1.0	37.0	100.0	100.0	13.3
#100	1.0	1.0	18.0	98.0	100.0	10.0
#200	1.0	1.0	6.0	90.0	100.0	8.0

Series	% AC	VMA	VFA
1	6.0	18.3	74.6

Mt. View 10% -4 RAP

Sieve size	Aggregate Components						
	007	089	M10	Marble dust	Lime	RAP	Blend
Proportions	77.0%	0.0%	7.0%	5.0%	1.0%	10.0%	100%
1"	100.0	100.0	100.0	100.0	100.0	100.0	100.0
3/4"	100.0	100.0	100.0	100.0	100.0	100.0	100.0
1/2"	97.0	100.0	100.0	100.0	100.0	100.0	98.0
3/8"	48.0	100.0	100.0	100.0	100.0	100.0	64.6
#4	3.0	22.0	99.0	100.0	100.0	100.0	24.6
#8	3.0	4.0	83.0	100.0	100.0	81.0	20.3
#16	2.0	2.0	66.0	100.0	100.0	65.0	17.2
#30	2.0	2.0	53.0	100.0	100.0	53.0	15.5
#50	2.0	1.0	37.0	100.0	100.0	40.0	13.3
#100	1.0	1.0	18.0	98.0	100.0	25.0	10.0
#200	1.0	1.0	6.0	90.0	100.0	15.0	8.0

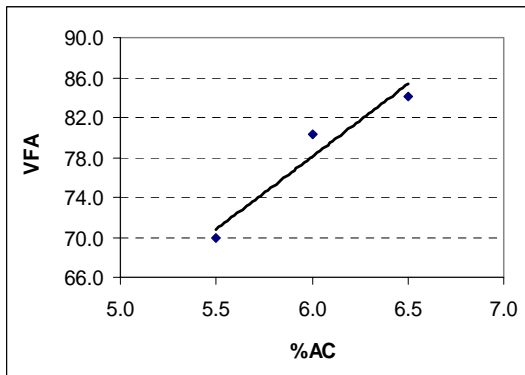
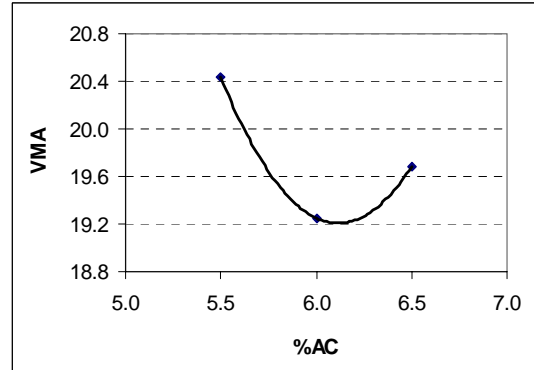
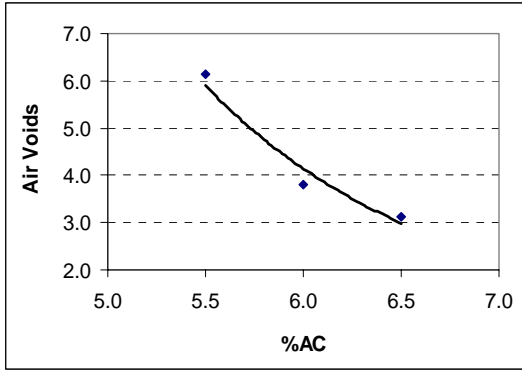
Series	% AC	VMA	VFA
1	4.5	17.3	66.8
2	5.0	17.1	74.7
3	5.5	18.2	77.2



Mt. View 20% DG2 RAP

Sieve size	Aggregate Components						
	007	089	M10	Marble dust	Lime	RAP	Blend
Proportions	67.0%	7.0%	0.0%	4.8%	0.9%	20.3%	100%
1"	100.0	100.0	100.0	100.0	100.0	100.0	100.0
3/4"	100.0	100.0	100.0	100.0	100.0	100.0	100.0
1/2"	97.0	100.0	100.0	100.0	100.0	100.0	98.0
3/8"	48.0	100.0	100.0	100.0	100.0	95.0	64.1
#4	3.0	22.0	99.0	100.0	100.0	77.0	24.9
#8	3.0	4.0	83.0	100.0	100.0	61.0	20.4
#16	2.0	2.0	66.0	100.0	100.0	50.0	17.3
#30	2.0	2.0	53.0	100.0	100.0	42.0	15.7
#50	2.0	1.0	37.0	100.0	100.0	32.0	13.6
#100	1.0	1.0	18.0	98.0	100.0	20.0	10.4
#200	1.0	1.0	6.0	90.0	100.0	12.0	8.4

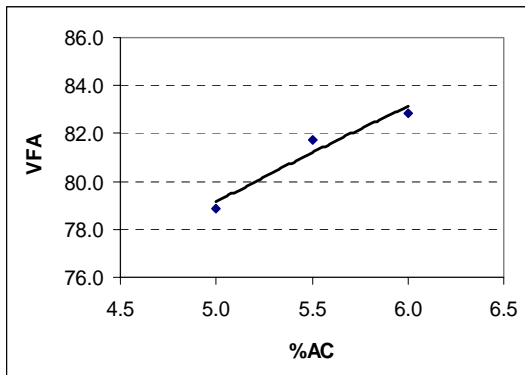
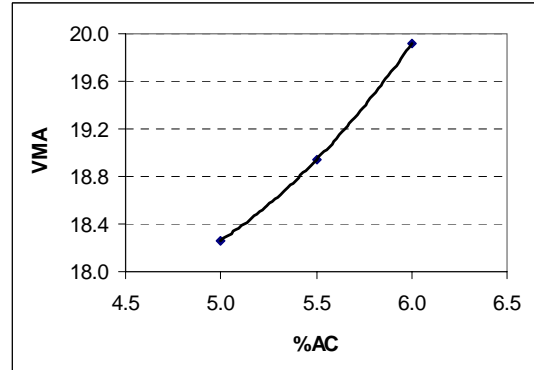
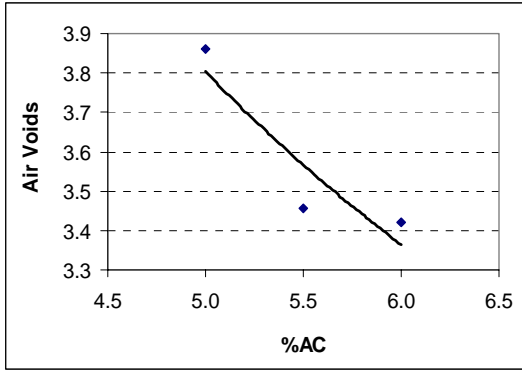
Series	% AC	VMA	VFA
1	5.5	20.4	69.9
2	6.0	19.3	80.3
3	6.5	19.7	84.1



Mt. View 30% +4 RAP

Sieve size	Aggregate Components						
	007	089	M10	Marble dust	Lime	RAP	Blend
Proportions	58.7%	0.0%	5%	5%	0.8%	30.5%	100%
1"	100.0	100.0	100.0	100.0	100.0	100.0	100.0
3/4"	100.0	100.0	100.0	100.0	100.0	99.0	99.7
1/2"	97.0	100.0	100.0	100.0	100.0	96.0	97.0
3/8"	48.0	100.0	100.0	100.0	100.0	84.0	64.6
#4	3.0	22.0	99.0	100.0	100.0	37.0	23.8
#8	3.0	4.0	83.0	100.0	100.0	25.0	19.3
#16	2.0	2.0	66.0	100.0	100.0	21.0	16.7
#30	2.0	2.0	53.0	100.0	100.0	18.0	15.1
#50	2.0	1.0	37.0	100.0	100.0	15.0	13.4
#100	1.0	1.0	18.0	98.0	100.0	10.0	10.2
#200	1.0	1.0	6.0	90.0	100.0	6.2	8.1

Series	% AC	VMA	VFA
1	5.0	18.3	78.9
2	5.5	18.9	81.8
3	6.0	19.9	82.8



A.2 Mix Designs for Lithia Springs Mixtures

Lithia Springs 0% RAP

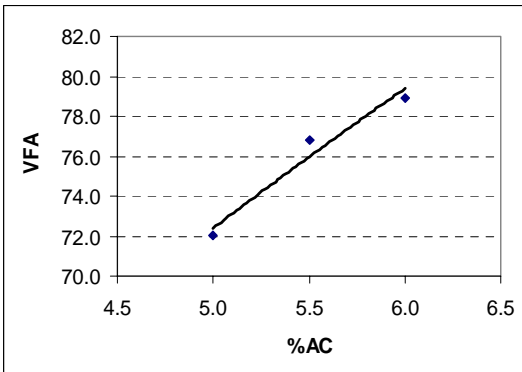
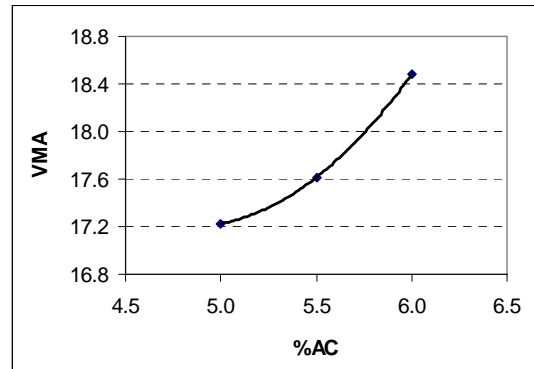
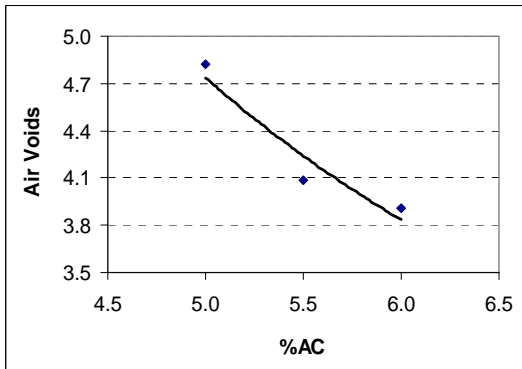
Sieve size	Aggregate Components					
	007	089	810	Marble dust	Lime	Blend
Proportions	67.0%	13.0%	13.0%	6.0%	1.0%	100%
1"	100.0	100.0	100.0	100.0	100.0	100.0
3/4"	100.0	100.0	100.0	100.0	100.0	100.0
1/2"	85.0	100.0	100.0	100.0	100.0	90.0
3/8"	50.0	100.0	100.0	100.0	100.0	66.5
#4	6.0	30.0	84.0	100.0	100.0	25.8
#8	2.0	2.0	62.0	100.0	100.0	16.7
#16	1.0	2.0	50.0	100.0	100.0	14.4
#30	1.0	1.0	41.0	100.0	100.0	13.1
#50	1.0	1.0	28.0	100.0	100.0	11.4
#100	1.0	1.0	21.0	98.0	100.0	10.4
#200	1.0	1.0	10.0	90.0	100.0	8.5

Series	% AC	VMA	VFA
1	6.0	17.8	75.8

Lithia Springs 10% DG1 RAP

Sieve size	Aggregate Components						
	007	089	810	Marble dust	Lime	RAP	Blend
Proportions	71.9%	0.0%	12.6%	4.5%	1.0%	10.0%	100%
1"	100.0	100.0	100.0	100.0	100.0	100.0	100.0
3/4"	100.0	100.0	100.0	100.0	100.0	100.0	100.0
1/2"	85.0	100.0	100.0	100.0	100.0	99.0	89.1
3/8"	50.0	100.0	100.0	100.0	100.0	93.0	63.4
#4	6.0	30.0	84.0	100.0	100.0	73.0	27.7
#8	2.0	2.0	62.0	100.0	100.0	58.0	20.6
#16	1.0	2.0	50.0	100.0	100.0	47.0	17.2
#30	1.0	1.0	41.0	100.0	100.0	38.0	15.2
#50	1.0	1.0	28.0	100.0	100.0	29.0	12.6
#100	1.0	1.0	21.0	98.0	100.0	19.0	10.7
#200	1.0	1.0	10.0	90.0	100.0	11.2	8.1

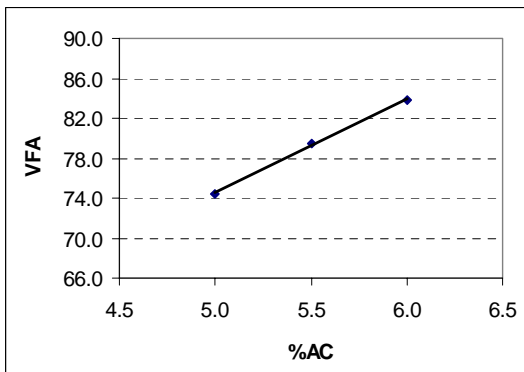
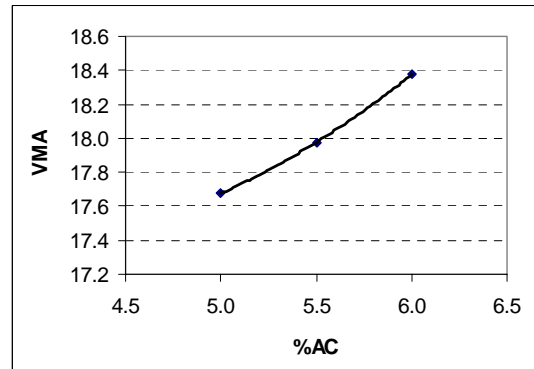
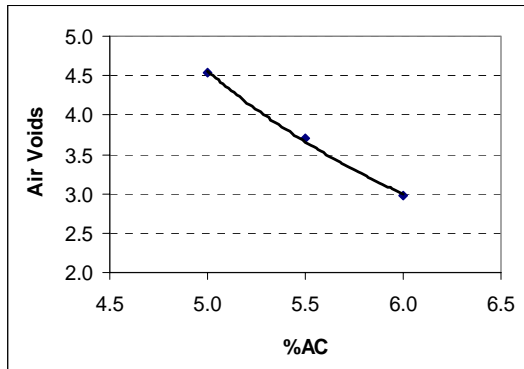
Series	% AC	VMA	VFA
1	5.0	17.2	72.0
2	5.5	17.6	76.8
3	6.0	18.5	78.9



Lithia Springs 20% +4 RAP

Sieve size	Aggregate Components						
	007	089	810	Marble dust	Lime	RAP	Blend
Proportions	61.8%	0.0%	12.0%	5.0%	0.9%	20.3%	100%
1"	100.0	100.0	100.0	100.0	100.0	100.0	100.0
3/4"	100.0	100.0	100.0	100.0	100.0	99.0	99.8
1/2"	85.0	100.0	100.0	100.0	100.0	96.0	89.9
3/8"	50.0	100.0	100.0	100.0	100.0	84.0	65.9
#4	6.0	30.0	84.0	100.0	100.0	37.0	27.2
#8	2.0	2.0	62.0	100.0	100.0	25.0	19.7
#16	1.0	2.0	50.0	100.0	100.0	21.0	16.8
#30	1.0	1.0	41.0	100.0	100.0	18.0	15.1
#50	1.0	1.0	28.0	100.0	100.0	15.0	12.9
#100	1.0	1.0	21.0	98.0	100.0	10.0	11.0
#200	1.0	1.0	10.0	90.0	100.0	6.2	8.5

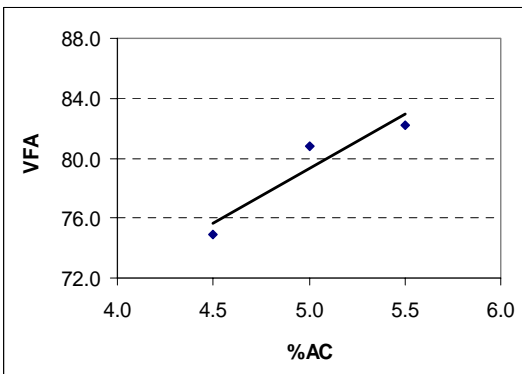
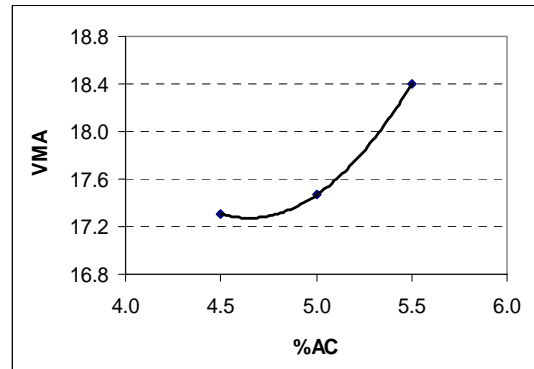
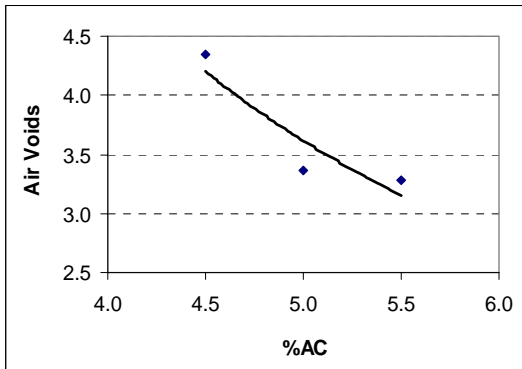
Series	% AC	VMA	VFA
1	5.0	17.7	74.4
2	5.5	18.0	79.4
3	6.0	18.4	83.8



Lithia Springs 30% DG2 RAP

Sieve size	Aggregate Components						
	007	089	810	Marble dust	Lime	RAP	Blend
Proportions	65.7%	0.0%	0.0%	3.0%	0.8%	30.5%	100%
1"	100.0	100.0	100.0	100.0	100.0	100.0	100.0
3/4"	100.0	100.0	100.0	100.0	100.0	100.0	100.0
1/2"	85.0	100.0	100.0	100.0	100.0	100.0	90.1
3/8"	50.0	100.0	100.0	100.0	100.0	95.0	65.6
#4	6.0	30.0	84.0	100.0	100.0	77.0	31.2
#8	2.0	2.0	62.0	100.0	100.0	61.0	23.7
#16	1.0	2.0	50.0	100.0	100.0	50.0	19.7
#30	1.0	1.0	41.0	100.0	100.0	42.0	17.3
#50	1.0	1.0	28.0	100.0	100.0	32.0	14.2
#100	1.0	1.0	21.0	98.0	100.0	20.0	10.5
#200	1.0	1.0	10.0	90.0	100.0	12.0	7.8

Series	% AC	VMA	VFA
1	4.5	17.3	74.9
2	5.0	17.5	80.8
3	5.5	18.4	82.2



A.3 Mix Designs for Camak Mixtures

Camak 0% RAP

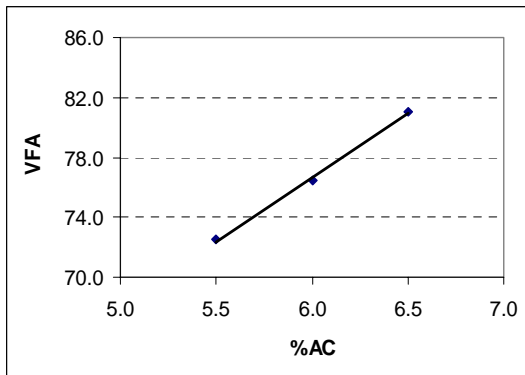
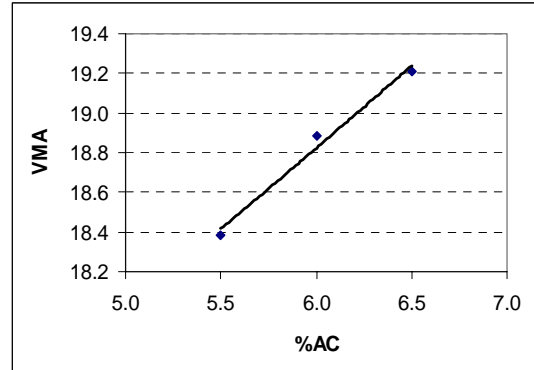
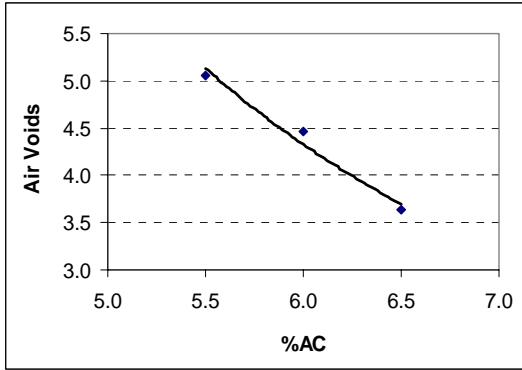
Sieve size	Aggregate Components				
	007	M10	Marble dust	Lime	Blend
Proportions	83.0%	10.0%	6.0%	1.0%	100%
1"	100.0	100.0	100.0	100.0	100.0
3/4"	100.0	100.0	100.0	100.0	100.0
1/2"	94.0	100.0	100.0	100.0	95.0
3/8"	46.0	100.0	100.0	100.0	55.2
#4	2.0	98.0	100.0	100.0	18.5
#8	1.0	82.0	100.0	100.0	16.0
#16	1.0	62.0	100.0	100.0	14.0
#30	1.0	50.0	100.0	100.0	12.8
#50	1.0	36.0	100.0	100.0	11.4
#100	1.0	25.0	98.0	100.0	10.2
#200	1.0	12.0	90.0	100.0	8.4

Series	% AC	VMA	VFA
1	6.0	21.1	73.3

Camak 10% DG2 RAP

Sieve size	Aggregate Components					
	007	M10	Marble dust	Lime	RAP	Blend
Proportions	73.0%	11.0%	4.9%	0.9%	10.2%	100%
1"	100.0	100.0	100.0	100.0	100.0	100.0
3/4"	100.0	100.0	100.0	100.0	100.0	100.0
1/2"	94.0	100.0	100.0	100.0	100.0	95.6
3/8"	46.0	100.0	100.0	100.0	95.0	60.1
#4	2.0	98.0	100.0	100.0	77.0	25.9
#8	1.0	82.0	100.0	100.0	61.0	21.8
#16	1.0	62.0	100.0	100.0	50.0	18.5
#30	1.0	50.0	100.0	100.0	42.0	16.3
#50	1.0	36.0	100.0	100.0	32.0	13.8
#100	1.0	25.0	98.0	100.0	20.0	11.2
#200	1.0	12.0	90.0	100.0	12.0	8.6

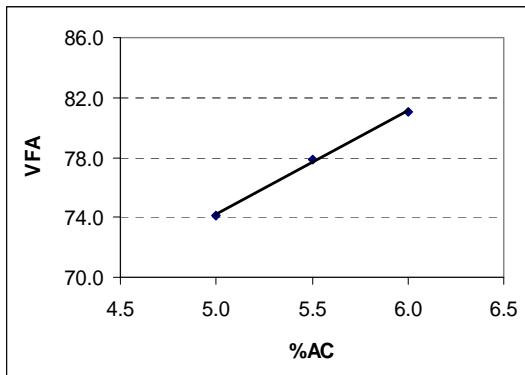
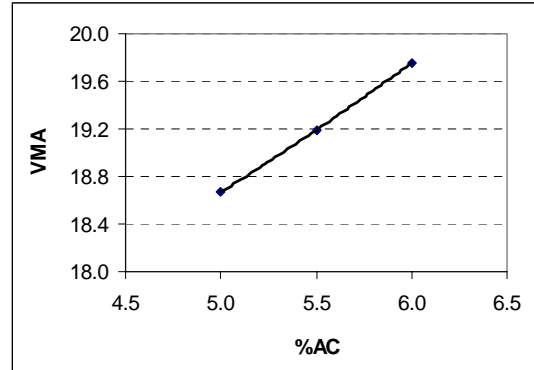
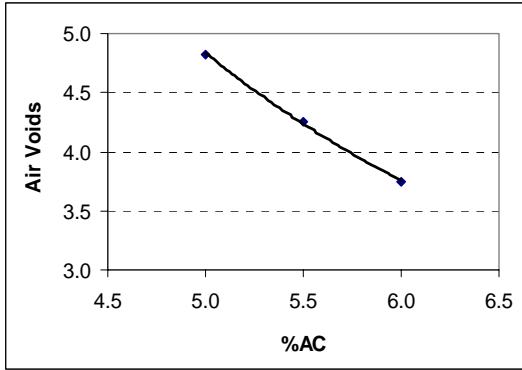
Series	% AC	VMA	VFA
1	5.5	18.4	72.5
2	6.0	18.9	76.4
3	6.5	19.2	81.1



Camak 20% -4 RAP

Sieve size	Aggregate Components					
	007	M10	Marble dust	Lime	RAP	Blend
Proportions	75.1%	0.0%	4.0%	0.9%	20.0%	100%
1"	100.0	100.0	100.0	100.0	100.0	100.0
3/4"	100.0	100.0	100.0	100.0	100.0	100.0
1/2"	94.0	100.0	100.0	100.0	100.0	95.5
3/8"	46.0	100.0	100.0	100.0	100.0	59.4
#4	2.0	98.0	100.0	100.0	100.0	26.4
#8	1.0	82.0	100.0	100.0	81.0	21.9
#16	1.0	62.0	100.0	100.0	65.0	18.7
#30	1.0	50.0	100.0	100.0	53.0	16.3
#50	1.0	36.0	100.0	100.0	40.0	13.7
#100	1.0	25.0	98.0	100.0	25.0	10.6
#200	1.0	12.0	90.0	100.0	15.0	8.3

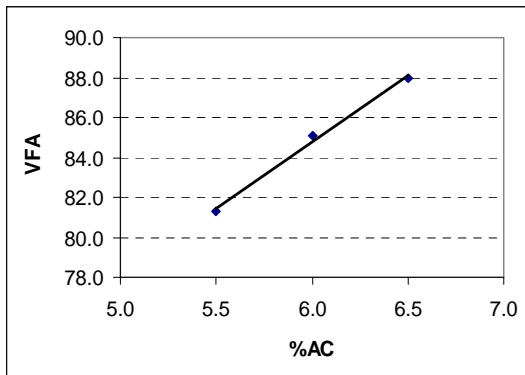
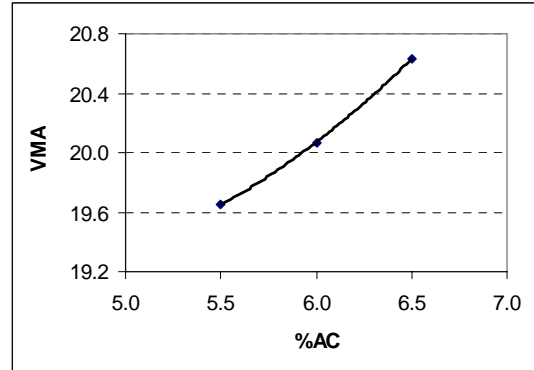
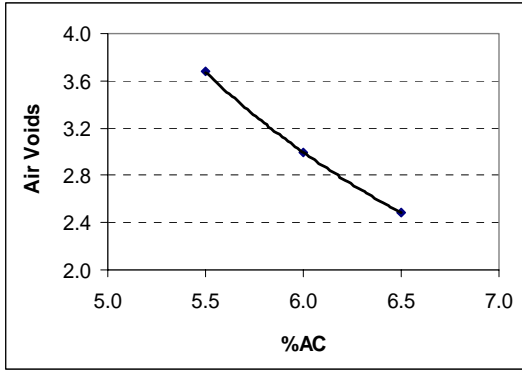
Series	% AC	VMA	VFA
1	5.0	18.7	74.2
2	5.5	19.2	77.8
3	6.0	19.8	81.1



Camak 30% DG1 RAP

Sieve size	Aggregate Components					
	007	M10	Marble dust	Lime	RAP	Blend
Proportions	65.6%	0.0%	3.5%	0.8%	30.1%	100%
1"	100.0	100.0	100.0	100.0	100.0	100.0
3/4"	100.0	100.0	100.0	100.0	100.0	100.0
1/2"	94.0	100.0	100.0	100.0	99.0	95.8
3/8"	46.0	100.0	100.0	100.0	93.0	62.5
#4	2.0	98.0	100.0	100.0	73.0	27.6
#8	1.0	82.0	100.0	100.0	58.0	22.4
#16	1.0	62.0	100.0	100.0	47.0	19.1
#30	1.0	50.0	100.0	100.0	38.0	16.4
#50	1.0	36.0	100.0	100.0	29.0	13.7
#100	1.0	25.0	98.0	100.0	19.0	10.6
#200	1.0	12.0	90.0	100.0	11.2	8.0

Series	% AC	VMA	VFA
1	5.5	19.6	81.3
2	6.0	20.1	85.1
3	6.5	20.6	88.0



A.4 Mix Designs for Ruby Mixtures

Ruby 0% RAP

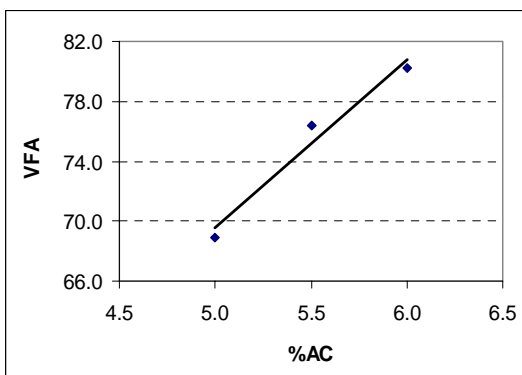
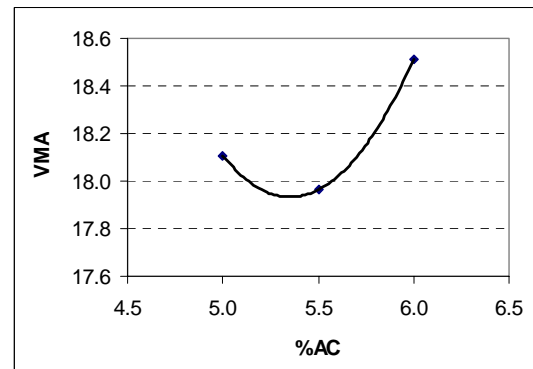
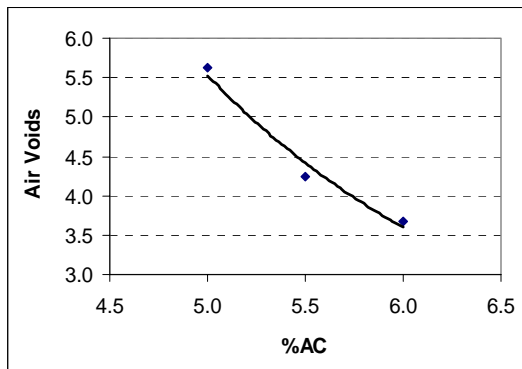
Sieve size	Aggregate Components				
	007	M10	Marble dust	Lime	Blend
Proportions	77.0%	18.0%	4.0%	1.0%	100%
1"	100.0	100.0	100.0	100.0	100.0
3/4"	100.0	100.0	100.0	100.0	100.0
1/2"	96.0	100.0	100.0	100.0	96.9
3/8"	55.0	100.0	100.0	100.0	65.4
#4	2.0	99.0	100.0	100.0	24.4
#8	1.0	82.0	100.0	100.0	20.5
#16	1.0	62.0	100.0	100.0	16.9
#30	1.0	49.0	100.0	100.0	14.6
#50	1.0	37.0	100.0	100.0	12.4
#100	1.0	27.0	98.0	100.0	10.6
#200	1.0	18.0	90.0	100.0	8.6

Series	% AC	VMA	VFA
1	6.5	19.4	76.7
2	7.0	18.8	86.5

Ruby 10% +4 RAP

Sieve size	Aggregate Components					
	007	M10	Marble dust	Lime	RAP	Blend
Proportions	69.9%	15.0%	4.0%	0.9%	10.2%	100%
1"	100.0	100.0	100.0	100.0	100.0	100.0
3/4"	100.0	100.0	100.0	100.0	99.0	99.9
1/2"	96.0	100.0	100.0	100.0	96.0	96.8
3/8"	55.0	100.0	100.0	100.0	84.0	66.9
#4	2.0	99.0	100.0	100.0	37.0	24.9
#8	1.0	82.0	100.0	100.0	25.0	20.4
#16	1.0	62.0	100.0	100.0	21.0	17.0
#30	1.0	49.0	100.0	100.0	18.0	14.8
#50	1.0	37.0	100.0	100.0	15.0	12.7
#100	1.0	27.0	98.0	100.0	10.0	10.6
#200	1.0	18.0	90.0	100.0	6.2	8.5

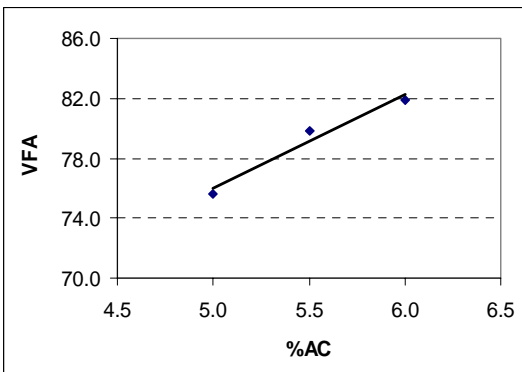
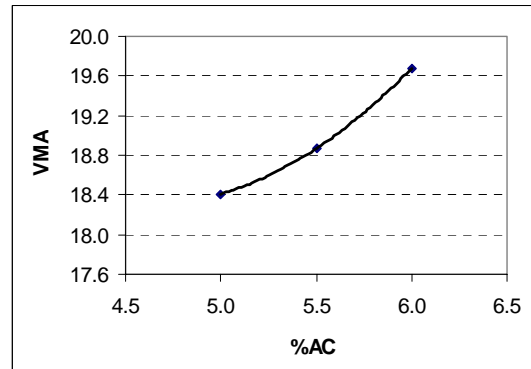
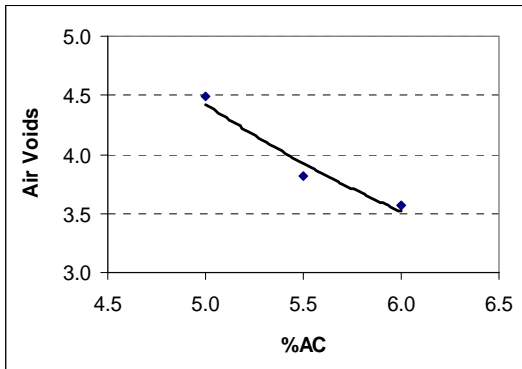
Series	% AC	VMA	VFA
1	5.0	18.1	68.9
2	5.5	18.0	76.4
3	6.0	18.5	80.2



Ruby 20% DG1 RAP

Sieve size	Aggregate Components					
	007	M10	Marble dust	Lime	RAP	Blend
Proportions	70.0%	5.0%	4.0%	0.9%	20.1%	100%
1"	100.0	100.0	100.0	100.0	100.0	100.0
3/4"	100.0	100.0	100.0	100.0	100.0	100.0
1/2"	96.0	100.0	100.0	100.0	99.0	97.0
3/8"	55.0	100.0	100.0	100.0	93.0	67.1
#4	2.0	99.0	100.0	100.0	73.0	25.9
#8	1.0	82.0	100.0	100.0	58.0	21.4
#16	1.0	62.0	100.0	100.0	47.0	18.1
#30	1.0	49.0	100.0	100.0	38.0	15.7
#50	1.0	37.0	100.0	100.0	29.0	13.3
#100	1.0	27.0	98.0	100.0	19.0	10.7
#200	1.0	18.0	90.0	100.0	11.2	8.4

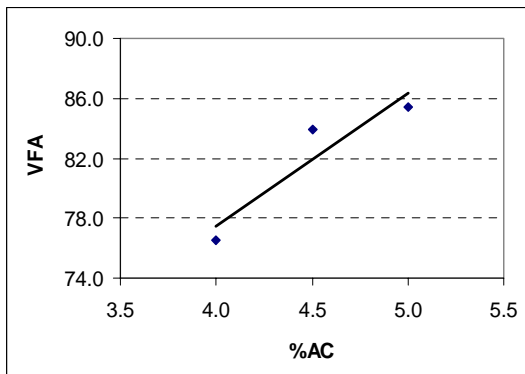
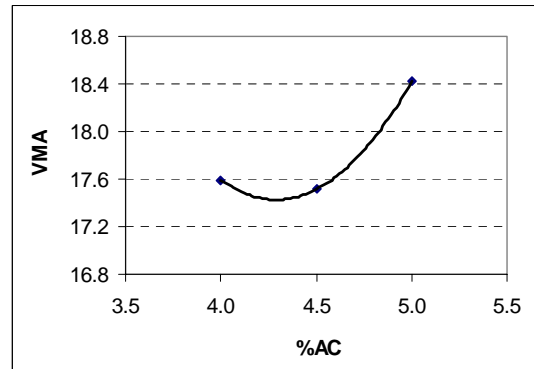
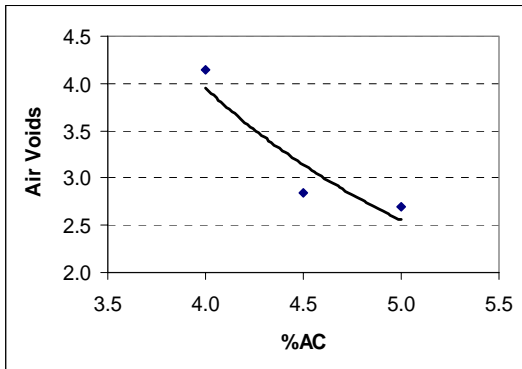
Series	% AC	VMA	VFA
1	5.0	18.4	75.6
2	5.5	18.9	79.8
3	6.0	19.7	81.9



Ruby 30% -4 RAP

Sieve size	Aggregate Components					
	007	M10	Marble dust	Lime	RAP	Blend
Proportions	66.7%	0.0%	2.5%	0.9%	29.9%	100%
1"	100.0	100.0	100.0	100.0	100.0	100.0
3/4"	100.0	100.0	100.0	100.0	100.0	100.0
1/2"	96.0	100.0	100.0	100.0	100.0	97.3
3/8"	55.0	100.0	100.0	100.0	100.0	70.0
#4	2.0	99.0	100.0	100.0	100.0	34.6
#8	1.0	82.0	100.0	100.0	81.0	28.3
#16	1.0	62.0	100.0	100.0	65.0	23.5
#30	1.0	49.0	100.0	100.0	53.0	19.9
#50	1.0	37.0	100.0	100.0	40.0	16.0
#100	1.0	27.0	98.0	100.0	25.0	11.5
#200	1.0	18.0	90.0	100.0	15.0	8.3

Series	% AC	VMA	VFA
1	4.0	17.6	76.5
2	4.5	17.5	83.9
3	5.0	18.4	85.4



APPENDIX B

Individual Test Results

Table B.1. Results from Moisture Susceptibility Test.

Agg. Source	% RAP	RAP Type	% Air Voids	Wet Strength, psi	Dry Strength, psi	TSR
Mt. View	0	DG1	7.2	69.90	77.86	0.90
Mt. View	0	DG1	7.2	77.09	64.94	1.19
Mt. View	0	DG1	7.1	67.67	71.94	0.94
Mt. View	10	-4	6.7	90.91	100.65	0.90
Mt. View	10	-4	6.9	86.45	83.21	1.04
Mt. View	10	-4	7.1	87.09	77.79	1.12
Mt. View	20	DG2	7.3	95.75	107.80	1.12
Mt. View	20	DG2	9.6	84.03	100.60	0.89
Mt. View	20	DG2	6.6	95.87	97.30	0.84
Mt. View	30	+4	6.7	101.99	107.84	0.95
Mt. View	30	+4	6.3	110.14	105.62	1.04
Mt. View	30	+4	7.3	87.28	103.77	0.84
Lithia Spr.	0	-4	7.6	67.55	91.80	0.74
Lithia Spr.	0	-4	7.9	74.36	97.08	0.77
Lithia Spr.	0	-4	7.5	70.79	79.26	0.89
Lithia Spr.	10	DG1	7.1	84.93	85.56	0.99
Lithia Spr.	10	DG1	6.8	73.78	79.96	0.92
Lithia Spr.	10	DG1	7.4	80.41	85.18	0.94
Lithia Spr.	20	+4	7.4	88.87	95.68	0.93
Lithia Spr.	20	+4	7.0	98.74	77.35	1.28
Lithia Spr.	20	+4	7.4	84.67	88.04	0.96
Lithia Spr.	30	DG2	7.3	98.99	98.55	1.00
Lithia Spr.	30	DG2	6.8	92.37	85.94	1.07
Lithia Spr.	30	DG2	6.5	95.94	99.76	0.96
Camak	0	+4	7.5	77.70	87.54	0.96
Camak	0	+4	8.0	78.80	90.34	0.89
Camak	0	+4	7.5	79.50	85.18	0.87
Camak	10	DG2	6.6	76.90	100.39	0.77
Camak	10	DG2	6.9	68.05	79.26	0.86
Camak	10	DG2	7.2	72.00	75.69	0.95
Camak	20	-4	6.8	96.58	108.54	0.89
Camak	20	-4	6.7	76.52	100.20	0.76
Camak	20	-4	7.8	84.03	86.64	0.97
Camak	30	DG1	6.4	127.39	136.81	0.93
Camak	30	DG1	7.1	114.78	124.08	0.93
Camak	30	DG1	6.2	112.05	113.51	0.99
Ruby	0	DG2	7.0	72.10	70.00	1.03
Ruby	0	DG2	6.0	71.60	70.00	1.02
Ruby	0	DG2	6.7	67.00	69.10	0.97
Ruby	10	+4	6.7	93.65	102.24	0.92
Ruby	10	+4	6.7	89.89	102.56	0.88
Ruby	10	+4	6.9	93.39	106.12	0.88
Ruby	20	DG1	6.1	81.42	84.54	0.96
Ruby	20	DG1	6.4	76.78	85.63	0.90
Ruby	20	DG1	6.1	92.69	79.13	1.17
Ruby	30	-4	6.1	154.89	168.96	0.92
Ruby	30	-4	6.9	134.77	139.99	0.96
Ruby	30	-4	6.3	135.54	125.16	1.08

Table B.2. Results from Rutting Susceptibility Test.

Agg. Source	% RAP	RAP Type	% Air Voids	Rut Depth, mm
Mt. View	0	DG1	5.4	3.13
Mt. View	0	DG1	5.0	2.94
Mt. View	0	DG1	5.2	1.76
Mt. View	0	DG1	5.3	3.39
Mt. View	0	DG1	5.0	0.95
Mt. View	0	DG1	5.1	6.50
Mt. View	10	-4	5.0	4.42
Mt. View	10	-4	5.1	3.18
Mt. View	10	-4	4.8	1.40
Mt. View	10	-4	4.9	3.11
Mt. View	10	-4	5.1	5.86
Mt. View	10	-4	5.1	1.41
Mt. View	20	DG2	5.1	4.23
Mt. View	20	DG2	4.7	6.01
Mt. View	20	DG2	4.9	3.34
Mt. View	20	DG2	4.8	2.05
Mt. View	20	DG2	4.4	8.33
Mt. View	20	DG2	5.0	2.50
Mt. View	30	+4	5.2	1.25
Mt. View	30	+4	4.9	2.35
Mt. View	30	+4	4.9	1.89
Mt. View	30	+4	4.9	1.23
Mt. View	30	+4	4.9	2.49
Mt. View	30	+4	4.8	0.99
Lithia Spr.	0	-4	4.7	3.14
Lithia Spr.	0	-4	4.2	1.86
Lithia Spr.	0	-4	4.3	1.89
Lithia Spr.	0	-4	4.7	3.59
Lithia Spr.	0	-4	4.7	1.98
Lithia Spr.	0	-4	4.3	1.76
Lithia Spr.	10	DG1	4.6	2.73
Lithia Spr.	10	DG1	4.7	2.37
Lithia Spr.	10	DG1	4.8	1.31
Lithia Spr.	10	DG1	4.6	2.15
Lithia Spr.	10	DG1	4.7	1.25
Lithia Spr.	10	DG1	4.7	2.19
Lithia Spr.	20	+4	4.7	2.69
Lithia Spr.	20	+4	4.8	2.48
Lithia Spr.	20	+4	4.7	1.77
Lithia Spr.	20	+4	4.9	0.93
Lithia Spr.	20	+4	4.4	3.33
Lithia Spr.	20	+4	4.2	3.45
Lithia Spr.	30	DG2	5.6	2.77
Lithia Spr.	30	DG2	5.2	5.75
Lithia Spr.	30	DG2	5.8	5.15
Lithia Spr.	30	DG2	5.3	2.88
Lithia Spr.	30	DG2	5.6	5.69
Lithia Spr.	30	DG2	5.4	4.76

Table B.2 (cont.). Results from Rutting Susceptibility Test.

Agg. Source	% RAP	RAP Type	% Air Voids	Rut Depth, mm
Camak	0	+4	4.9	6.83
Camak	0	+4	4.8	4.27
Camak	0	+4	4.7	2.39
Camak	0	+4	4.5	4.42
Camak	0	+4	4.2	3.45
Camak	0	+4	4.3	0.68
Camak	10	DG2	4.7	1.62
Camak	10	DG2	4.6	2.14
Camak	10	DG2	4.4	1.97
Camak	10	DG2	4.9	1.58
Camak	10	DG2	4.5	2.56
Camak	10	DG2	4.6	1.89
Camak	20	-4	4.3	1.40
Camak	20	-4	4.4	1.83
Camak	20	-4	4.1	1.93
Camak	20	-4	4.8	0.95
Camak	20	-4	4.2	1.87
Camak	20	-4	5.2	0.91
Camak	30	DG1	4.7	4.04
Camak	30	DG1	4.8	2.95
Camak	30	DG1	4.7	2.53
Camak	30	DG1	5.0	4.20
Camak	30	DG1	4.3	2.75
Camak	30	DG1	4.1	3.04
Ruby	0	DG2	5.1	5.89
Ruby	0	DG2	5.4	1.73
Ruby	0	DG2	4.5	3.85
Ruby	0	DG2	4.2	4.05
Ruby	0	DG2	4.8	2.70
Ruby	0	DG2	4.4	3.30
Ruby	10	+4	5.4	4.40
Ruby	10	+4	5.2	5.60
Ruby	10	+4	5.3	6.17
Ruby	10	+4	5.6	5.83
Ruby	10	+4	5.0	5.03
Ruby	10	+4	5.0	3.92
Ruby	20	DG1	4.8	5.74
Ruby	20	DG1	4.7	4.56
Ruby	20	DG1	4.8	5.99
Ruby	20	DG1	5.0	6.47
Ruby	20	DG1	5.2	5.84
Ruby	20	DG1	4.5	3.67
Ruby	30	-4	5.4	4.95
Ruby	30	-4	5.2	3.08
Ruby	30	-4	5.8	4.03
Ruby	30	-4	5.2	4.84
Ruby	30	-4	5.3	3.25
Ruby	30	-4	4.4	2.97

Table B.3. Results from Creep Compliance Test.

Agg. Source	% RAP	RAP Type	Creep Compliance @ 50 sec, 1/psi			log a _T		m-value
			- 20 °C	- 10 °C	0 °C	- 10 °C	0 °C	
Mt. View	0	DG1	8.35E-07	1.13E-06	2.68E-06	-0.87	-1.75	0.574
Mt. View	10	-4	6.46E-07	9.91E-07	1.87E-06	-0.82	-1.64	0.410
Mt. View	20	DG2	5.89E-07	1.55E-06	3.37E-06	-1.03	-2.07	0.386
Mt. View	30	+4	9.63E-07	2.59E-06	3.12E-06	-0.78	-1.55	0.372
Lithia Springs	0	-4	4.58E-07	9.69E-07	2.14E-06	-1.15	-2.29	0.339
Lithia Springs	10	DG1	5.00E-07	1.03E-06	2.32E-06	-1.27	-2.54	0.320
Lithia Springs	20	+4	7.38E-07	1.13E-06	1.88E-06	-0.70	-1.40	0.484
Lithia Springs	30	DG2	1.42E-06	2.38E-06	6.63E-06	-1.34	-2.68	0.432
Camak	0	+4	1.15E-06	2.70E-06	7.89E-06	-1.14	-2.27	0.440
Camak	10	DG2	1.69E-06	1.60E-06	2.60E-06	-0.31	-0.62	0.599
Camak	20	-4	9.82E-07	1.50E-06	3.35E-06	-0.83	-1.66	0.518
Camak	30	DG1	1.61E-06	1.85E-06	6.03E-06	-0.86	-1.71	0.687
Ruby	0	DG2	1.83E-06	3.37E-06	1.03E-05	-0.92	-1.84	0.598
Ruby	10	+4	1.61E-06	2.40E-06	4.71E-06	-0.61	-1.21	0.548
Ruby	20	DG1	1.48E-06	2.51E-06	6.77E-06	-0.85	-1.70	0.630

Table B.4. Results from Fatigue Test (400 $\mu\epsilon$).

Agg. Source	% RAP	RAP Type	% Air Voids	N_f	Initial Stiffness, MPa	Diss. Energy (kPa)
Mt. View	0	DG1	6.8	1,202,320	3,102	0.247
Mt. View	0	DG1	6.5	6,365,620	3,374	0.277
Mt. View	0	DG1	6.9	3,236,690	3,632	0.288
Mt. View	10	-4	6.6	5,319,730	3,194	0.246
Mt. View	10	-4	6.3	4,017,630	3,236	0.254
Mt. View	10	-4	6.3	6,123,740	3,921	0.302
Mt. View	20	DG2	5.3	1,755,400	3,660	0.272
Mt. View	20	DG2	5.5	2,890,920	3,366	0.277
Mt. View	20	DG2	5.7	2,367,890	3,430	0.288
Mt. View	30	+4	7.4	2,450,210	4,314	0.197
Mt. View	30	+4	6.9	342,580	5,572	0.197
Mt. View	30	+4	6.5	1,205,860	4,260	0.203
Lithia Spr.	0	-4	6.4	6,098,480	3,564	0.277
Lithia Spr.	0	-4	5.9	4,917,110	3,738	0.298
Lithia Spr.	0	-4	5.4	5,562,870	3,656	0.295
Lithia Spr.	10	DG1	5.4	5,434,130	3,972	0.298
Lithia Spr.	10	DG1	5.6	3,055,130	3,896	0.299
Lithia Spr.	10	DG1	6.0	2,568,770	3,667	0.278
Lithia Spr.	20	+4	6.1	6,648,340	3,472	0.278
Lithia Spr.	20	+4	6.1	2,593,300	3,674	0.285
Lithia Spr.	20	+4	6.7	5,134,130	3,494	0.275
Lithia Spr.	30	DG2	5.8	2,274,170	4,160	0.296
Lithia Spr.	30	DG2	5.2	2,053,980	4,126	0.265
Lithia Spr.	30	DG2	5.1	268,000	4,213	0.894
Camak	0	+4	5.8	3,062,380	3,480	0.277
Camak	0	+4	6.0	3,576,160	3,252	0.273
Camak	0	+4	6.4	6,421,250	2,830	0.251
Camak	10	DG2	6.0	3,149,900	3,605	0.513
Camak	10	DG2	5.8	4,033,030	3,463	0.513
Camak	10	DG2	5.3	6,877,810	3,644	0.288
Camak	20	-4	5.2	3,163,080	3,542	0.265
Camak	20	-4	7.0	4,225,320	3,077	0.247
Camak	20	-4	6.8	679,370	2,798	0.224
Camak	30	DG1	5.7	3,771,280	2,858	0.238
Camak	30	DG1	5.0	4,144,106	3,267	0.258
Camak	30	DG1	5.1	3,656,092	3,730	0.258
Ruby	0	DG2	6.7	5,528,870	3,636	0.221
Ruby	0	DG2	6.2	4,984,710	3,568	0.224
Ruby	0	DG2	6.2	5,701,660	3,302	0.224
Ruby	10	+4	5.6	5,364,710	3,726	0.311
Ruby	10	+4	6.3	2,020,360	3,466	0.296
Ruby	10	+4	5.4	6,271,490	3,519	0.275
Ruby	20	DG1	6.2	8,368,160	3,074	0.257
Ruby	20	DG1	5.7	3,557,870	3,488	0.289
Ruby	20	DG1	5.5	1,454,590	3,623	0.275
Ruby	30	-4	6.9	543,000	4,411	0.308
Ruby	30	-4	6.4	1,091,240	4,863	0.321
Ruby	30	-4	6.2	645,220	4,588	0.321

Table B.5. Results from Fatigue Test (800 $\mu\epsilon$).

Agg. Source	% RAP	RAP Type	% Air Voids	N_f	Ini. Stiffness, MPa	Diss. Energy (kPa)
Mt. View	0	DG1	6.7	78,940	2,929	0.989
Mt. View	0	DG1	6.1	35,440	3,030	1.004
Mt. View	0	DG1	6.6	23,020	2,898	0.963
Mt. View	10	-4	6.7	62,700	3,156	0.995
Mt. View	10	-4	5.2	57,900	3,599	0.900
Mt. View	10	-4	6.0	29,830	2,752	0.916
Mt. View	20	DG2	5.0	37,600	4,480	0.898
Mt. View	20	DG2	6.3	37,420	4,277	0.910
Mt. View	20	DG2	5.4	18,020	4,219	0.873
Mt. View	30	+4	6.9	22,860	4,372	0.701
Mt. View	30	+4	7.2	20,520	4,331	0.670
Mt. View	30	+4	6.7	16,260	4,243	0.698
Lithia Spr.	0	-4	7.0	49,280	3,003	1.017
Lithia Spr.	0	-4	5.9	73,420	3,325	1.119
Lithia Spr.	0	-4	7.0	53,410	2,941	0.980
Lithia Spr.	10	DG1	5.9	44,850	3,506	1.095
Lithia Spr.	10	DG1	5.6	32,990	3,480	1.087
Lithia Spr.	10	DG1	5.5	56,790	3,248	1.024
Lithia Spr.	20	+4	6.3	43,640	3,226	1.041
Lithia Spr.	20	+4	6.4	80,150	3,064	0.997
Lithia Spr.	20	+4	6.1	50,030	3,246	1.045
Lithia Spr.	30	DG2	5.2	25,850	5,029	0.526
Lithia Spr.	30	DG2	5.4	11,150	4,569	0.586
Lithia Spr.	30	DG2	5.0	13,260	5,250	0.513
Camak	0	+4	5.7	109,140	3,323	0.894
Camak	0	+4	5.0	109,470	3,273	0.867
Camak	0	+4	5.9	57,600	3,065	0.801
Camak	10	DG2	5.5	58,090	3,265	1.075
Camak	10	DG2	6.5	21,880	3,277	1.025
Camak	10	DG2	5.6	42,870	3,121	1.001
Camak	20	-4	5.0	82,650	3,556	1.084
Camak	20	-4	6.9	33,500	3,253	1.012
Camak	20	-4	6.1	97,060	3,331	0.799
Camak	30	DG1	5.0	93,550	3,679	1.128
Camak	30	DG1	5.0	65,730	3,578	0.799
Camak	30	DG1	6.1	65,000	3,043	1.007
Ruby	0	DG2	6.8	78,700	3,096	0.896
Ruby	0	DG2	5.2	50,660	3,133	0.885
Ruby	0	DG2	6.5	88,680	2,854	0.806
Ruby	10	+4	6.8	59,420	3,192	1.065
Ruby	10	+4	7.0	26,920	2,969	1.013
Ruby	10	+4	5.6	36,460	3,262	1.087
Ruby	20	DG1	6.4	37,170	2,978	0.978
Ruby	20	DG1	5.8	11,390	3,550	1.199
Ruby	20	DG1	5.6	14,810	3,515	1.138
Ruby	30	-4	6.6	5,180	4,933	0.722
Ruby	30	-4	6.7	4,340	4,709	0.638
Ruby	30	-4	6.7	3,300	4,753	0.627